NPS / Multi Agency Critical Loads Project

Steady-State Critical Loads and Exceedance for Terrestrial and Aquatic Ecosystems in the Northeastern United States

Technical Report

12/30/2010

Prepared by: Eric K. Miller, Ecosystems Research Group, Ltd.

Prepared For: Ellen Porter and Tamara Blett
National Park Service
Air Resources Division

First Revision 1/18/2011

Second Revision 8/18/2011 to incorporate peer-review comments

Table of Contents

Appendices

Introduction

Sulfur and nitrogen emissions upwind of the northeastern US have decreased since the implementation of the Clean Air Act in 1970 and its amendments in 1990 (Driscoll et al. 2001; Stoddard et al. 2003; Sickles and Shadwick 2007). Still, levels of atmospheric deposition associated with present emissions of both sulfur and nitrogen compounds are expected to have continuing negative impacts on forest and aquatic ecosystem health and productivity. Sulfur and nitrogen deposition can cause excessive nutrient cation (calcium, magnesium, and potassium) leaching, reducing the supply of nutrient cations available for plant growth, a process called cation depletion (e.g., Johnson et al. 1994; Lawrence and Huntington 1999; Watmough and Dillon 2003; Bailey et al. 2005). Inadequate nutrient supplies frequently lead to increased susceptibility to climate, pest and pathogen stress, and result in reduced forest health, reduced growth, and eventual changes in forest species composition (Schaberg et al. 2001; Schaberg et al. 2007; Long et al. 2009). Reduced calcium levels in forests have been shown to reduce the reproductive success of forest-dwelling birds (Hames et al. 2002). Reduced soil base cation levels and high loads of sulfate and nitrate lead to reduced pH in aquatic ecosystems. Chronic and episodic pH reductions lead to fish kills, poor fish growth, and changes in plankton and diatom communities (Blouin, 1989; Buckler et al. 1994; Dixit et al. 1999; Driscoll et al. 2001).

The Northeast States for Coordinated Air Use Management (NESCAUM), a regional air quality planning organization, estimated the change in sulfur and nitrogen deposition expected to occur in the Northeast between 2002 and 2018 in response to planned and enacted air pollution control programs in the eastern US (NESCAUM 2008a; NESCAUM 2008b). Sulfur deposition is expected to decrease by an average of 36% and nitrogen deposition is expected to decrease by an average of 24% across the region. However, some locations within the region are estimated to experience increases over 2002 levels. This study was undertaken to estimate the location and extent of the forest and aquatic resources likely to remain at risk to projected 2018 levels of sulfur and nitrogen deposition. The percentage of forest and aquatic resources that might ***begin*** to recover from the effects of historically higher sulfur deposition levels as deposition drops to the levels projected for 2018 were also estimated. Possible future changes in the climate of the region or changes in timber utilization rates may affect the capacity of forest and aquatic ecosystems to tolerate acidity. However, due to budget limitations, these potential changes to environmental conditions were not considered in the present study.

The primary goals of the project were to obtain estimates of the percentage of forest and aquatic resources for which the current and c.a. 2018 sulfur and nitrogen deposition exceed the steady-state critical load and to identify areas that would benefit from further studies and refined estimates of risk. Steady-state critical loads modeling has been used extensively throughout Europe and Scandinavia (ICP 2004) and to a lesser extent in North America (e.g. Miller et al. 2006, Ouimet et al. 2006, Dupont et al. 2005, NEG/ECP 2001) and China (e.g. Ye et al. 2002) to produce first-order estimates of the spatial extent and spatial location of ecosystems likely to be at risk under different atmospheric deposition scenarios.

This study differs from previous regional assessments covering the region (e.g. Mc Nulty et al. 2007, Dupont et al. 2005) because it was designed to improve the identification of potentially impaired ecosystems by conducting critical loads analysis at high spatial resolution. EPA's Clean Air Science Advisory Committee (CASAC 2011, page ES-6) has specifically identified the issue of extreme local heterogeneity in environmental conditions as a major challenge for the assessment of critical loads. Coarse (1-km or greater) grids may be adequate in areas of flat-lying geologic units and limited topographic relief (e.g. Morrison et al. 1994). However, in regions of complex geology and mountainous terrain such as the northeastern US, surface waters in close proximity may have substantially different pH. Forest ecosystems known to be impacted by acidic deposition in the northeastern US are dispersed widely on the landscape with damage often restricted to small areas less than 1 km^2, although the total amount of sensitive area may be significant. Sub-kilometer scale variations in geology, climate, and hydrology (e.g., Lazarus et al. 2004; Schaberg et al. 2006) as well as steep gradients in deposition rates at small scales in complex mountainous terrain (e.g., Miller et al. 1993) give rise to the fine-scale, patchy distribution of observed acidification impacts. In coarse-grid analyses of complex terrain, the landscape parameters contributing to sensitivity or the deposition rates average to values such that the large grid cell mean values fail to detect the minimum critical load or maximum exceedance within a grid cell where significant negative ecological effects may be occurring a sub-grid scale.

This section provides an overview of the technical tasks undertaken to produce estimates of steady-state critical loads of sulfur and nitrogen deposition and atmospheric deposition exceedance of critical loads for forested and aquatic ecosystems in the Northeastern United States. Additional details relating to specific tasks are included in subsequent sections. The study was undertaken as a pilot project to explore the feasibility and utility of regionalized and integrated forest and aquatic ecosystem critical load calculations. Methods were employed that allowed a consistent method of calculation, common data sources, and a consistent spatial resolution across the wide variety of ecosystems present in the Northeast.

Due to the requirements of conducting the regional study using consistent methods, data sources, and spatial resolution, some types of environments are better represented in the analysis than others. The most appropriate use of these results is at the regional scale for which they were developed. Therefore, the end user of the estimates must take care to evaluate how the regional study assumptions relate to known conditions at a local scale when using either assessment components or the results of this study at scales smaller than the full Northeast Region. The project was primarily designed to produce an assessment useful for regional air-quality managers, providing a regional perspective of forest and aquatic resource vulnerability under different pollutant emissions and atmospheric deposition scenarios. End-users of the data whose interests lie in evaluation or management of specific land parcels are encouraged to use the regional study results as guidance providing information on the general magnitude of critical loads and exceedance expected to prevail on a given parcel. The regional assessment identifies areas most likely to be at continued risk from sulfur and nitrogen deposition and provides resource managers with information that can effectively guide decisions about where and what type of additional data should be collected to reduce uncertainty in critical load estimates at the local scale.

Structure of the Northeast Regional Steady-State Critical Loads Project

Methods for critical load estimation were employed that allowed a consistent method of calculation, common data sources, and a consistent spatial resolution across the wide variety of ecosystems present in the Northeast. The methods used followed previous work (Miller et al. 2006, Ouimet et al. 2006) in the New England States as part of the New England Governors' and Eastern Canadian Premiers' (NEG/ECP) Acid Deposition Assessment for forested ecosystems (NEG/ECP 2001). This project extended the New England assessment to include New York State (see Section 3). In contrast to the NEG/ECP study, this project also estimated the exceeedance of the critical load under a potential future atmospheric deposition scenario (see Section 2). The aquatic ecosystem assessment deviated from prior NEG/ECP work (Dupont et al. 2005) by making an effort to assess conditions in all surface waters rather than a small population of sampled lakes (see Section 4). The aquatic component of the assessment made use of the extensive data layers generated in the terrestrial ecosystem assessment and employed a modification of the simple-mass-balance type models used widely in Europe and North America (see section 4).

In both the forested terrestrial and aquatic ecosystem cases, the assessment follows the well-established steady-state mass-balance approach to accounting for the sources and sinks of acidification potential (ICP Mapping Manual 2004). A steady-state approach was required to meet the goal of a comprehensive (all areas considered) regional assessment. There were not adequate data available to employ dynamic (time course simulation) modeling approaches to a comprehensive regional assessment. Dynamic modeling was applied by a separate project team (Sullivan and Cosby) to specific watersheds within the northeastern US where suitable data were available.

The federal multi-agency working group sponsoring the project, along with primary stakeholders (state air and water quality agencies), were briefed on the methodologies, atmospheric deposition scenarios, and key modeling assumptions. Feedback on approaches, assumptions, and critical thresholds was obtained from the federal agencies and stakeholders and incorporated into the assessment design. Results of the assessment were reviewed with the sponsoring federal agencies and stakeholders. Model input data and assessment results were stored and transmitted on portable USB disks to the lead sponsoring agency for archival and distribution.

Interpreting the results of steady-state critical loads analysis

It is important for the end-user of the assessment results to understand the concept of a "**steady-state**" critical load and the difference between steady-state and dynamic models of ecosystem processes. The concept of steady-state refers to a condition when external influences (e.g. atmospheric deposition) and internal processes of a system (e.g. growth rates) are unchanging and in-balance such that system state properties (e.g. biomass, soil base saturation, surface water pH) are not changing. Steady-state models make the assumption that external factors (e.g. atmospheric deposition) and internal processes (e.g. growth) remain constant indefinitely. This assumption greatly simplifies model structure and data requirements. The representations of ecosystem properties in steady-state models are the

values of properties for a system ***in equilibrium*** with the specified values of external and internal driving parameters. ***There is no information about time-varying properties of a system in a steady-state critical loads model.*** However, it is common to compare the steady-state ecosystem properties resulting from equilibrium with different sets of driving parameters. Frequently the differences in parameters represent different values of the driving variables known or anticipated at different times. Thus, steady state models are used primarily to estimate ***the ecosystem properties toward which a system is likely to evolve*** under the specified values of external and internal parameters at some future time from the equilibrium properties associated with external and internal parameter values at a previous time. Steady-state models can also be used to estimate the direction of change in ecosystem properties from observed (non-steady state) conditions if external and internal parameters were to remain constant at observed values indefinitely.

Natural systems are not typically in a steady state. Natural and anthropogenic disturbances (e.g. fire, climate variability, harvesting, pollution) continually perturb natural systems shifting biomass, species composition, nutrient stocks etc. For this reason, ecosystems are often referred to as "dynamic[1]" or time-varying systems. Ecological and biogeochemical models that are capable of simulating the time-varying properties of an ecosystem are often employed to interpret an observational record of changes over time in system properties and to predict likely future values of ecosystem properties in response to anticipated future changes in external influences or internal processes. Dynamic models can provide time-series representations of the trajectories and the ***lag-time*** of ecosystem properties responding to temporal variation in driving factors. Such models provide detailed representations of how ecosystem properties have evolved to present conditions and the rate at which they are likely to change in response to estimated changes in driving factors.

Given the inherent time-varying nature of properties in natural systems, why did this project use a steady-state modeling framework to assess critical loads and exceedance? While dynamic models provide representations the temporal variation of natural system properties, they are very data intensive. Most dynamic ecosystem/biogeochemical models suitable for critical loads analysis require time series of observations for one or more parameters in order to calibrate the value of other parameters in the model that are not easily directly measured (ICP Mapping Manual 2004). This approach works very well when evaluating critical loads and exccedance for specific locations or watersheds that have been extensively studied and for which time series observations of the required parameters are available. This approach works less well where no observations are available. A primary objective of the current study was to provide ***estimates*** of critical loads and exceedance for all forested and aquatic ecosystems, not just those systems for which extensive observations were available. The form of steady-state models permits simplifications of the descriptions of ecosystem processes such that fewer data are required, and the required data are more amenable to estimation.

The representations of ecosystem properties in steady-state models are the values of a property for a system in equilbrium with the specified values of external and internal parameters. Frequently, steady-state models are also used to provide information on the long-term-average rate of change of ecosystem properties as a system shifts from one steady-

[1] Active and changing

state (equilibrium with one set of external and internal parameters) to a different steady-state (equilibrium with a different set of external and internal parameters). Long-term average rates of change provide only a general sense of the rate of change, as the representation of ecosystem processes are too simplified in a steady-state model to provide information on non-linear variation with respect to time. Except for the unusual case where a natural system is in equilibrium with the specified external and internal parameters, ***the ecosystem properties estimated with steady-state models represent "potential" conditions at some future time rather than current conditions.*** Thus, it is frequently the case that ecosystem properties (e.g. pH) predicted by a steady-state model on the basis of observed driving parameters (e.g. climate, atmospheric deposition) do not match temporally coincident observations of ecosystem properties. [2]This does not represent a failure of the model, because the model is not designed to predict the time-varying, non-equilibrium ecosystem condition reflected in the observed properties. Rather, when the equilibrium value of an ecosystem property indicated by a steady-state model differs from the observed value of an ecosystem property, this indicates that the ecosystem is not in equilibrium with the observed driving external and internal parameters. In such a case the difference between the steady-state estimate of the property and the observed value of the property provides an indication of the direction and long-term average rate of change of the property, should the driving parameters remain constant long enough for the system to equilibrate.

For example, if the steady-state aquatic critical load associated with a target surface water pH of 6.6 is ***not*** exceeded by the observed rate of atmospheric deposition this does not mean that the observed surface water pH will be 6.6 or greater. ***It means that the surface water pH should be expected to change from the observed value toward a value of 6.6 or greater as the system moves toward equilibrium with the new conditions. Time-lags due to repopulation of the soil-exchange complex with base cations or release of stored S and N may delay observed changes in surface water pH.*** To estimate the rate of change in surface water pH or the time at which the target surface water pH will be reached requires dynamic modeling of ecosystem processes. As discussed above, dynamic modeling is, at present, only possible for a relatively small number of sites with suitable observations.

The New England States and New York have experienced significant large-scale disturbances in recent centuries, which make it unlikely that many terrestrial and aquatic ecosystems are in equilibrium with external and internal driving factors. The implications of the known disturbances need to be considered when interpreting the results of the steady-state critical loads analysis from this study. Much of the region was subject to extensive deforestation during the 1700s and 1800s, exporting significant amounts of base cations from ecosystems. Regrowth of forests during the 1900s shifted base cations from the soil exchangeable pool to growing vegetation. Significant forest harvesting and associated nutrient export continues in some parts of the region at present. Industrialization, urbanization, and associated increases in sulfur and nitrogen atmospheric deposition

---

[2] Therefore, the end-user should not harbor the expectation that a map of steady-state critical load exceedance should have a 1:1 correspondence with current or historic observations of ecosystem condtions (e.g. pH, ANC). The map conveys information about a ***potential future condition*** of the ecosystem ***if it were to reach steady-state*** with respect to the inputs and conditions of the modeled scenario.

increased base cation losses from soil exchangeable pools during the last century. Since the mid 1970s sulfur deposition has declined in the region. Thus, ecosystems in the region are transitioning from a state of generally greater base cation exports on an annual basis (1800 through 1970s) to lesser base cation exports on an annual basis (1970s to present).

In the recent past, base cation exports may have been greater than the capacity of many ecosystems to replenish available base cations through mineral weathering. As a result, available pools of base cations declined in forest soils and pH declined in many surface waters. The period of base cation depletion persisted for an extended period of time, significantly reducing soil nutrient levels and aquatic pH. At present (and under the somewhat lower sulfur deposition rates anticipated in 2018) many areas of the landscape are projected to experience much lower rates of nutrient exports due to harvesting and acid-deposition induced leaching than in previous decades. In many locations, the nutrient loss rates appear to be less than the rate of replenishment due to mineral weathering. Therefore, soil-available base cation pools are likely increasing from minimum values. However, due to the large prior draw-down of exchangeable base cation pools and small to modest projected net annual increases in these pools, soil base saturation and aquatic pH may be slow to recover.

When steady-state analysis indicates that current or projected future rates of atmospheric deposition of sulfur and nitrogen do not exceed the critical load at a location where prior rates of atmospheric deposition did exceed the critical load, this condition indicates the system is likely beginning recovery of soil base cation reserves and/or aquatic pH. Numerically this condition is represented by a negative value of "exceedance" (ICP Mapping Manual 2004). Generally, the more negative the exceedance, the more rapid the rate of recovery. The specific trajectory of recovery will depend on factors that are not considered in steady-state models but which are considered in dynamic models such as the size of the exchangeable pool of base cations and the base saturation. However, given the significant degree of base cation depletion that has occurred in many areas due to prior conditions, the recovery of soil base saturation and aquatic pH may take decades or longer. Figures 1.1-1.3 which are hypothetical, generalized time series of key system parameters illustrate these concepts.

Figures 1.1 to 1.3 below provide hypothetical, generalized examples of the complex relationships discussed above between time-varying ecosystem properties such as soil base saturation and surface water pH, the rate of sulfur + nitrogen deposition, and the steady-state critical loads for forest and aquatic ecosystems that would be calculated under different sets of assumptions that an observer/analyst would make during different time periods in three different hypothetical non-equilibrium systems. These figures do not represent a dynamic simulation of any specific location in the region. These figures are constructed hypothetical examples designed to help the end-user of the steady-state critical loads analysis understand how steady-state critical load modeling results calculated using different assumptions relate to commonly measured parameters such as soil base saturation and surface water pH in a non-steady state system. The examples should help an end-user interpret the steady state regional assessment results in the context of non-equilibrium soil base saturation and surface water pH conditions observable on the landscape today.

The steady-steady state critical loads analysis in this study was designed to provide an objective approach for identifying ecosystems where recovery is possible and where recovery is unlikely under present and future atmospheric deposition scenarios. This study identified areas where additional data should be collected in order to apply dynamic models to estimate the likelihood of and the expected recovery trajectory toward a specific target soil base saturation or a surface water pH. The study was not designed to be a final assessment of risk to terrestrial and aquatic ecosystems, but rather as an initial step toward objectively identifying areas that may be in early stages of recovery or that likely will continue to degrade under the anticipated 2018 deposition. Resource managers can use the results of this study to identify areas where the detailed field studies required before dynamic modeling would be most cost-effective for estimating the temporal response of ecosystems to future changes in atmospheric deposition.

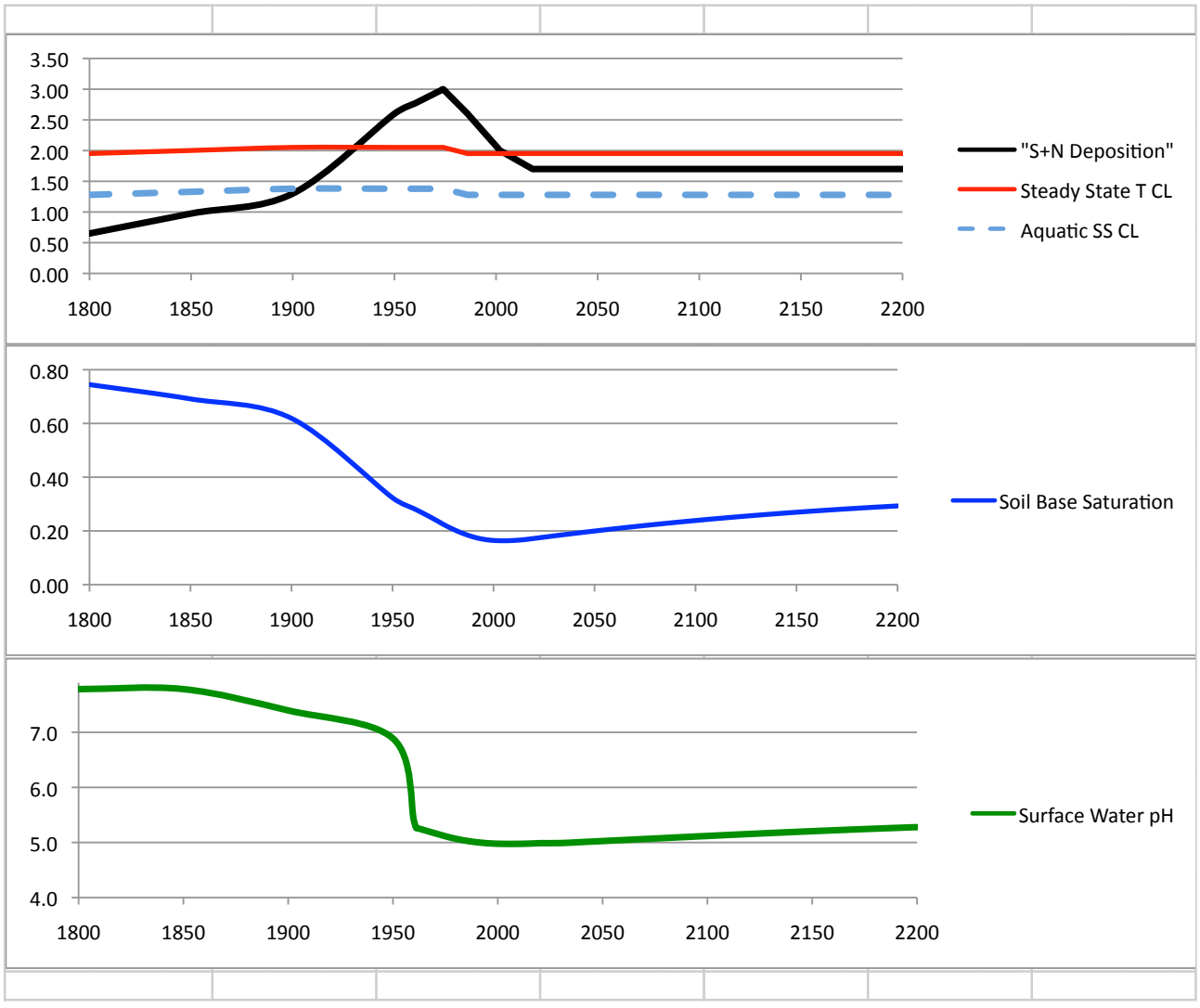

Figure 1.1. A hypothetical, generalized example of the relationship between steady-state critical loads calculated under assumptions representative of different time periods, atmospheric deposition rate and transient ecosystem conditions. The example time-series are intended to aid in understanding steady-state critical load concepts and interpretation. In this first example there is no deforestation with settlement and there is no "deep weathering" contributing to buffering of surface water. A hypothetical representative time

Figure 1.1 caption continued ...

course of the external driving factor atmospheric sulfur plus nitrogen (S+N) deposition in the Northeastern US in comparison to the steady-state terrestrial and critical loads calculated for an ecosystem using assumptions representative of different time periods is shown in the top panel. Atmospheric deposition of S+N increased substantially from presumed background levels through 1974 after which it declines significantly through 2018, but not to pre-industrial levels. The example assumes deposition remains constant indefinitely after 2018. In this example, no settlement deforestation or current harvesting is assumed and the steady-state critical load for S+N deposition that would be calculated by and observer during different time periods differs very little due to the as atmospheric base cation deposition declined after 1974. For a steady-state analysis conducted at any given time period, deposition exceeds the steady-state aquatic critical load from about 1900 through the remainder of the example time period. For a steady-state analysis conducted at any given time period, deposition exceeds the terrestrial critical load from about 1930 through 2000. The middle panel shows an example time course of soil base saturation in response to changing atmospheric deposition rates. Soil base saturation declines significantly in response to the elevated flux of anions through the ecosystem associated with the onset of increased S+N deposition. As deposition falls below the estimated critical load after 2000, soil base saturation begins to recover. Because deposition remains only slightly below the critical load, recovery is protracted and base saturation remains far below pre-industrial conditions 200 years after recovery begins. Surface water pH declines slightly as anion levels in the system (due to S+N deposition) rise, but soil base saturation remains relatively high (bottom panel). In the example system, as base saturation falls significantly, surface water pH declines substantially to well below the critical load target level (6.6). Because deposition remains above the steady-state aquatic critical load, pH will not recover to 6.6, but does increase slightly from its minimum value in response to reduced sulfur deposition.

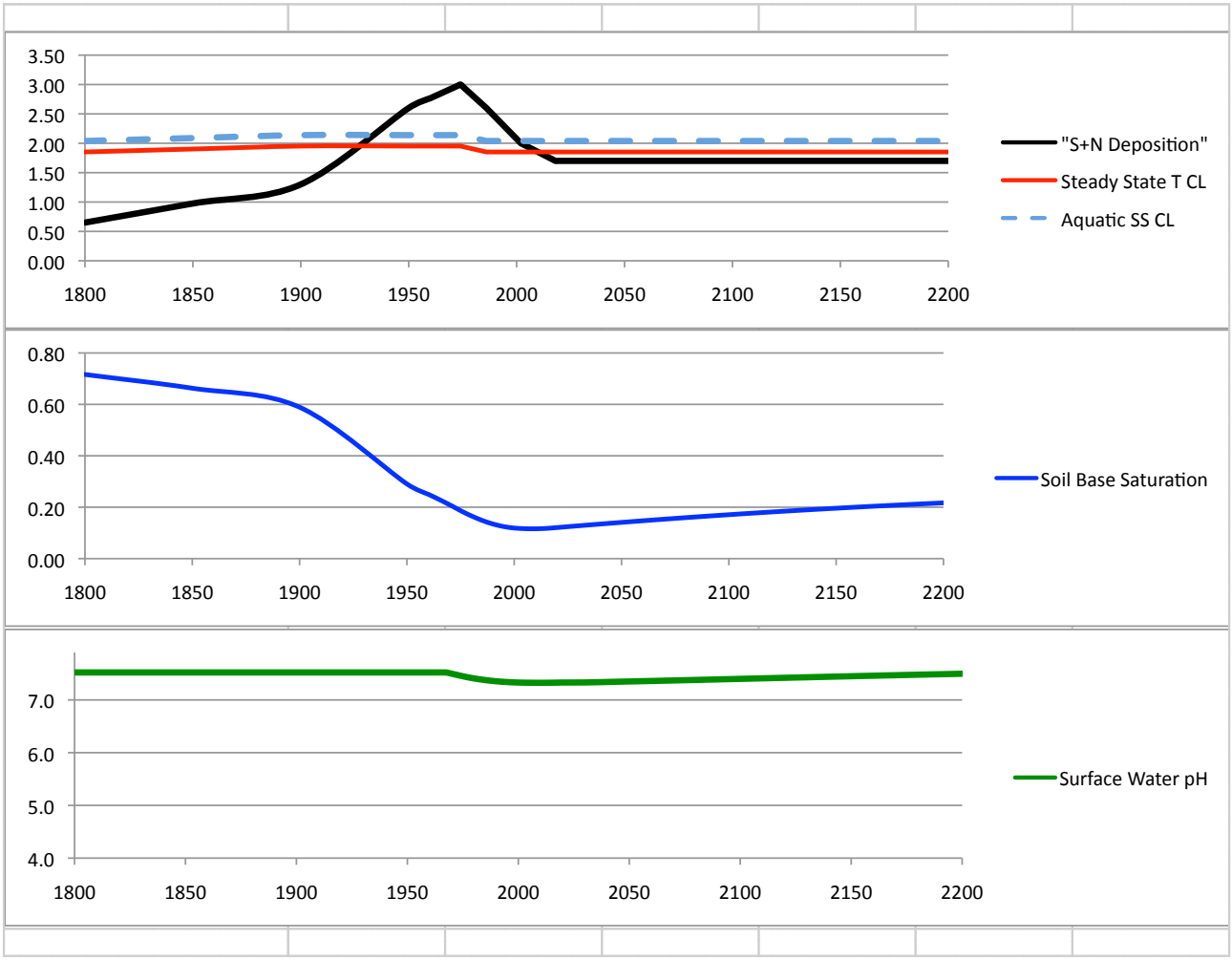

Figure 1.2. A hypothetical, generalized example of the relationship between steady-state critical loads calculated under assumptions representative of different time periods, atmospheric deposition rate and transient ecosystem conditions. In this example (and similar to Figure 1) there is no deforestation with settlement included. However, in this example there is a "deep weathering" (below the soil rooting zone) contribution of mineral weathering in deep till materials or bedrock along hydrologic flow paths included in addition to the root zone soil mineral weathering. The example illustrates how additional weathering (relative to the thin-soil example in Figure 1) raises the calculated steady-state aquatic critical load above the steady-state terrestrial critical load (top panel) at any given time period. In this hypothetical example, because the deep weathering contribution provides additional buffering, surface water pH remains relatively stable and above the target pH of 6.6 used to establish the aquatic steady-state critical load (bottom panel).

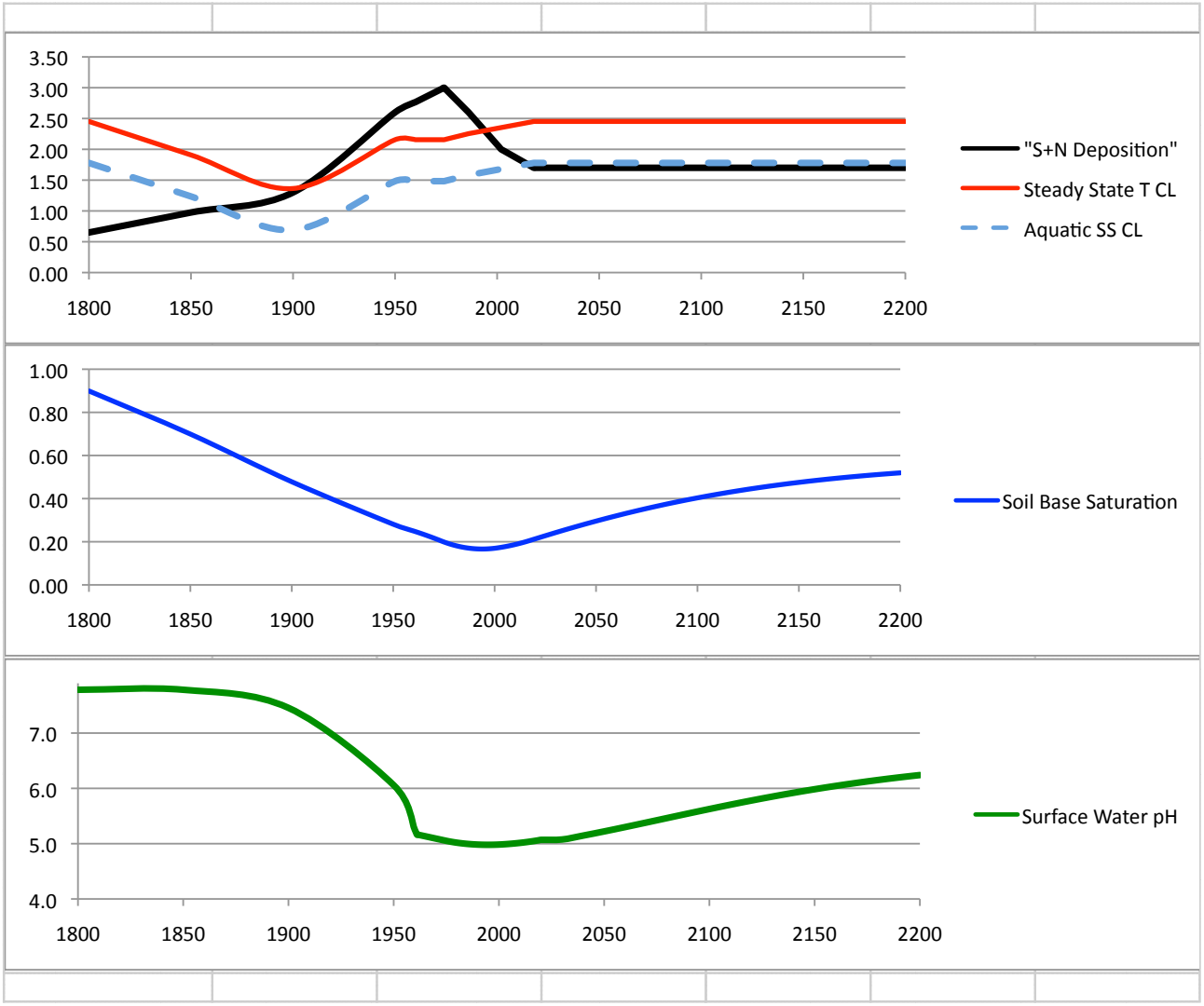

Figure 1.3. A hypothetical, generalized example of the relationship between steady-state critical loads calculated under assumptions representative of different time periods, atmospheric deposition rate and transient ecosystem conditions. This hypothetical example uses the same deposition assumptions as Figures 1-2 and the same panel arrangement. Soil root zone weathering rates in this example are higher than in the example shown in Figure 1. In this example significant forest harvesting (similar to present rates in Maine) is maintained for an extended period from 1800 through 1900. After 1900 harvesting rates are simulated to fall gradually to rates similar to the present NY state average and stabilize at that level through 2200. This example illustrates how different assumptions about base cation removal due to harvesting significantly affect both the terrestrial and aquatic steady-state critical load calculations. The difference in steady-state critical loads calculated with respect to different harvesting rates representative of different time periods is shown in the top panel. In the example, as increases in S+N deposition follow the period of high harvesting rates (much like the history of Northeastern forests), both harvesting and acid deposition act to remove base cations from the soil exchangeable pool (middle panel). As in the example scenario shown in Figure 1, surface water pH (bottom panel) declines as the soil base saturation declines, falling below the target level (6.6) in the mid 1900s. Soil base saturation begins to recover after deposition falls below the terrestrial critical load that would be calculated using the assumed harvesting rate in the example for the late 1990s. In this example, soil base saturation does not recover to pre-settlement levels by 2200. Once the deposition falls below the aquatic steady-state critical load calculated to be representative of 2018 conditions, surface water pH begins to recover. Due to the higher weathering rates used in this example relative to those used in Figure 1, a modest recovery of soil base saturation occurs and surface water pH nearly reaches the pH 6.6 target by 2200.

Overview of Technical Report

The technical report of assessment tasks is divided into multiple sections for ease of use. Each document describes a component task of the assessment. The major tasks are outlined below with reference to the detailed documentation associated with each task.

Section 1 – Assessment Domain
Definition of assessment domain, spatial resolution of data layers, data formats, and geographic reference system used in modeling

Section 2 – Atmospheric Deposition
Atmospheric Deposition Scenarios

- Estimation of "current" sulfur, nitrogen and base cation deposition
- Estimation of 2018 sulfur and nitrogen deposition

Section 3 – NY Terrestrial Critical Loads
Estimation of forest ecosystem critical loads and exceedance in New York State

- Development of the forested ecosystem critical threshold
- Steady-state mass balance model
- Estimation of forest nutrient demand
- Soil mineral weathering
- Forest ecosystem critical loads

Section 4 – Aquatic Critical Loads

- Development of aquatic ecosystem critical threshold scenarios
- Steady-state aquatic critical load modeling using the SSWC method
- Steady-state aquatic critical load modeling using the first-order-acidity-balance

Section 5 – Integration
Integration of forested and aquatic ecosystem critical loads and exceedance maps

Section 6 – Uncertainty in Critical Load and Exceedance Estimates

References – Introduction

Dupont, J., T.A. Clair, C. Gagnon, D.S. Jeffries, J.S. Kahl, S J. Nelson, and J.M. Peckenham. 2005. Estimation of critical loads of acidity for lakes in northeastern United States and eastern Canada. *Environmental Monitoring and Assessment*. 109:275-291.

CASAC 2011. http://yosemite.epa.gov/sab/sabproduct.nsf/264cb1227d55e02c85257402007446a4/0FC13C821EE6181A85257473005AE1EC/$File/NOxSOx+PA+2nd+Ext+Rev+Draft+9-15-2010.pdf

ICP Mapping Manual (2004) International Cooperative Programme on Modelling and Mapping of Critical Loads and Levels and Air Pollution Effects, Risks and Trends, UNECE Convention on Long-range Transboundary Air Pollution. *Manual on Methodologies and criteria for Modelling and Mapping of Critical Loads and Levels and Air Pollution Effects, Risks and Trends.* (http://icpmapping.org/cms/zeigeBereich/5/manual-und-downloads.html)

Miller, E.K. (2006) Assessment of Forest Sensitivity to Nitrogen and Sulfur Deposition in Maine. Technical report submitted to Maine Dept. of Environmental Protection, Bureau of Air Quality, Statehouse Station #17, Augusta, Maine 04333. Ecosystems Research Group, Ltd., Norwich, VT.

NEG/ECP Forest Mapping Group. 2001. Protocol for assessment and mapping of forest sensitivity to atmospheric S and N deposition. The Conference of the New England Governors and Eastern Canadian Premiers. 76 Summer St. Boston, MA 02110. 79 pp.

Ouimet, R., P. Arp, S. Watmough, J. Aherne, and I. DeMercant. 2006. Determination and mapping critical loads of acidity and exceedances for upland forest soils in Eastern Canada. *Water, Air, and Soil Pollution* 172: 57-66.

Ye, X., J. Hao, L. Duan, and Z. Zhou. 2002. Acidification sensitivity and critical loads of acid deposition for surface waters in China. Science of the Total Environment. 289:189-203.

Section 1 – Analysis Domain, Spatial Resolutions, Geographic Reference System, and Data Storage Format

This section describes the analysis domain, spatial resolutions, geographic reference system, and data storage format for the NPS / Multi Agency Critical Loads Project: Steady-State Critical Loads and Exceedance for Terrestrial and Aquatic Ecosystems in the Northeastern United States.

Analysis Domain, Spatial Resolutions, and Geographic Reference System

This project makes use of previously generated estimates of forested ecosystem critical loads for sulfur and nitrogen deposition for the New England States (see NEG/ECP 2001, Miller 2006, Schaberg et al. 2007) and extends the domain to include New York State. This project adopted the spatial resolutions and modeling geographic reference system employed in the previous study. Miller (2006) employed data and modeling at mixed resolutions appropriate to the data source and tier in the modeling stack. Specific grid resolution documentation is included with each file. The highest resolution data layers were developed at 30-meter grid cell resolution. The grid cells correspond to USGS National Land Cover Data (NLCD) resolution. For some data layers (notably soil parameters and mineralogy) the resolution is 90-meter grid cells. Where 90-meter and 30-meter resolution data were used together in modeling the 90-meter data were bilinearly interpolated to 30-meter resolution using the IDRSI™(www.clarklabs.org) PROJECT module.

Due to the very large amount of data associated with the 30-meter resolution modeling, the full modeling domain (NY, VT, NH, ME, MA, CT, RI) was divided into 2 sub-domains (NY and New England). The file names for the New England domain are prefixed with the abbreviation “neweng” in the accompanying data files. The file names for the New York domain are prefixed with the abbreviation “ny” in the accompanying data files. Data files at 30-meter resolution for each domain are on the order of 1.7 GB.

Geographic Reference System

All geographic data are supplied in the EPA standard Albers Equal Area Projection for North America (defined below). Unless otherwise specified in the documentation all modeling was conducted on this grid.

```
ref. system : Alber's Equal Area Conic for EPA
projection  : Alber's Equal Area Conic
datum       : NAD83
delta WGS84 : 0 0 0
ellipsoid   : GRS80
major s-ax  : 6378137
minor s-ax  : 6356752.314
origin long : -96.0
origin lat  : 23.0
origin X    : 0
origin Y    : 0
scale fac   : na
units       : m
parameters  : 2
stand ln 1  : 29.5
stand ln 2  : 45.5
```

Native GIS Format of Project Data

Analysis and modeling was conducted using a combination of tools including IDRISI™ (www.clarklabs.org) geographic information system software and task-specific custom software. For ease of data manipulation, processing, and display, the IDRISI™ raster format was used for preparing and storing data. The geographic data developed for this project are were archived and transmitted to the primary sponsoring agency in IDRISI™ raster format (file suffix ".rst").

IDRISI™ raster format is a flat binary floating-point file that can be imported into all major GIS or image processing software using flat binary tools such as BSQ (band-sequential format) import. An ASCII text raster documentation file (file suffix ".rdc") accompanies each data file and contains the necessary file structure and georeferencing information. An annotated example documentation file is provided on the following page.

Example IDRISI™ raster grid documentation file.

```
file format : IDRISI Raster A.1
file title  : HRDM Annual Total (wet+dry) S Deposition (kg/ha/y)
data type   : real
file type   : binary
columns     : 23769
rows        : 18127
ref. system : alberepa
ref. units  : m
unit dist.  : 1.0000000
min. X      : 1297410.0000000
max. X      : 2010480.0000000
min. Y      : 2122980.0000000
max. Y      : 2666790.0000000
pos'n error : unknown
resolution  : 30.000000
min. value  : 0.0000000
max. value  : 19.7469902
display min : 0.0000000
display max : 19.7469902
value units : kg/ha/y
value error : unknown
flag value  : none
flag def'n  : none
legend cats : 0
lineage     : This file was created by Ecosystems Research Group, Ltd.
```

References – Section 1

Miller, E.K. 2006. Assessment of Forest Sensitivity to Nitrogen and Sulfur Deposition in Maine. Technical report prepared on behalf of the Conference of New England Governors' and Eastern Canadian Premiers' Forest Mapping Group, 15 December 2006, for the Maine Department of Environmental Protection, Bureau of Air Quality, Statehouse Station #17, Augusta, ME 04333.

NEG/ECP Forest Mapping Group. 2001. Protocol for assessment and mapping of forest sensitivity to atmospheric S and N deposition. The Conference of the New England Governors and Eastern Canadian Premiers. 76 Summer St. Boston, MA 02110. 79 pp.

Schaberg, P.G., Miller, E.K., Eagar, C. Assessing the Threat that Anthropogenic Calcium Depletion Poses to Forest Health and Productivity. 2007. USDA Forest Service General Technical Report PNW-GTR-806 (a peer-reviewed, combined publication of the Southern and Pacific Northwest Research Stations) and a chapter on the web-based forestry encyclopedia: www.threats.forestencyclopedia.net

Section 2 – Atmospheric Deposition Estimates circa 2000 and 2018 for the Northeastern United States

The project developed high-resolution atmospheric deposition estimates for NY and New England. The Northeast States for Coordinated Air Use Management (NESCAUM), a regional air quality planning organization, estimated the change in sulfur and nitrogen deposition expected to occur in the Northeast between 2002 and 2018 in response to planned and enacted air pollution control programs in the eastern US (NESCAUM 2008a; NESCAUM 2008b). Sulfur deposition is expected to decrease by an average of 36% and nitrogen deposition is expected to decrease by an average of 24% across the region. However, some locations within the region are estimated to experience increases over 2002 levels. This study was undertaken to estimate the location and extent of the forest and aquatic resources likely to remain at risk to projected 2018 levels of sulfur and nitrogen deposition. The percentage of forest and aquatic resources that might begin to recover from the effects of historically higher sulfur deposition levels as deposition drops to the levels projected for 2018 were also estimated.

The original design of the project was to use air and precipitation concentration data from CMAQ model runs conducted by NESCAUM to define the air and precipitation concentration fields for 30-meter resolution runs of a high spatial resolution deposition model (HRDM, Miller et al. 2005, Miller 2000) for seasonal average conditions. The high-resolution deposition runs were to be conducted with 30-year normal climate parameters to provide an appropriate representation of long-term climatic conditions for steady-state critical loads modeling.

Upon receipt of CMAQ data from NESCAUM, ERG conducted an analysis comparing the CMAQ-generated estimates with NADP and CASTNET data and with prior modeling based on 30-year normal climate and interpolated air and precipitation concentration fields derived from NADP and CASTNET data. This analysis included consultation with John Graham (formerly) at NESCAUM and Robbin Dennis at EPA. We compared the NESCAUM CMAQ runs with more recent CMAQ runs and corrections prepared by EPA. This comparative analysis is described in the accompanying document (Appendix-NPSCL-TD2a-CMAQ-Comparative-Analysis.pdf) "Comparative analysis of MANE-VU 2002 Simulation with EPA NERL CMAQ 2002 Simulation Internal Documentation for Multi-Agency Eastern Critical Loads Project Deposition Estimates – 5/29/2009".

Briefly, CMAQ (both NESCAUM and EPA runs) was found to under predict S and N in the Northeastern US relative to NADP and CASTNET data and prior HRDM runs based on NADP and CASTNET observations with 30-year normal climate. CMAQ performance and EPA's correction routines have been optimized for both the national model domain and a much larger eastern domain that includes the Mid-Atlantic States. While CMAQ performance is reasonable when summarized over the full model domain or the eastern domain, there are areas of better and poorer model performance. CASAC (2011, page 3 and table 7-1) also noted that while the S mass-balance is handled reasonably well "overall" (meaning nationally) there are "difficulties in spatial pairing of observations and modeled results of wet deposition" and "this spatial pairing has improved with the more recent PRISM adjustments**."** CASAC (2011) provides a similar statement for NO_3 and NH_4, however, these species' mismatch with

observations is much greater than for SO_4. The difficulties in "spatial pairing" (i.e. accuracy of the estimates at any given observation point) were evaluated (with the PRISM adjustments included) for the Northeastern States as part of this project. The northeastern US is an area where the level of disagreement between model output and observations is large enough to be significant when calculating critical load exceedances (Appendix-NPSCL-TD2a-CMAQ-Comparative-Analysis.pdf). The apparent model bias in the northeastern US, ***while not large in the context of deposition variance across the nation***, is of the same order of magnitude as the anticipated changes in Northeastern US deposition resulting from the combined effects of CAIR, Federal Fuel and Motor Vehicle Programs and SIPs.

A conference call with stakeholders and project participants was organized to review this issue, and to develop an alternative approach for generating deposition estimates. To provide estimates of near current (circa 2000) and 2018 deposition for use with steady-state critical loads modeling it was decided to modify the approach used previously by ERG for the NEG/ECP critical loads project (NEG/ECP 2001, Miller 2006). For the circa 2000 deposition estimates atmospheric depositions of sulfur (S), nitrogen (N), chloride (Cl), calcium (Ca), magnesium (Mg), sodium (Na), and potassium (K) were estimated using the best available observational data for each state. The 5-year average (1999-2003) was used in order to provide some smoothing of year-to-year variations in climate and patterns of atmospheric transport. The period 1999-2003 was selected based on data availability and the timing of funding for atmospheric deposition modeling. Total deposition, including precipitation, cloud droplet interception, and dry deposition, was estimated for all jurisdictions. Total deposition to the region was modeled at a 30-m ground resolution using atmospheric chemistry data from the NADP and CASTNet, deposition monitoring networks using Ecosystems Research Group, Ltd.'s High-Resolution Deposition Model (Miller et al. 2005, NEG/ECP Forest Mapping Group, 2001, Miller, 2000). Deposition monitoring sites are sparsely distributed in the region and factors affecting deposition rates are highly variable, particularly in mountainous regions (see Miller et al., 1993), thus the deposition estimates carry considerable unquantifiable uncertainty.

For circa 2018 estimates, the ratio of the MANE-VU CMAQ (NESCAUM 2006) estimated deposition for 2018/2002 was computed and multiplied by the 1999-2003 HRDM simulation results. This approach produced 2018 S and N deposition estimates with a basis and magnitude tied to NADP and CASTNet observations, but with the MANE-VU CMAQ simulation inference of the spatial distribution of proportional change in deposition between circa 2000 and circa 2018 resulting from the combined effects of CAIR, Federal Fuel and Motor Vehicle Programs and SIPs.

As originally planned, 1971-2000 normal climate fields generated from the NOAA network of observing stations (Miller et al. 2005) were used to drive the HRDM. Using climate normals rather than individual year climate is more appropriate for developing input layers for steady-state critical loads modeling. The steady state loads need to represent long-term average climatic conditions rather than conditions in a specific year. As there were no CMAQ 2018/2002 change data available for Ca, Mg, K, Na, and Cl, 2018 deposition was not estimated for these elements. In critical loads modeling the deposition of these elements is assumed to be the same in circa 2018 as in circa 2000.

High Resolution Deposition Model (HRDM)

The HRDM (Miller et al. 2005) was developed to provide estimates of atmospheric deposition to complex landscapes in support of ecosystem analysis and modeling. It is well understood that in the complex landscape of northeastern North America that atmospheric deposition can vary by a factor of 4 on small (< 2 km) spatial scales (Figure 2.1). It is also well established that ecosystem effects of atmospheric deposition vary on small spatial scales in response to deposition variance and other landscape factors (Schaberg et al. 2007). The HRDM was developed to provide atmospheric deposition estimates that include the influence landscape variance and receptor characteristics on < 1 km spatial scales.

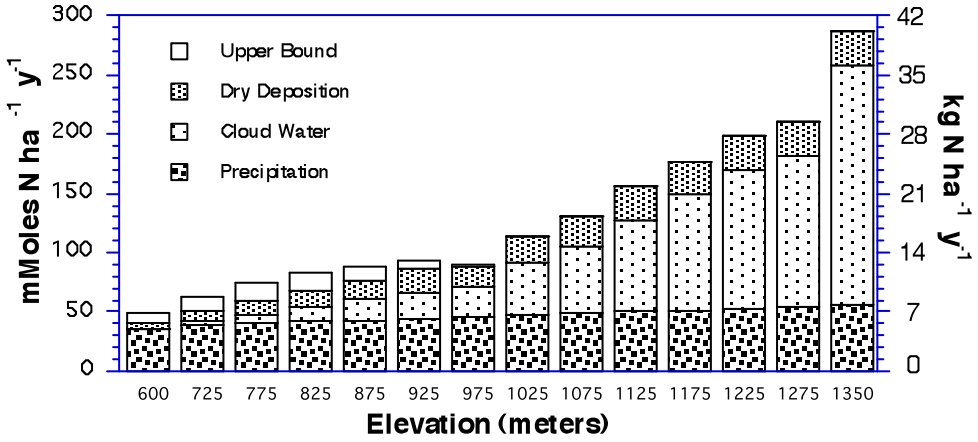

Figure 2.1. Variation in nitrogen deposition along a 750-meter elevational gradient and 1.6 km map distance in NY state (from Miller et al. 1993).

The HRDM is described in detail by Miller et al. (2005) as applied to estimating mercury deposition. In this project the HRDM was used to estimate, sulfur, nitrogen and base cation deposition. The differences between the application of the HRDM by Miller et al. (2005) and in this project are described below.

The HRDM makes use of both point and continuous data (Figure 2.2). Data on landscape properties necessary to describe the characteristics of the receptor surface and microclimatic conditions at the receptor surface were assimilated into a geographic information system at 30-meters ground resolution. The 30-meter resolution was selected to take advantage of the native resolution of USGS National Land Cover Data (NLCD) product. As described elsewhere (Miller et al. 2005) and in Section 3 of this document the NLCD was a key component of a method for estimation of the vegetation type present in a grid cell using the NLCD satellite derived information along with microclimate information (see Section 3 of this document).

Data on air and precipitation concentrations of different elements at the surface were collected at point locations by the national monitoring networks NADP and CASTNet (Figure 2.3). Continuous air and precipitation concentration fields were interpolated for the region following Miller et al. (2005) from the network observations. Meteorology and climate observations measured at point locations (CASTNet and NWS) were reduced to seasonal hourly averages representative of a diurnal cycle and interpolated to continuous fields following Miller et al. (2005). Temperature and precipitation fields were computed from 30-year climate normals in order to generate estimates representative of long-term average conditions rather than a particular year (see discussion of steady-state critical loads analysis requirements in the Introduction). These fields together with the landscape and receptor characteristics fields were used to drive inferential models of the cloud-water and dry deposition processes (see Miller et al. 2005, and Miller et al. 1993). Sulfur deposition was modeled individually for aqueous SO_4, particulate SO_4, and vapor-phase SO_2. Nitrogen deposition was modeled individually for aqueous NO_3 and NH_4, particulate NO_3 and NH_4, and vapor-phase HNO_3 (Miller et al. 1993). Aerosol dry deposition was modeled for the base cations Ca^{2+}, Mg^{2+}, K^+, and Na^+ with base cation air concentrations estimated by means of observed mass scavenging ratios from precipitation concentrations (Miller et al. 1993).

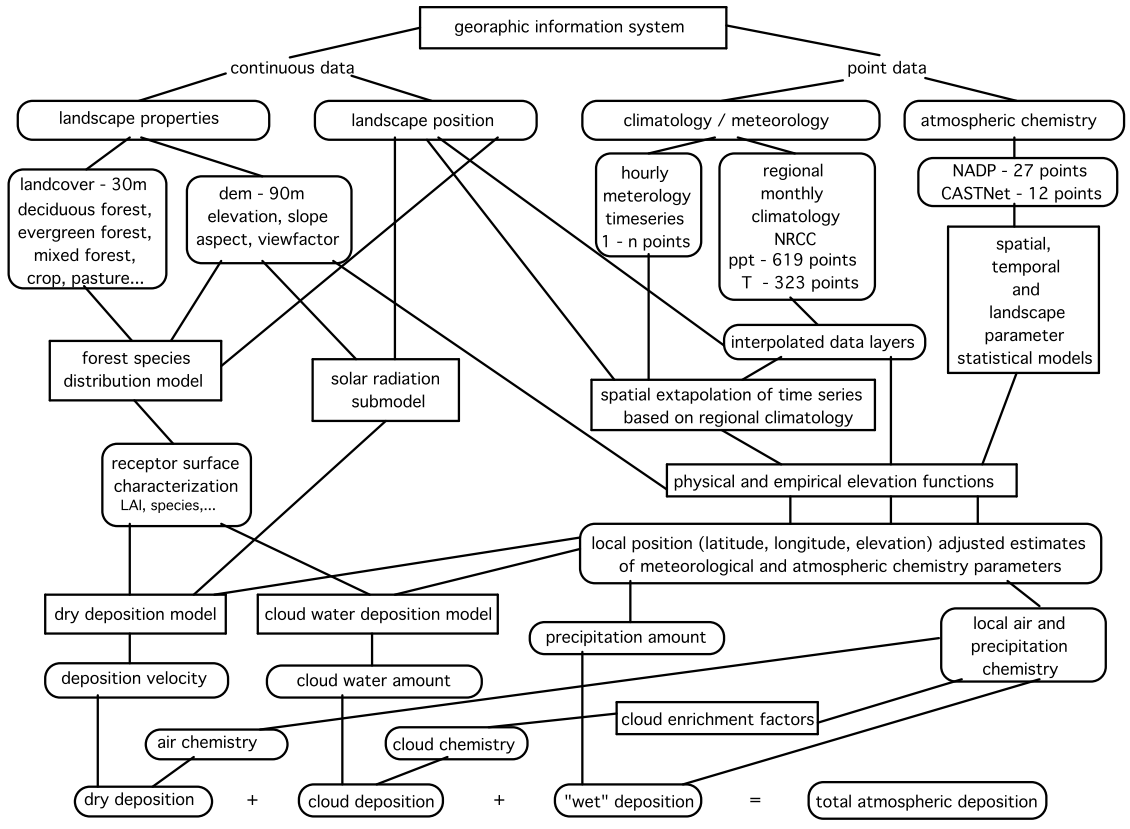

Figure 2.2. Schematic representation of the application of the HRDM (Miller et al. 2005) to estimation of sulfur, nitrogen, and base cation deposition.

The dry deposition and cloud water submodels were run for 6 representative model days representing the average diurnal meteorological cycles of winter, spring with leaves off, spring with leaves on, summer, fall with leaves on, and fall with leaves off. The average deposition rates for these model days were multiplied by the number of days associated with these meteorological conditions in order to scale estimates to a full year. Seasonal (winter, spring, summer, fall) precipitation deposition was calculated as the product of the estimated seasonal precipitation and estimated average seasonal precipitation concentration. The seasonal values were summed to scale estimates to a full year.

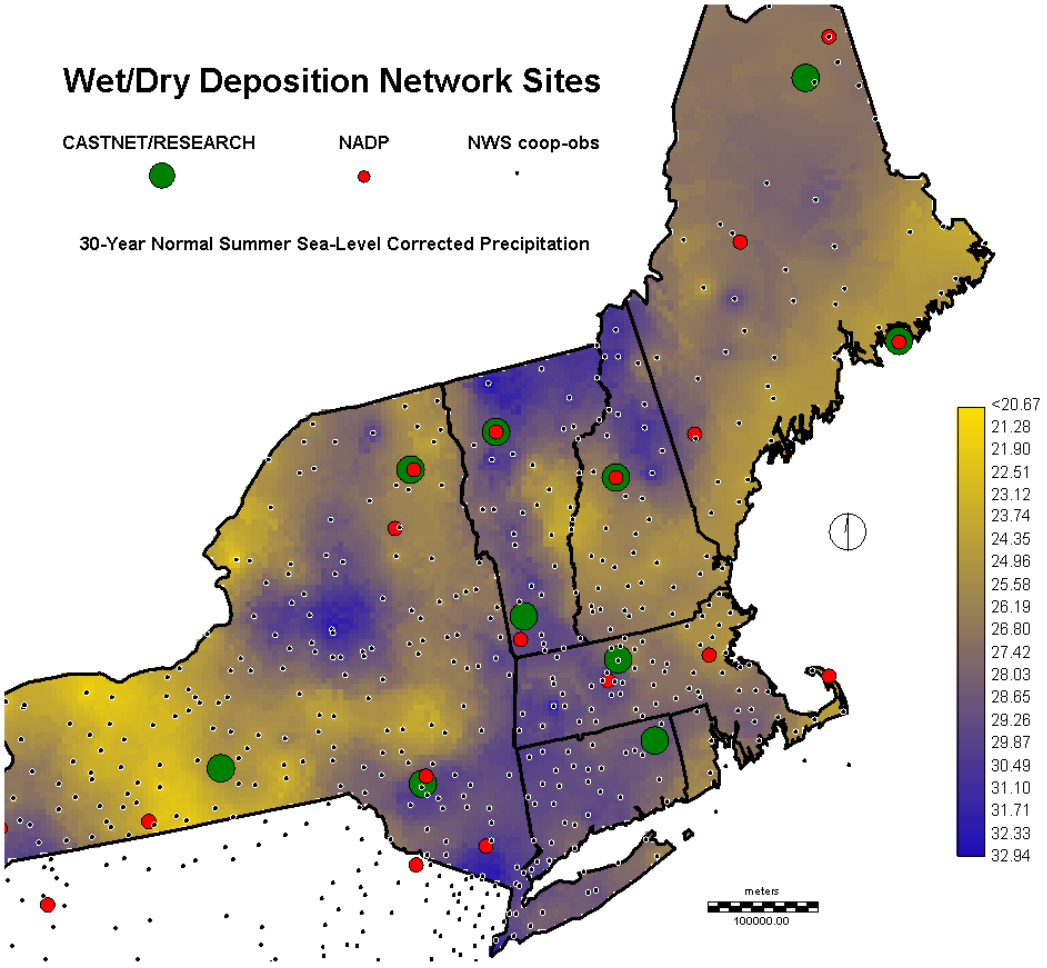

Figure 2.3. Locations NADP (red circles), CASTNET (green circles) and NWS (black dots) cooperative observer network precipitation stations used in preparing grids for the HRDM. One NADP/NOAA AirMon station in northern VT is also shown as a green circle. The continuous color scale shows the 30-year normal (1971-2000) summer season sea-level corrected (see Miller et al. 2005) precipitation (cm) field as an example of an interpolated input grid derived from point observations.

Deposition Scenario Output

Files for total nitrogen deposition, wet nitrogen deposition, and dry nitrogen deposition are distributed with units of kg N per ha per year (kg/ha/y). Files for total sulfur deposition, wet sulfur deposition, and dry sulfur deposition are provided with units of kg S per ha per year (kg/ha/y). The total steady-state acidifying potential of S + N is provided in terms of the charge-equivalent deposition rate in kiloequivalents (SO_4^{2-} + NO_3^-) per hectare per year (keq/ha/y) (Figure 2.4). This formulation assumes all forms of N will be converted to oxidized-N (NO_3^-) at steady state as the soil C/N ratio drops to a level conducive to nitrification. This assumption is implicit in the steady-state modeling framework (see NEG/ECP 2001). The conversion of N must be accounted for in the development of the loading term for steady-state modeling with form of model used in this project (NEG/ECP 2001). Files for all other elements (Ca, Mg, K, Na, Cl) are provided in terms of the charge-equivalent deposition rate in kiloequivalents (Ca^{2+}, Mg^{2+}, K^+, Na^+, Cl^-) per hectare per year (keq/ha/y).

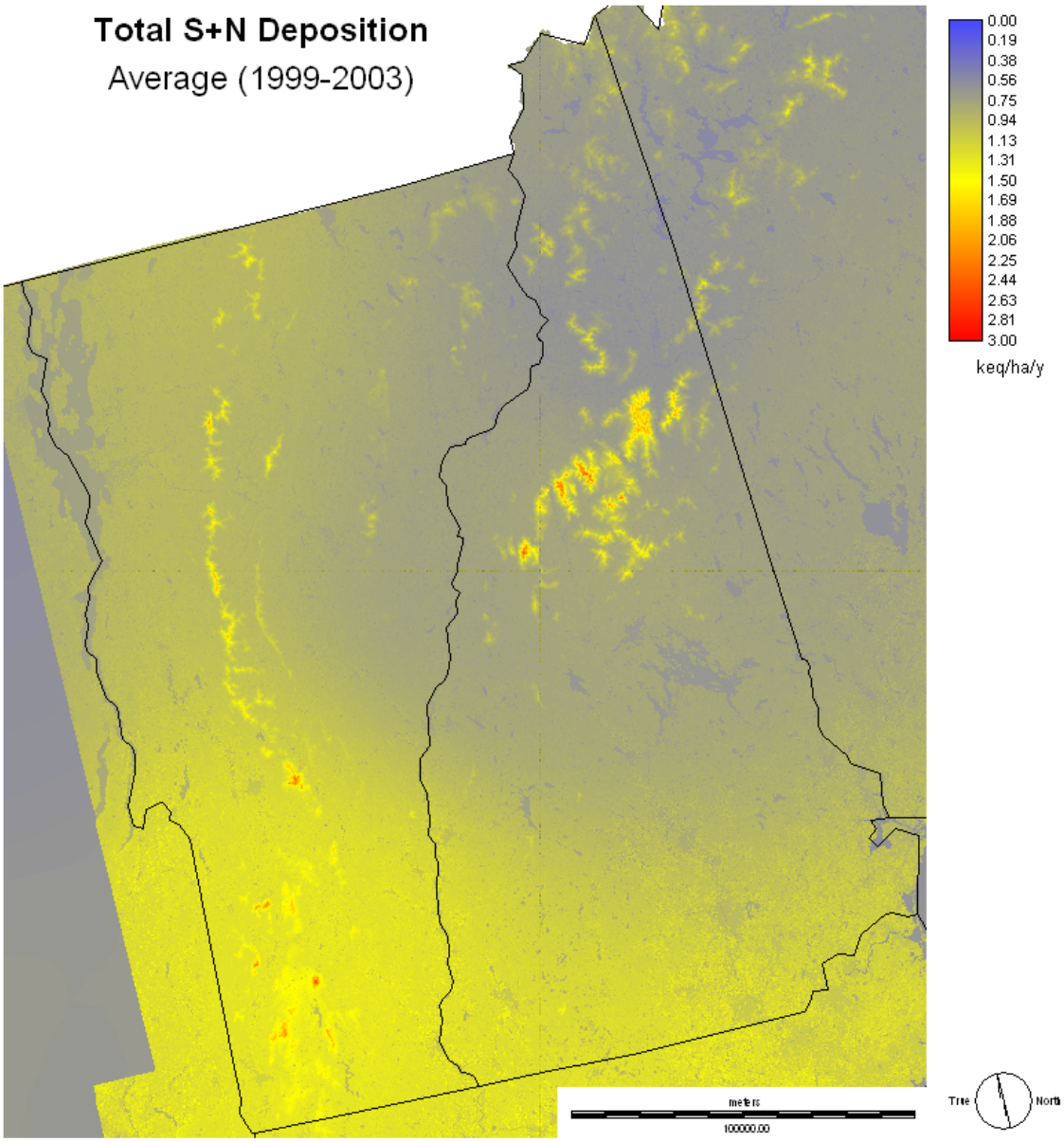

Figure 2.4. Example of HRDM output formatted as total steady-state acidifying potential of S + N (keq/ha/y) for VT and NH. Only VT and NH are shown in order to reveal some of the high-resolution information captured, such as elevated deposition in the Green Mountains of VT and White Mountains of New Hampshire. For steady-state critical loads modeling all deposited N is assumed to be converted to NO_3^- at steady state (see NEG/ECP (2001). A general southwest to northwest decline in deposition is indicated as well as higher deposition rates in the mountainous areas.

References – Section 2

Miller, E.K. 2000. Atmospheric Deposition to Complex Landscapes: HRDM – A Strategy for Coupling Deposition Models to a High-Resolution GIS. Proceedings of the National Atmospheric Deposition Program Technical Committee Meeting, October 17-20, 2000, Saratoga Springs, New York.

Miller, E.K., A.J. Friedland, E.A. Arons, V.A. Mohnen, J.J. Battles, J.A. Panek, J. Kadlecek and A.H. Johnson. 1993. Atmospheric Deposition to Forests Along an Elevational Gradient at Whiteface Mountain, NY USA. *Atmospheric Environment* 27A: 2121-2136.

Miller, E.K., A. VanArsdale, G.J. Keeler, A. Chalmers, L. Poissant, N. Kamman, and R. Brulotte. 2005. Estimation and Mapping of Wet and Dry Mercury Deposition Across Northeastern North America. *Ecotoxicology* 14: 53-70.

NEG/ECP Forest Mapping Group. 2001. Protocol for assessment and mapping of forest sensitivity to atmospheric S and N deposition. The Conference of the New England Governors and Eastern Canadian Premiers. 76 Summer St. Boston, MA 02110. 79 pp.

NESCAUM, 2006. Contributions to Regional Haze in the Northeast and Mid-Atlantic United States, Technical Report for the MANE-VU Regional Planning Organization, NESCAUM, Boston, MA, August, 2006 (See http://www.nescaum.org/documents/ contributions-to-regional-haze-in-the-northeast-and-mid-atlantic--united-states/).

Schaberg, P.G., Miller, E.K., Eagar, C. Assessing the Threat that Anthropogenic Calcium Depletion Poses to Forest Health and Productivity. 2007. USDA Forest Service General Technical Report PNW-GTR-806 (a peer-reviewed, combined publication of the Southern and Pacific Northwest Research Stations) and a chapter on the web-based forestry encyclopedia: www.threats.forestencyclopedia.net

Section 3 – Estimation of Forest Ecosystem Critical Loads and Exceedance (2002 and 2018) in New York State

This section describes the estimation of forest ecosystem critical loads and exceedance in New York State. Forest ecosystem critical loads analysis for New York followed the previously established methods used for the New England Governors' and Eastern Canadian Premiers' Forest Mapping Inititative (NEG/ECP 2001, Miller 2006, Ouimet et al. 2006). The methodology is reviewed here providing information specific to the data sources used in the New York assessment.

Development of the forest ecosystem critical threshold

Although sulfur emissions have decreased as a result of SO_2 control programs, projected emissions of both sulfur and nitrogen compounds are expected to have continuing negative impacts on forests, presenting long-term threats to forest health and productivity in northeastern North America. Anthropogenic sulfur and nitrogen deposition can cause excessive nutrient cation (calcium, magnesium, and potassium) leaching, reducing the supply of nutrient cations available for plant growth, a process called cation depletion (e.g. Watmough and Dillon 2003). Inadequate nutrient supplies frequently lead to increased susceptibility to climate, pest and pathogen stress, and result in reduced forest health, reduced growth, and eventual changes in forest species composition (Figure 3.1, see also Schaberg et al. 2001, Schaberg et al. 2007).

The approach used to estimate the critical load of sulfur and nitrogen deposition is an ecological assessment based on a steady-state, ecosystem mass balance for nutrient cations[3] (ICP mapping manual 2004, Ouimet et al. 2006) as implemented by the NEG/ECP (2001). The critical load of sulfur + nitrogen is the level of deposition below which, to the best of available knowledge, no harmful ecological effects occur in a forest ecosystem. Excess acidic deposition to forest ecosystems can adversely affect forest growth and productivity. Forest health consequences of elevated nitrogen and sulfur deposition have been documented in the literature and are variable depending on many site-related characteristics (e.g. Ouimet et al. 2001, Schaberg et al. 2001, Schaberg et al. 2006). In general, acidic deposition can cause soil and surface water acidification, increase soluble soil aluminum to toxic levels, and lead to a depletion of soil base cations, especially those required for plant growth and health (Ca, Mg and K).

The symptoms of plant nutrient deficits manifest themselves at the cellular level, but also become visible as primary indicators of tree health (Figure 3.1). Notable tree health problems include increased susceptibility to winter injury, increased crown dieback, and

[3] Base cations were evaluated individually to determine whether there was an insufficient supply of any individual base cation. If there was an inadequate supply of any one base cation, the ecosystem was considered sensitive to the current levels of S+N deposition. The critical load was, therefore, calculated based on the most limiting nutrient cation.

increased proliferation of insect or disease activities. All of these may reduce forest growth (Figure 3.2) and increase mortality. Over time, stand productivity may decrease, and the accumulation of health problems may lead to shifts in species composition and diversity (Schaberg et al. 2007). After extensive deliberation and international peer review, the NEG/ECP Forest Sensitivity Mapping Initiative adopted a forest ecosystem steady-state critical threshold corresponding to a condition of all nutrient base cation mass balances equal to zero (NEG/ECP 2001). If the steady-state Ca, Mg, or K mass-balance is negative, this indicates the ecosystem is on a path to reduced critical nutrient availability (state of nutrient depletion). If the steady-state mass balances for all nutrient cations are positive then the ecosystem has the capacity to maintain (and rebuild stocks) of critical nutrients. The magnitude of the steady state nutrient depletion or accretion rate provides information on severity of nutrient depletion or the buffering capacity of the system.

Previous studies have compared modeled critical load exceedances based on a critical threshold of exchangeable nutrient base cation depletion/non-depletion with many of independent indicators of forest health. For example, figure 3.2 shows the association between tree growth of hardwood and softwood stands in Québec, and the plot-specific deposition index[4]. Similar associations were obtained between the regional assessment derived deposition index and crown dieback and canopy transparency (Schaberg et al. 2007) and soil chemistry (pH, Ca/Al, percent base saturaton, Ca amount), canopy dieback, and tree growth (Miller 2006, Figure 3.3).

[4] Different studies have used different terminology to express the difference between the atmospheric deposition rate of a pollutant and the critical load of a pollutant. Deposition index was the terminology used by the NEG/ECP project to quantify the difference between atmospheric deposition and the critical load (critical load minus atmospheric deposition). A negative deposition index indicates that atmospheric deposition exceeds the critical load. The current project has adopted the European standard terminology of critical loads analysis (ICP Mapping Manual 2004). The "exceedance" of the critical load is defined as the atmospheric deposition rate minus the critical load. Thus, **"exceedance" and "deposition index" have the same absolute numeric value, but opposite signs**.

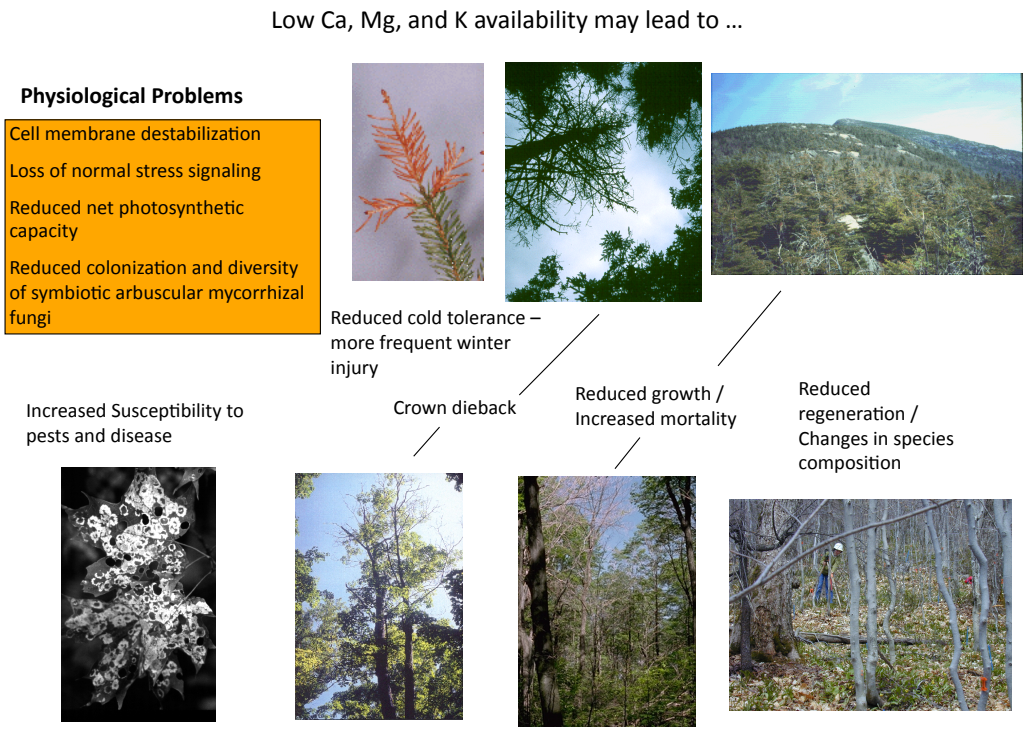

Figure 3.1. Cascade of physiological problems, plant symptoms, and ecosystem effects as the result of low Ca, Mg, or K availability (after the concepts of Schaberg et al. 2001 and Schaberg et al. 2007).

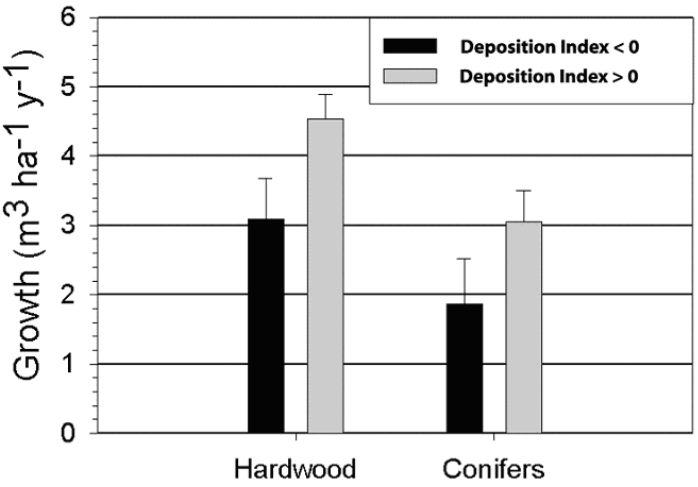

Figure 3.2. Growth rates of northern hardwood and boreal coniferous forest stands relative to the deposition index (see footnote 2, page 2 for definition). Forest growth was significantly lower over a 19-year period at hardwood and softwood stands in Québec where current deposition levels exceed the critical load (deposition index < 0) than at sites where deposition is less than the critical load (deposition index > 0). Data presented are means adjusted for plot initial volume and stand age. Error bars represent standard errors of the adjusted means (Ouimet et al., 2001).

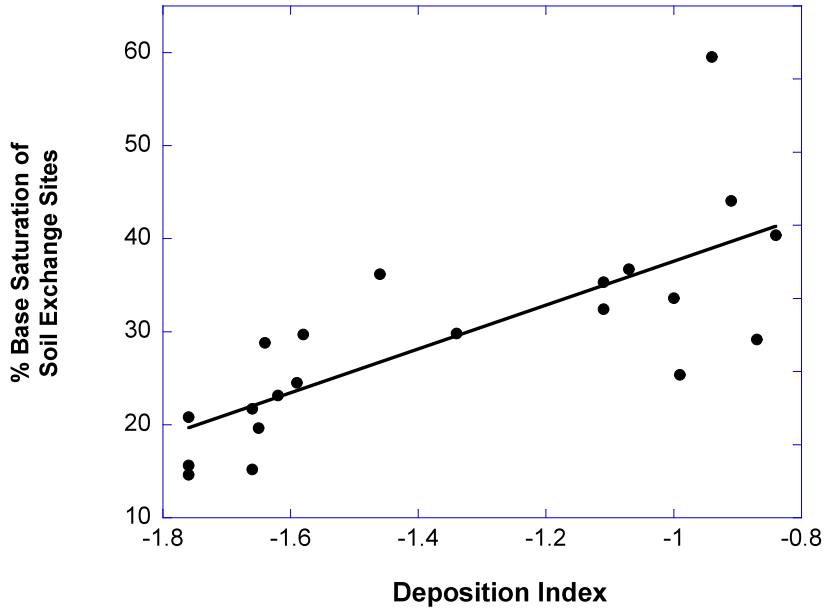

Figure 3.3. Comparison of soil measurements to modeled deposition index: Root-zone base cation availability expressed as base saturation (the percent of exchange sites populated by base cations) as a function of the modeled deposition index for soil pits in Massachusetts. Soil base saturation was correlated with the deposition index ($r^2 = 0.56$, $p < 0.0001$, $n = 21$ pits). From Miller (2006).

Steady-state nutrient mass balance model

To maintain consistency with the New England States analysis (NEG/ECP 2001, Miller 2006), the NY assessment employed the same steady-state nutrient mass balance modeling approach. The NEG/ECP steady-state model is described elsewhere (NEG/ECP 2001, Ouimet et al. 2006). This analysis follows the approach applied in much of Europe (ICP Mapping Manual 2004) with each jurisdiction choosing a critical threshold or thresholds (discussed above) appropriate for the ecosystems present in a jurisdiction. The critical load of S + N deposition (CL_{S+N}) was estimated by computing the steady-state mass balance for sources and sinks of acidity in a forest ecosystem (Figure 3.4).

$$CL_{S+N} = BC_{wx} + BC_{dep} + N_{sinks} - ANC_{leaching} - Cl_{dep} - BC_{cuptake} ,$$

where BC_{wx} is the base cation weathering rate, BC_{dep} is the atmospheric deposition of base cations, N_{sinks} is the sum of all ecosystem processes that remove nitrogen from the system,

$ANC_{leaching}$ is the loss of base cations and organic acid anions from the system with percolating soil water, Cl_{dep} is atmospheric deposition of chloride, and $BC_{cuptake}$ is the uptake of base cations from soil required to regrow biomass that is removed by fire or harvesting.

The first three terms on the right hand side of the mass-balance equation are the ecosystem sinks of acidity. The methods for estimating BC_{wx} are discussed below. The estimation of BC_{dep} is discussed in Section 2 of this document. The principle nitrogen sinks in a terrestrial ecosystem are denitrification, long-term immobilization in recalcitrant soil organic matter, and export of nitrogen with biomass removed by fire or harvesting. Following the assumptions made in the NEG/ECP project (NEG/ECP 2001, Ouimet et al. 2006), denitrification and net immoblization of nitrogen are assumed to be zero at steady state[5] (see also Aber et al. 1998, Galloway et al. 2003). Nitrogen removal due to fire and harvesting (N_{uptake}) is discussed below.

The second three terms on the right hand side of the mass-balance equation are the ecosystem sources of acidity. The leaching of acid neutralizing capacity ($ANC_{leaching}$) includes base cation leaching in conjunction with leaching of SO_4^{2-} and NO_3^- fluxing through the ecosystem as well as the leaching of organic acid anions. The methods for estimating $ANC_{leaching}$ in the NEG/ECP model used here are described in detail in Ouimet et al. (2006). The NEG/ECP approach is based on a constraint of maintaining a minimum soil base saturation of 25% to be consistent with conditions of stable base cation pools representing adequate nutrition (NEG/ECP 2001, Ouimet et al. 2006, Schaberg et al. 2007). "The observed soil pH – base saturation relationship for forest soils in the region indicated that the constants used in the calculation of [ANC] leaching should be set to 10 (M/M) for the molar Bc/Al ratio in soil leachate and 109 (mol L^{-1})[2] for the gibbsite dissolution constant" (Ouimet et al. 2006). Estimation of Cl_{dep} is discussed in Section 2 of this document. The methods for estimating $BC_{cuptake}$ are described below.

Expressed simply, the mass balance model evaluates whether the base cations (Ca^{2+}, Mg^{2+}, K^+, Na^+) lost in conjunction with leaching of SO_4^{2-} and NO_3^- from the ecosystem and via harvesting or fire can be replaced on an ongoing basis by base cations released into the soil by mineral weathering reactions and those deposited from the atmosphere (Figure 3.4). Mass balances for Ca, Mg, K, and Na were evaluated individually. If the steady-state mass balance for any one individual cation is negative, the critical load is exceeded. A negative mass-balance for Ca, Mg or K indicates a long-term condition of nutrient depletion. If all cation mass balances are positive, the critical load is not exceeded and this indicates the system has the capacity to tolerate additional S or N deposition.

The difference between the critical load and atmospheric deposition, termed "exceedance" (ICP Mapping Manual 2004), indicates the severity of the nutrient imbalance or the capacity to tolerate additional deposition. At sites where the deposition exceeds the critical load, the time required for the manifestation of declines in forest health and growth rate is governed, in part, by the size of the soil-exchangeable pool of nutrient cations.

---

[5] The assumption that net nitrogen storage is zero ***at the steady-state*** (see Aber et al 1998, Galloway et al. 2003) does not imply we are claiming any system is presently at steady-state with respect to N or that any particular system necessarily ever will achieve steady-state. This is a useful simplifying assumption appropriate for a steady-state condition.

Exchangeable cations are those that are loosely retained in the soil, and can be thought of as the short-term supply of nutrients, while soil mineral weathering provides the long-term supply. If the exchangeable pool is large, the forest may be able to buffer a small nutrient input-output imbalance for tens to hundreds of years, delaying the onset of health and growth limitations. This buffering period allows time for the implementation of air-pollution emissions reductions.

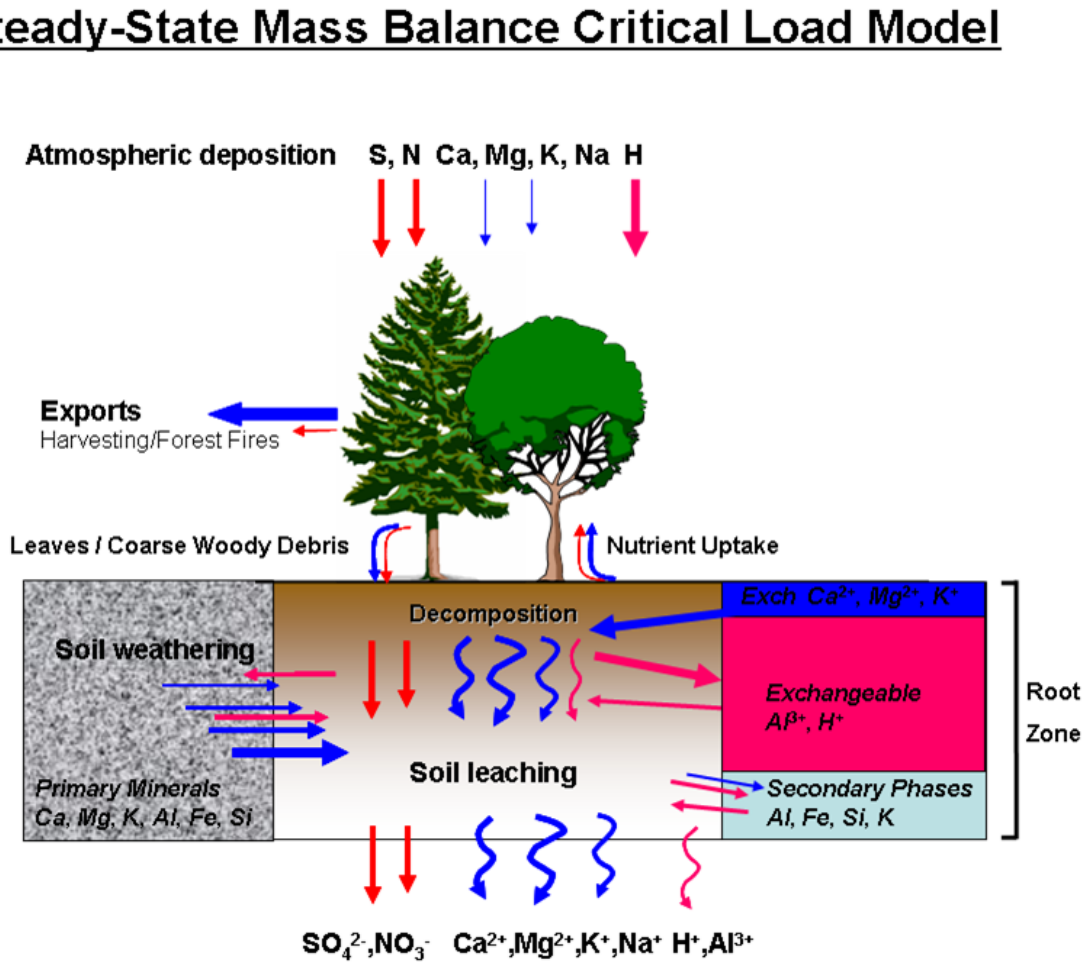

Figure 3.4. Cartoon of steady state mass balance model described in Ouimet et al. (2006) and the ICP Mapping Manual (2004).

The size of the exchangeable cation pool is governed by a variety of factors including soil depth, texture, organic matter content and the history of nutrient input-output imbalance or surplus. This is an extremely local condition. It is not currently possible to reliably estimate the size of exchangeable nutrient pools on a regional basis. Observations from specific sites throughout the Northeast indicate exchangeable cation pools in the general range of 2 to 80 keq ha^{-1}. Frequently, sites with low weathering rates and a history of nutrient depletion will also have small exchangeable pools of cations. Thus, we can generally assume that where the critical load is exceeded today, it was also exceeded in the recent past (1960's to present) and the buffering capacity of the exchange pools at such sites has already been diminished. At sites where deposition does not currently exceed the critical load,

exchangeable cation reserves are expected to be increasing. Therefore, the magnitude of the exceedance provides an indication of the time to the onset of nutrient shortages. These concepts are illustrated in Figure 3.3b, based on measurements from several plots in Massachusetts. Where exceedance values are high (the deposition index is strongly negative), health problems and growth declines should be evident now or within decades (Schaberg et al. 2007). Where exceedance is only slightly higher than the critical load (the deposition index is only slightly negative), problems may take 100 to several hundred years to develop.

Meaningful differences between different applications of the steady-state mass-balance approach occur in the development of estimates (data layers) for specific terms in the model. The methods used to estimate different terms in the nutrient cation mass balances are described below.

Estimation of Forest Nutrient Demand (BC_{uptake} and N_{uptake})

Forest nutrient demand was quantified as part of the mass balance. In undisturbed forests that have reached their climatic potential biomass there is no net annual requirement for nutrients because nutrients in dead trees are recycled into new forest growth. When forests are burned or harvested, part of the nutrient capital of the stand is removed with the ash or timber. The amount removed depends on the intensity of the fire or harvest and the parts of the tree that are removed. In order to calculate a critical load that will adequately protect a working forest, it is necessary to quantify the demand for nutrients required for growth after harvest. Forest tree species and communities vary substantially in their inherent growth rates, demand for specific nutrients, fire recurrence interval, and level of forest management activity in different parts of the study landscape. There are also variations in harvesting rates and practices on privately and publicly owned lands and in different jurisdictions. For these reasons, we characterized the rate of nutrient extraction associated harvest by forest type, land-ownership category[6], and location. Fire recurrence intervals average tens of thousands of years in most parts of New York and New England; therefore, nutrient losses due to fire were ignored.

Distribution of Forest Types

A 30-m resolution spatial data layer describing the distribution of 9 major forest types was produced by determining the probability of forest type occurrence as a function of climate, and using the USEPA/USGS National Land Cover Data to discriminate between evergreen, deciduous or mixed forest types that could potentially occupy the same climatic conditions. Forest type niche in microclimate space was determined separately for deciduous and evergreen forest types by analysis of USFS FIA plot data (Miller and McLane, Appendix NPSCL-TD3a-Forest-Type-Model.pdf). A ground truth survey conducted in the New England

[6] The public and private land ownership categories refer to all lands where harvesting would be permissible. There was no harvesting modeled from state and federal reserves or wilderness areas. There was no data available on private reserves, thus harvesting was allowed on all private lands in the model.

States as part of the NEG/ECP project determined that the New England forest type map was 75% accurate overall, with higher accuracies for the dominant forest types (Miller and McLane, Appendix NPSCL-TD3a-Forest-Type-Model.pdf). There was no funding in the current project for a similar ground-truth effort in New York. Therefore, there is an unknown uncertainty level for forest type classification in New York.

Nutrient Exports Associated with Harvesting

The annual demand for nutrients required to regrow the biomass exported via harvesting was estimated from timber extraction rates and wood nutrient content. This information was available for New York from a combination of state and federal sources. In New York, annual biomass extraction was estimated by county, land-ownership category (public, private), and forest type (softwood, hardwood, mixed) from forest inventory data provided by the USDA Forest Service Forest Inventory and Analysis Program (FIA)[7]. FIA does not directly determine timber extraction rates, but rather how much of the inventory is removed between surveys. Therefore, when land is converted from forestry to residential and industrial uses, the trees harvested are counted as a removal from inventory. However, this type of removal does not reflect a long-term recurring harvest, because the harvested land is no longer in forest production. Due to these limits on information, rates of average recurring biomass extractions are probably over estimated in rapidly developing counties.

The New York state-wide public lands GIS data layer used to map harvesting rates by land-ownership categories may contain inconsistencies or omissions that influence the estimated spatial distribution of nutrient extraction rates. It was beyond the scope and budget of this project to address any problems with the state-wide land-ownership coverage. Due to lack of information on management plans for specific land parcels, all forest type-ownership categories were assigned the FIA county-wide average rate of timber extraction for that class. The effect of these assumptions is that nutrient losses due to recurring timber extraction may be overestimated on some lands and underestimated on others. Nutrient concentrations for each tree species for healthy foliage, branch, bark, and stem wood were compiled from the literature (Pardo et al. 2005).

The Appendix "NPSCL-TD3b-Biomass-Extraction.pdf" describes the generalization of FIA county level data in more detail.

Soil Mineral Weathering (BC_{wx})

The chemical breakdown of rock-forming minerals and their conversion to soil minerals, termed *soil mineral weathering*, is the primary means of replenishing the nutrients Ca, Mg and K that are lost from soils via acidic deposition-induced leaching and/or biomass removal. The landscape and geologic factors that control the rate of weathering are: 1) mineral assemblage, 2) climate, and 3) physical properties of the soil. Common minerals that may co-occur in the same rock or soil may have widely varying Ca, Mg, and K contents and

[7] FIA data by county was obtained from the FIA web interface (http://fia.fs.fed.us/).

inherent rates of chemical breakdown that could vary by up to 8 orders of magnitude (Table 3.1 and see Lasaga et al. 1994). Thus, the proportion of easily weathered minerals (which are often the highest in Ca and Mg) exerts the dominant control on the overall soil weathering rate. The mineral assemblage is governed by the geologic history of a site including the bedrock mineralogy, transport of minerals to the site by water, wind or glaciers, and the length of time the assemblage has been subject to weathering. Weathering rates increase with increasing temperature and water flux through a soil. The more mineral surface area that is exposed to water, the higher the weathering rate and this factor is governed by soil mineralogy, texture, and climate. The depth to which roots can penetrate the soil (a function of both plant and soil characteristics) and the presence or absence of a fluctuating water table at this depth influence the volume of soil over which weathering is relevant to plant nutrition. Not surprisingly, the weathering rate is a highly localized parameter and very difficult to evaluate on a regional basis given the complexity of factors involved and data required. The estimation approach employed provides values of the average weathering rate for upland soils (NEG/ECP-FMG, 2001). Local weathering rates may depart substantially from the averages derived, but the estimates provide a rational basis for differentiating the ability of different areas within the region to replenish lost nutrients.

In areas with upwelling groundwater, weathering rates would include deep till and bedrock contributions below the root zone and along 3-dimensional ground water transport pathways. To attempt to include such upwelling water contributions in the weathering rate estimates would require complex and data intensive groundwater modeling that was beyond the scope and budget of this project. Thus, the end user of the information in this report must be aware that the weathering rates used represent the minimum likely weathering rates in areas of upwelling waters.

Table 3.1. Mean lifetime of a 1 mm crystal of common primary minerals at 25°C and pH 5.0. From compilation by Lasaga et al. (1994).

Mineral	Mean Lifetime of a 1 mm crystal (years)
Anorthite	112
Nepheline	211
Diopside	6,800
Enstatite	10,100
Gibbsite	276,000
Sanidine	291,000
Albite	575,000
Microcline	921,000
Epidote	923,000
Muscovite	2,600,000
Kaolinite	6,000,000
Quartz	34,000,000

The mountainous landscape, range of climate, diverse bedrock geology, glacial history, and lack of any data that were scale-appropriate for the entire region presented a series of challenges to estimating mineral weathering rates. Through a combination of field studies, modeling, and literature review we developed an empirical model describing the glacial transport of minerals in the <2mm size fraction, developed a comprehensive state-wide database of bedrock mineralogy to be used with the glacial transport model, developed landscape context sensitive empirical models of key climatic factors and soil characteristics, and used the PROFILE (Sverdrup and Warfvinge, 1993; see also NEG/ECP-FMG, 2001) weathering rate model to process this information stored in a geographic information system. The process of developing the input data for the PROFILE model (Sverdrup and Warfvinge, 1993) is described below.

Bedrock Mineralogy

A digital version of the bedrock geologic map for NY was obtained from the NY State Museum (see http://www.nysm.nysed.gov/publications/). The map was imported into Clark Laboratories Cartalinx™ vector GIS software (www.clarklabs.org). The geologic literature and unpublished documents (senior, masters, Ph.D. theses, technical reports, etc.) were searched for all possible mineralogical descriptions of specimens collected from documented locations. A description of the development of this database and a complete listing of sources used are provided in Appendix NPSCL-TD3c-Bedrock-Minearlogy.pdf. In some cases a report of the mineral composition for a specimen was accompanied by coordinates for the sampling location. In other cases the location of the sample could be determined from a text description or sample map along with consultation of topographic and geologic maps. A systematic attempt was made to locate samples representative of each map unit and each polygon representing an occurrence of a map unit. Sample mineralogy, source reference information, and sample coordinates were compiled into a data table (Appendix NPSCL-TD3d-NYBedrockMineralogyTable.xls). As certain bedrock types contained minerals that were not represented in the PROFILE model, rational substitutions were made to classify the non-PROFILE minerals into minerals of similar chemistry and reactivity following the suggestions of Sverdrup and Warfvinge (1993), the model documentation, and Hurlbut and Klein (1977).

Not all map units or map polygons were represented by a sample. When this situation occurred, the textual descriptions on the geologic map and in relevant references in the geologic literature reviewed were consulted and used to assign values of mineralogy consistent with the description of the map unit. Most often missing values were replaced with the average values of mineral percentages from all other samples from the map unit. When no samples were available for a map unit, the average value of the most similar map unit as determined from unit descriptions and the literature was used. This type of replacement was typically only necessary for map polygons of minor units with very limited geographic extent. The data table includes information on the type of data (measurement type or estimation) used to assign mineralogy to each map polygon. With all map polygons associated with a measured or estimated mineralogy, the data table was joined to the map polygon coverage to map the spatial distribution of bedrock mineral occurrences as weight percents of the specific minerals used in the profile model. The vector coverages were rasterized to a 90-meter resolution grid in the modeling geographic reference system (see Section 1 of this document).

In the development of the New England States bedrock mineralogy database, funding was available for fieldwork and sample analysis to establish the mineralogy of major map units and major map polygons for which there were no prior samples available. There was no funding for similar work for New York as part of this study, which resulted in a higher rate of estimation of mineralogy (as described above) for New York. The end user should be aware that because the mineralogy of many major map polygons is estimated, the quality of the New York State mineralogy database is somewhat lower than the New England States mineralogy database.

Glacial Redistribution of Bedrock Minerals

As part of the NEG/ECP project, Eric Miller (ERG), Peter Ryan (Middlebury College) and colleagues developed an empirical model of the glacial redistribution of bedrock materials in the <2mm size fraction of soil parent materials. They focused on the <2mm size fraction because this size fraction of material contains the vast majority of mineral surface area available for weathering reactions (White et al. 1996, Malmström et al. 2000). The PROFILE model simulates weathering reactions in this size fraction. The methods and results of this effort are largely reported in Munroe et al. (2008). Ryan and Miller and Munroe et al. (2008) used the bedrock mineralogy database developed for Vermont to locate small map polygons containing unique minerals that were not present in surrounding map polygons at distances of 20 or more km. They treated these map polygons as small area or point sources of these minerals to be redistributed by glacial activity. They dug a series of soil pits at progressive distances from the source locations along the direction of glacial transport as indicated by maps of glacial motion (Ackerly and Larsen 1987). C-horizon (unweathered soil parent material) was sampled and the <2mm size fraction separated. Quantitative X-ray diffraction methods (Munroe et al. 2008) were used to quantify the percentage of different minerals present in the < 2mm size fraction. They found that for minerals that are fairly resistant to weathering, mineral concentrations declined linearly with distance from the source to near zero at a distance of 18 km along the direction of glacial transport (Figure 3.5). Highly weatherable minerals such as calcite were not detected greater than 2 km from the source in the glacial transport direction (Figure 3.6).

Because of the high potential contribution of the minerals calcite and dolomite to soil mineral weathering rates, further investigations were made to verify the inferred 2 km net transport distance for these minerals. Because of the significant expense involved with digging soil pits and quantitative X-ray diffraction analysis, McLane and Miller (unpublished) quantified the proportion of trees and herbaceous plants known to require high levels of calcium along transects from calcium-rich geologic formations (e.g. limestone) along the direction glacial transport into calcium-poor geologic formations (e.g. slates, sandstones). Their study confirmed a 2-km effective glacial transport limit for Ca. The difference in effective glacial transport distance is likely due to the very high rates of calcite and dolomite chemical breakdown during and immediately post glaciation (Taylor and Blum 1995, White et al. 1996).

The observations of declining concentrations of minerals in the < 2 mm soil parent material size fraction away from their geologic sources were used to derive an empirical dispersion function. This function was applied to each 90-meter grid cell to estimate the contribution of minerals from glacially upstream grid cells. The process generated a series of

grids describing the estimated weight percentage of different minerals present in the <2mm parent material. Additional information derived from the Ryan and Miller and Munroe et al. (2008) quantitative X-ray diffraction studies on weathered soil horizons in the same pits was used to adjust the parent material weight percentages for the amount of secondary clay and amorphous minerals formed in the weathering zone due to weathering since glaciation. The weight percentages of reactive minerals were reduced to account for weathering since glaciation (see Taylor and Blum 1995). The adjusted mineral weight percentages were used as input for the PROFILE weathering rate model.

Because funding was not available to conduct similar studies in New York, we assumed that bedrock materials in the less than 2 mm size fraction underwent similar glacial redistribution and post-glacial weathering to that observed in the Vermont study.

Soil Depth and Texture

Estimates of soil depth (to rock or effective root penetration depth), bulk density, and texture (percent sand, silt, and clay), which are required input for the PROFILE model, were taken from the USDA NRCS STATSGO soils database (http://soils.usda.gov/survey/geography/statsgo/). The STATSGO data were used (as opposed to the higher resolution SSURGO data) because at the time of initiation of the NEG/ECP project digital SSURGO data were not available for the entire project domain. The STATSGO vector coverages were rasterized and associated data values interpolated to the project 90-meter grid. These grids were modified using information on the depth of till and depth of stratified materials taken from the USGS coverage describing the surficial geologic deposits of New York and New England (Sollor 1990 and http://geo-nsdi.er.usgs.gov/metadata/digital-data/38/qsurf.html).

Climatic Parameters

Climate and Runoff values required by PROFILE were generated by the HRDM climate module (see Miller et al. 2005) using 30-year (1971-2000) normal precipitation and temperature data from the National Climatic Data Center and Environment Canada. Evapotranspiration was estimated using the method of Dingman (1994) accounting for differing vegetation types and soil conditions (see section 4 for more detail). It was assumed that mean annual soil temperature in the rooting zone was equivalent to mean annual air temperature.

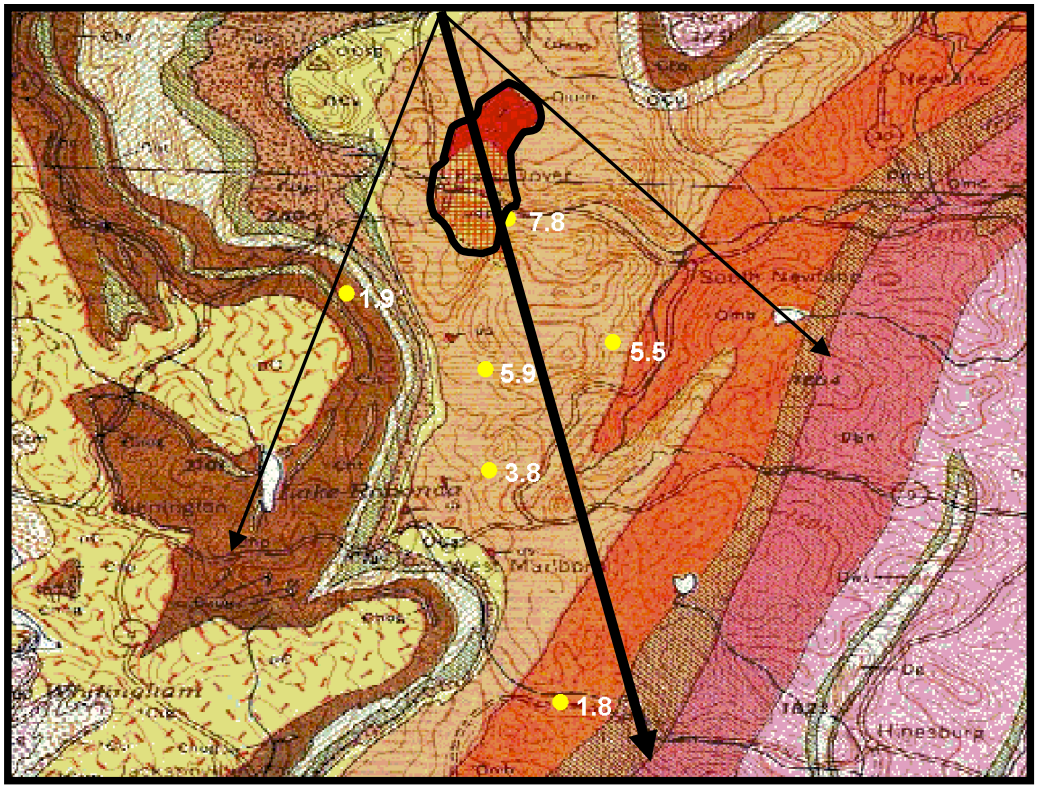

Figure 3.5. Weight percentage sepentine in the < 2mm size fraction of soil parent material (C Horizon) in the direction of glacial transport from an isolated outcrop of the mineral (red shaded area within bold black outline). Bold arrow indicates the dominant direction of glacial transport as revealed by glacial striae. From unpublished research by E. Miller (ERG) and P. Ryan (Middlebury College).

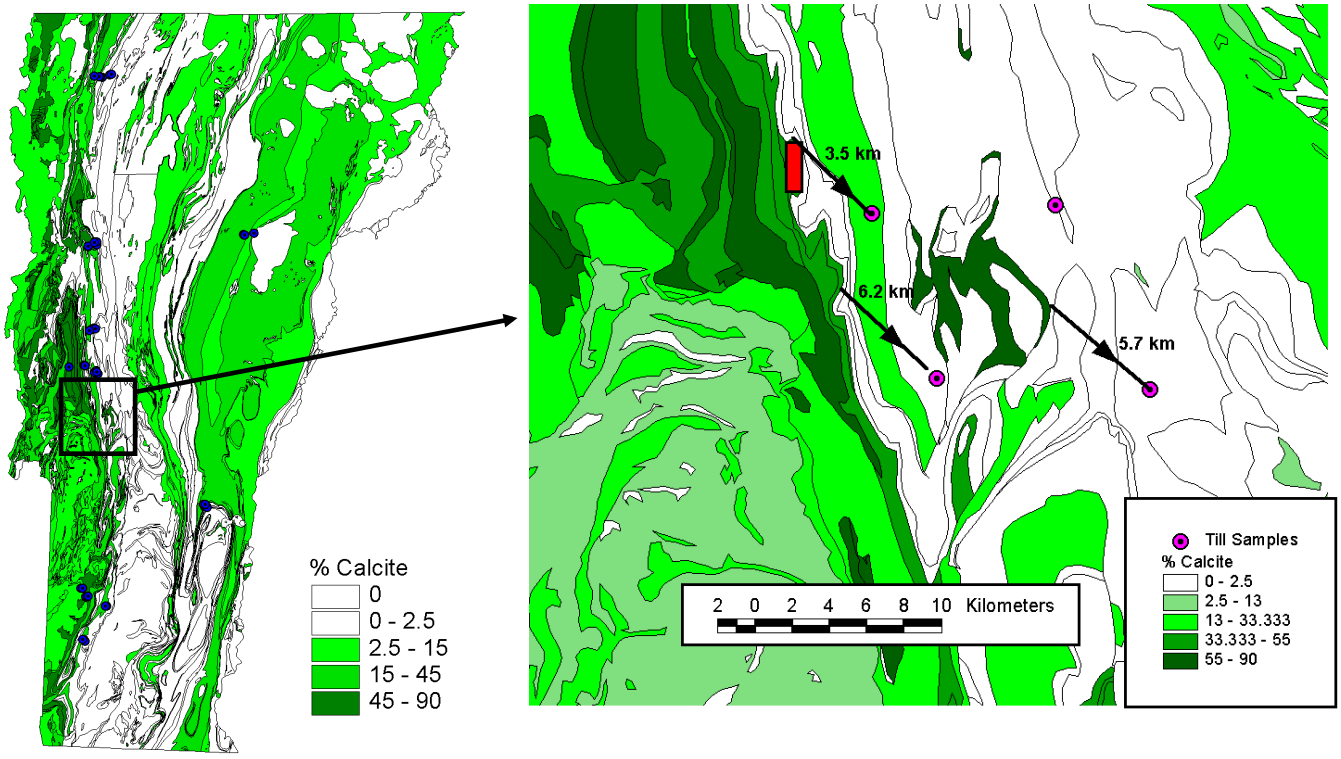

Figure 3.6. (Left) Map illustrating the spatial distribution of calcite in Vermont bedrock. (Right) Enlargement of boxed area on left figure. Soil pit locations are shown along with their distance from major calcite bearing rock formations. No calcite was found in these soil pits demonstrating that calcite experiences different net transport to more weathering resistant minerals (see Figure 5 and also Munroe et al. 2008).

PROFILE Modeling

The PROFILE soil mineral weathering rate model (Sverdrup an d Warfvinge 1993) was run for each grid cell using the data layers described above as input. For this regional modeling effort it was not possible to estimate soil parameters according to different soil horizons. Therefore, weathering rates were computed for a single soil layer with average properties of the soil profile over the root zone depth (typically 0.5 to 1.5 meters). Output from the model included the weathering flux of Ca, Mg, K, and Na.

Forest Ecosystem Critical Loads

The estimated critical load of sulfur + nitrogen for NY and the New England States is shown in figure 3.7). Critical loads in NY are highest in areas of sediments and metasediments containing limestone or calcite vein fillings. Critical loads are fairly high in the Adirondack park due to the presence of abundant anorthite and hornblende in the anorthosite bedrock. Anorthite, the Ca end-member of the plagioclase feldspar solid solution series is one of the most highly weatherable primary minerals (Table 3.1 and Lasaga et al, 1994). Areas of low critical loads occur in the higher elevations of the Adirondack Mountains where cooler temperatures and thin soils reduce weathering rates. Very low critical loads occur in the Catskills and other areas were sandstone bedrock prevails.

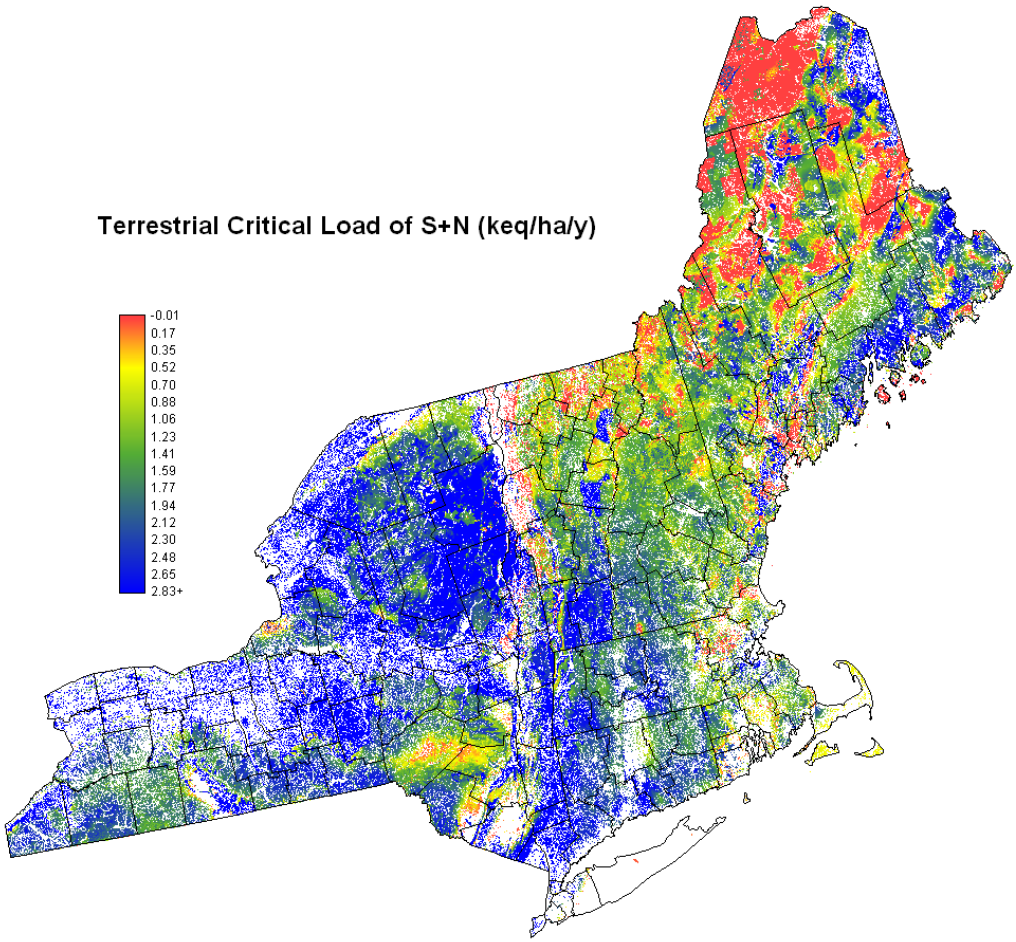

Figure 3.7. Terrestrial ecosystem critical load of sulfur + nitrogen in the northeastern US. White areas on the map are urban, agricultural, or water areas where the terrestrial critical load was not mapped.

Table 3.2 compares statewide averages of the critical load and its key components. New York has lower statewide estimated base cation removals due to harvesting than the New England states. In contrast, New York has a high statewide average weathering rate and a high statewide average critical load relative to the New England States due to the abundance of calcareous rocks and anorthosite[8] in the state. New York, with its large land area, has a wide range of geologic materials and a wide range of climatic conditions leading to a large variance in the weathering rate.

Table 3.2. Comparison of statewide average critical loads, base cation weathering, and base cation uptake due to harvesting. [1]WX SD refers to the standard deviation of the base cation weathering rate.

State	Base Cation Harvest keq ha^{-1} y^{-1}	Base Cation Weathering keq ha^{-1} y^{-1}	WX SD[1]	Critical Load keq ha^{-1} y^{-1}
Maine	0.41	2.44	1.87	1.28
New Hampshire	0.26	1.80	0.43	1.35
Vermont	0.23	2.50	2.09	1.60
Rhode Island	0.33	2.20	0.33	1.13
Massachusetts	0.21	2.27	1.24	1.77
Connecticut	0.17	2.68	1.15	2.29
New York	0.13	6.50	11.6	5.30

Figure 3.8 shows the areas where sulfur plus nitrogen atmospheric deposition is estimated to exceed the critical load for forested ecosystems for New York and New England under c.a. 2000 and 2018 atmospheric deposition rates. All states show a reduction in estimated forest area where deposition exceeds the critical load between 2002 and 2018 (Figure 3.9).

[8] Anorthosite is composed primarily of the mineral anorthite. Anorthite is the Ca-end member of the plagioclase solid solution series. Anorthite is one of the most readily weatherable minerals after calcite and dolomite (see Table 3.1). The mineral hornblende is also frequently a significant constituent of anorthosite, contains significant calcium, and is readily weathered.

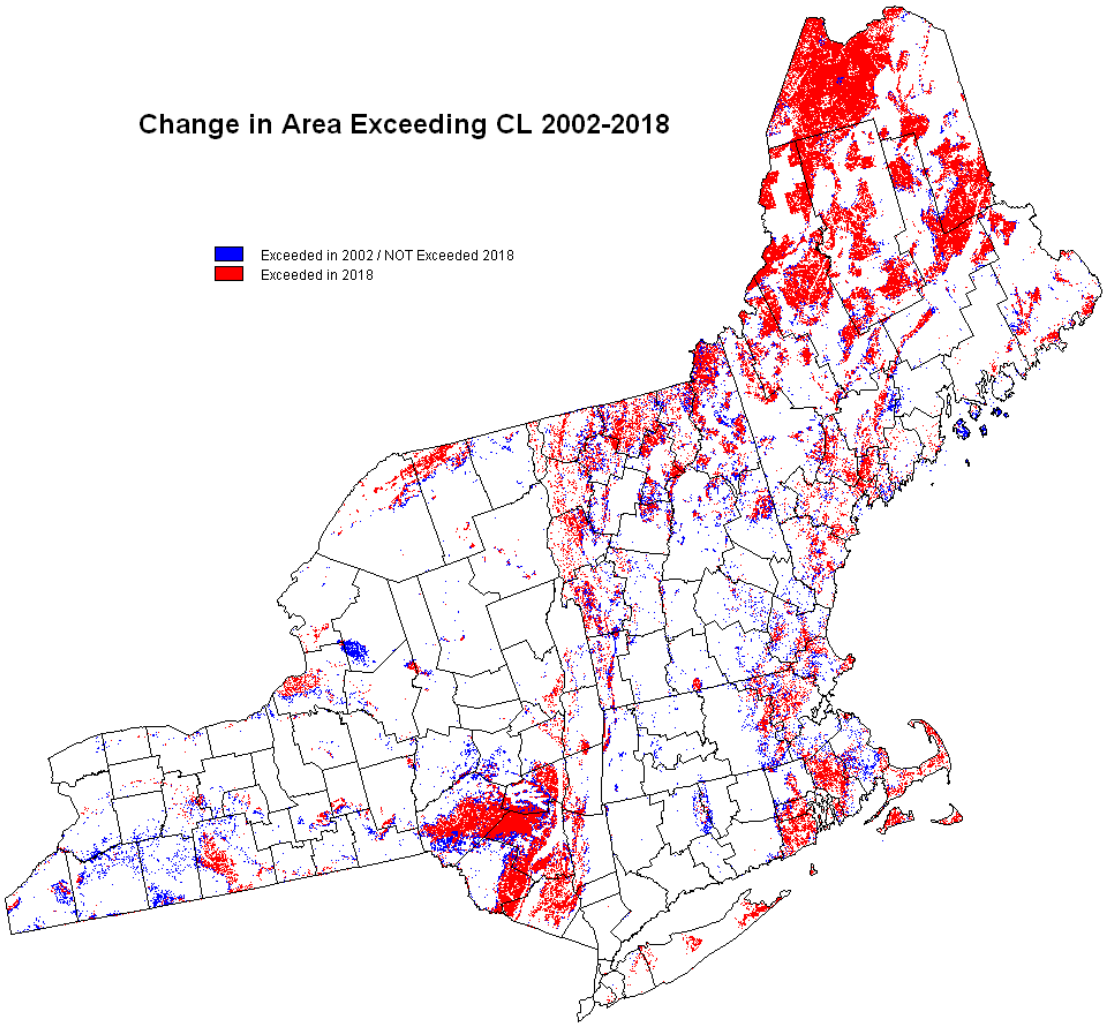

Figure 3.8. Areas where atmospheric deposition of sulfur and nitrogen is estimated to exceed the critical load for forest ecosystems in 2018 (red) and in 2002, but not in 2018 (blue). Atmospheric deposition is estimated to be below the critical load in both modeled time periods for the white areas.

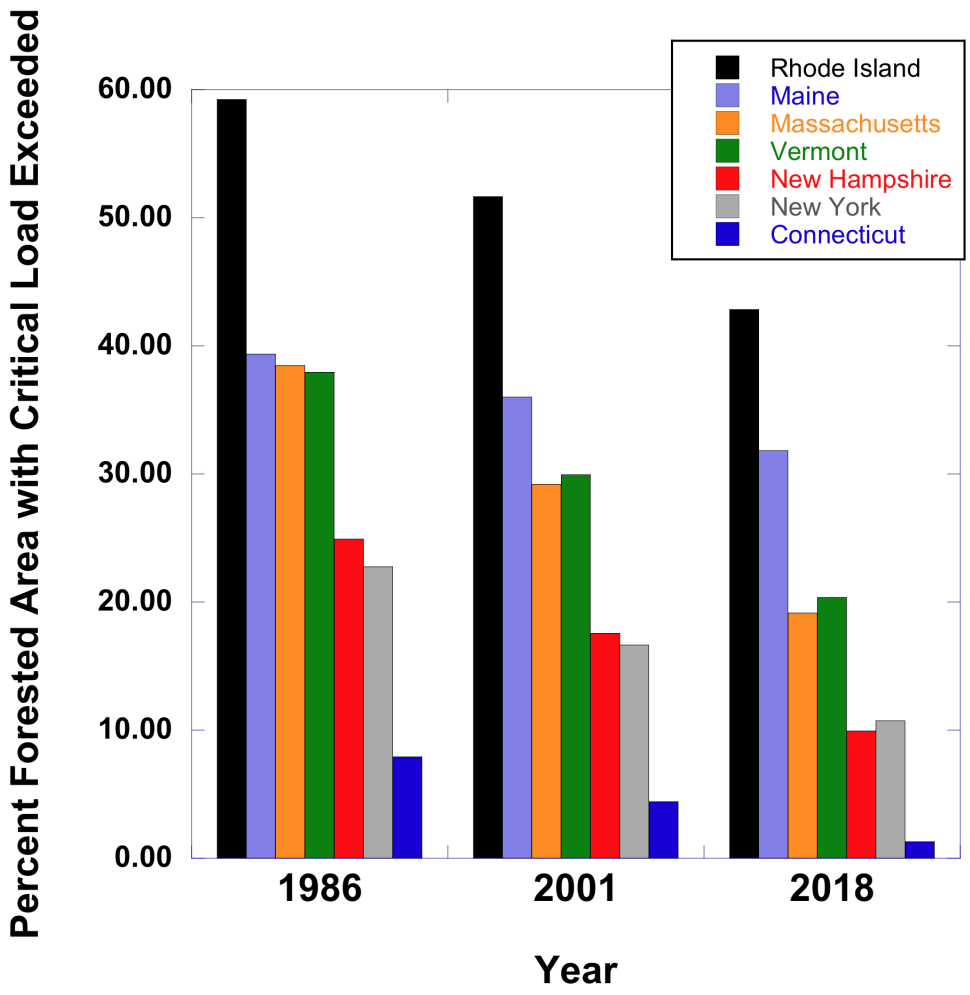

Figure 3.9. Percentage of forested area (by state and time period) where atmospheric deposition of sulfur and nitrogen is estimated to exceed the critical load. Differences between years for individual states generally represent declining sulfur deposition. Differences between states within years result from differences in geology, harvesting rates, and atmospheric deposition rates.

References – Section 3

Ackerly, S.C. and Larsen, F.D. 1987. Southwest-trending striations in the Green Mountains, central Vermont, in New England Intercollegiate Geological Conference, 79th Annual Meeting, Guidebook for Field Trips in Vermont. New England Intercollegiate Geological Conference, p. 369-382.

De Vries, W. 1991. Methodologies for the assessment and mapping of critical loads and of the impact of abatement strategies on forest soils. DLO Winand Staring Centre, Wageningen, the Netherlands. Rep. 46.

Fernandez, I.J., L.E. Rustad, S.A. Norton, J.S. Kahl, and B.J. Cosby. 2003. Experimental Acidification Causes Soil Base-Cation Depletion at the Bear Brook Watershed in Maine. Soil Science Society of America Journal 67: 1909-1919.

Hurlbut, C.S. and C. Klein. 1977. *Manual of Mineralogy*. John Wiley and Sons, New York. 532pp.

Lasaga, A.C. 1984. Chemical kinetics of water-rock interactions. *Journ. Geophys. Res*. 89:4009-4025.

Lasaga, A.C., J.M. Soler, J.G. Ganor, T.E. Burch, and K.L. Nagy. 1994. Chemical weathering rate laws and global geochemical cycles. *Geochim. et Cosmochim. Acta* 58:2361-2386.

Malmström, M.E., G. Destouni, S.A. Banwart and B.H.E. Strömberg. 2000. Resolving the scale-dependence of mineral weathering rates. *Environmental Science and Technology* 34:1375-1378.

Miller, E.K. 2000. Atmospheric Deposition to Complex Landscapes: HRDM – A Strategy for Coupling Deposition Models to a High-Resolution GIS. Proceedings of the National Atmospheric Deposition Program Technical Committee Meeting, October 17-20, 2000, Saratoga Springs, New York.

Miller, E.K. 2006. Assessment of Forest Sensitivity to Nitrogen and Sulfur Deposition in Maine. Technical report prepared on behalf of the Conference of New England Governors' and Eastern Canadian Premiers' Forest Mapping Group, 15 December 2006, for the Maine Department of Environmental Protection, Bureau of Air Quality, Statehouse Station #17, Augusta, ME 04333.

Miller, E.K., A.J. Friedland, E.A. Arons, V.A. Mohnen, J.J. Battles, J.A. Panek, J. Kadlecek and A.H. Johnson. 1993. Atmospheric Deposition to Forests Along an Elevational Gradient at Whiteface Mountain, NY USA. *Atmospheric Environment* 27A: 2121-2136.

Miller, E.K., A. VanArsdale, G.J. Keeler, A. Chalmers, L. Poissant, N. Kamman, and R. Brulotte. 2005. Estimation and Mapping of Wet and Dry Mercury Deposition Across Northeastern North America. *Ecotoxicology* 14: 53-70.

Moore, J-D. and R. Ouimet. 2006. Ten-year effect of dolomitic lime on the nutrition, crown vigor, and growth of sugar maple. *Canadian Journal of Forest Research* 36:1834-1841.

Morrison, H.A., et al. 2005. 2004 Canadian Acid Deposition Science Assessment. Environment Canada – Meteorological Service of Canada, 4905 Dufferin Street, Downsview, Ontario, Canada M3H 5T4.

Munroe J.S., Ryan P.C., Carlson H.A., and Miller E.K., 2008, Testing Latest Wisconsinan Ice Flow Directions in Vermont through Quantitative X-ray Diffraction Analysis of Soil Mineralogy. *Northeastern Geology and Environmental Sciences*, 29(4): 263-275.

NEG/ECP Forest Mapping Group. 2001. Protocol for assessment and mapping of forest sensitivity to atmospheric S and N deposition. The Conference of the New England Governors and Eastern Canadian Premiers. 76 Summer St. Boston, MA 02110. 79 pp.

NEG/ECP Forest Mapping Group. 2003. Assessment of Forest Sensitivity to Nitrogen and Sulfur Deposition in New England and Eastern Canada: Conference of New England Governors and Eastern Canadian Premiers Forest Mapping Group Pilot Phase Report. The Conference of the New England Governors and Eastern Canadian Premiers. 5161 George Street, Suite 1006, Halifax, NS, B3J 1M7. 16pp.

NSTC. 1998. National Acid Precipitation Assessment Program Biennial Report to Congress: An Integrated Assessment. National Science and Technology Council, Committee on Environment and Natural Resources, Silver Spring, MD.

Ouimet, R., L. Duchesne, D. Houle, and P.A. Arp. 2001. Critical loads of atmospheric S and N deposition and current exceedances for Northern temperate and boreal forests in Québec. *Water Air, and Soil Pollution*. *Focus* 1(1/2):119-134.

Ouimet, R., P. Arp, S. Watmough, J. Aherne, and I. DeMercant (2006) Determination and mapping critical loads of acidity and exceedances for upland forest soils in Eastern Canada. *Water, Air, and Soil Pollution* 172: 57-66.

Pardo, L.H., M. Robin-Abbott, N. Duarte, and E.K. Miller. 2005. Tree Chemistry Database (Version 1.0). USFS General Technical Report NE-324. USDA Forest Service, 11 Campus Blvd. Suite 2000, Newtown Square, PA.

Schaberg, P.G., D.H. DeHayes, and G.J. Hawley. 2001. Anthropogenic Calcium Depletion: A Unique Threat to Forest Ecosystem Health? *Ecosystem Health* 7: 214-228.

Schaberg, P.G., Miller, E.K., Eagar, C. Assessing the Threat that Anthropogenic Calcium Depletion Poses to Forest Health and Productivity. 2007. USDA Forest Service General Technical Report PNW-GTR-806 (a peer-reviewed, combined publication of the Southern and Pacific Northwest Research Stations) and a chapter on the web-based forestry encyclopedia: www.threats.forestencyclopedia.net

Schaberg, P.G., J.W. Tilley, G.J. Hawley, D.H. DeHayes, and S.W. Bailey. 2006. Associations of calcium and aluminum with the growth and health of sugar maple trees in Vermont. *Forest Ecology and Management* 223: 159-169.

Sverdrup, H. and P. Warfvinge. 1993. Calculating field weathering rates using a mechanistic geochemical model PROFILE. *Applied Geochemistry* 8: 273-283.

Taylor, A. and J.D. Blum. 1995. Relation between soil age and silicate weathering rates determined from the chemical evolution of a glacial chronosequence. *Geology* 23:979-982.

Watmough, S.A. and P.J. Dillon. 2003. Calcium losses from a forested catchment in South-Central Ontario, Canada. *Environ. Sci. Technol.* 37: 3085-3089.

White, A.F., A.E. Blum, M.S. Schulz, T.D. Bullen, J.W. Harden, and M.L. Peterson. 1996. Chemical weathering rates of a soil chronosequence on granitic alluvium: I. Quantification of mineralogical and surface area changes and calculation of primary silicate reaction rates. *Geochimica et Cosmochimica Acta* 60:2533-2550.

Section 4 – Northeast Steady State Aquatic Critical Loads and Exceedance (2002/2018)

Steady-state aquatic ecosystem critical loads were calculated for regional surface waters. Two approaches were evaluated. One approach was to use surface water chemistry data available for 1482 waters to estimate critical loads using the Steady-State Water Chemistry method (SSWC) as described in the ICP Mapping Manual (2004). It was hoped that these specific water body critical loads could be extrapolated to the region by developing statistical models of either critical load or critical load parameters as functions of the information in the terrestrial critical loads data layers on geology, soils, vegetation, climate, and landscape elements (see Section 3 of this document). Despite considerable effort, it was not possible to achieve a satisfactory regional extrapolation. This failure to achieve a satisfactory regionalization using a scaling approach is likely due to the extreme diversity of landscapes, geology, and surface waters across the Northeast region. The failure of this approach is also related to weaknesses in the SSWC method of estimating a base cation weathering from observed surface water data that are strongly influenced by dynamic processes such as cation depletion/accretion (Rapp 2001, Rapp and Bishop 2009) and sulfur retention/release (Mitchell et al. 2010).

A second approach was employed that involved calculating aquatic critical loads using a modified form of the first-order acidity balance variant of the steady-state simple mass balance model (ICP Mapping Manual 2004). For this method that we call the "landscape mass-balance method" (LMB), sources and sinks of acidity to the surface water system within a watershed were calculated from data developed for the terrestrial ecosystem analysis, thus directly regionalizing the estimates of aquatic critical loads. We explicitly do not consider in-lake processes retention or release as these are dynamic processes. Models that estimate in-lake retention and release from observations are not true steady state models, as they depend on a flawed assumption that the in-lake processing deduced from observations will properly represent the steady state condition. The pure steady-state approach we adopted was well suited to the project goal of strong integration between the terrestrial an aquatic ecosystem analyses.

For both approaches, data for surface water chemistry were obtained from state and federal land-management and environmental agencies through a data request. Additional federal data were obtained from the USEPA National Stream Survey and EMAP Eastern Lake Survey. These data were used to derive a method for calculating the effects of dissolved organic carbon on the charge-balance ANC required to achieve a specific pH target.

Critical loads with respect to two ecosystem protection levels (pH 6.6, ANC=50 μeq/L at DOC = 0 mg/L and pH 7.5, ANC = 100 μeq/L at DOC = 0 mg/L) were evaluated. The anticipated change in exceedance of aquatic critical loads was assessed between 2002 and 2018 based on CMAQ modeling of current "on-the-books" state and federal air pollution control measures (see Section 2 of this document). Sensitivity analyses were conducted to elucidate uncertainty in assessment results associated with DOC and salt corrections.

Goals of the Aquatic Critical Loads Study

The specific goals of this aquatic critical loads and exceedance analysis differ somewhat from prior regional studies in the Northeast (e.g Dupont et al. 2005, NHDES 2004, VTDEC 2003). The primary goal of this study was to conduct aquatic critical loads analysis within data and analytical frameworks that harmonized with a parallel terrestrial critical loads and exceedance analysis for the Northeast US region. An important objective of the project was to generate an integrated aquatic and terrestrial critical loads map. A critical loads and exceedance analysis based on observed surface water chemistry was intended to provide a foundation data layer from which empirical relationships would be developed to estimate critical loads for unsampled surface waters in order to create a comprehensive surface water assessment for the region. An alternative approach calculating aquatic critical loads directly from the watershed parameters was ultimately required to a complete regional assessment.

As integration of terrestrial and aquatic analyses was paramount, several constraints often employed in earlier aquatic critical loads assessments needed to be relaxed – and alternative approaches developed for selecting training site data. The integrated assessment approach and extrapolation goal required the following deviations or expansions from previous efforts.

- Broad geographic and landscape position representation (not just known sensitive sites)
- Inclusion of well-buffered surface waters
- Inclusion of surface waters impacted by de-icing agents
- Inclusion of surface waters impacted by non-atmospheric point and non-point nitrogen inputs
- Explicit inclusion of DOC effects on pH

Prior studies in the northeast US either focused on subregions or sacrificed broad geographic and landscape position characterization in order to avoid the complexities introduced by high salt contamination and non-atmospheric nitrogen inputs (Dupont et al. 2005, NHDES 2004, VTDEC 2003). Thus, the present study accepts some amount of additional uncertainty introduced by handling these non-standard conditions in exchange for increased geographic and landscape representation.

Development of the Aquatic Critical Threshold Scenarios

Target pH and the ANC limit

In order to calculate a critical load, a critical threshold condition must be established with respect to a biogeochemical metric that can be modeled and which is associated with ecosystem health or the condition of key organisms in an ecosystem (ICP Mapping Manual 2004, Henriksen and Posch 2001). For aquatic ecosystems subject to acidification by sulfur and nitrogen, the parameter most often related to the condition of key organism and aquatic ecosystem health is pH (ICP Mapping Manual, 2004, Dupont et al. 2005). For historical reasons – due primarily to the complications associated with modeling DOC (discussed below) a target pH critical threshold has been translated to a corresponding value of the acid neutralizing capacity termed the ANC limit (see discussion in Dupont et al. 2005). This is done because the charge-balance form of the acid neutralizing capacity (see Morel and Hering 1993) is simpler to model than pH in a steady-state context with limited data (ICP Mapping Manual 2004).

Discussions were held with stakeholders and project participants to establish model scenarios to be evaluated with respect to the ANC limit used in the model and the implied or "target" pH associated with an ANC limit. Stakeholders and participants were provided information on the difference between the calculated charge-balance ANC employed in the SSWC or LMB models and alkalinity (often informally referred to as "ANC"), which is an operational measurement of acid neutralizing capability of a solution (see Morel and Hering 1993). Enough confusion exists in the literature that occasionally investigators mistakenly equate alkalinity and charge-balance ANC when setting the charge balance ANC limit for critical load modeling.

The observed strong and predictable relationship between pH and alkalinity is not transferable to allow direct inference of the charge-balance ANC limit corresponding to a given pH indicative of ecosystem conditions. DOC and charge-balance ANC together control the alkalinity and pH of a system as explained in the Appendix (NPSCL-TD4a-DOC-correction-of-ANC-limit.pdf, see also Morel and Hering 1993, pg. 199).

Stakeholders and project participants established two model scenarios to be evaluated.

1. Target pH = 6.6, Implied ANC limit = 50 μeq/L at DOC = 0 mg/L
2. Target pH = 7.15, Implied ANC limit = 100 μeq/L at DOC = 0 mg/L

The DOC correction for the charge balance ANC limit (Appendix NPSCL-TD4a-DOC-correction-of-ANC-limit.pdf) was applied on the basis of measured DOC values. For practical reasons, the assumption was made that observed DOC would represent steady-state DOC, although this assumption is not likely valid (see Monteith et al. 2007). The implications of this assumption for critical loads and exceedance were explored via sensitivity analysis (25% DOC increase through 2018).

Surface Water Data

Data for surface water chemistry were obtained from state and federal land-management and environmental agencies through a data request. Additional federal data were obtained from the USEPA National Stream Survey and EMAP Eastern Lake Survey.

Surface water data records were evaluated with respect to data completeness, geographic representation, and temporal representation. In order to achieve the broadest geographic and landscape position representation, some samples lacking DOC, NO_3^-, or NH_4^+ measurements were accepted.

Preferences for data inclusion in the analysis:

- Preference for data collected from approximately 1995 through 2005
- Include data from other time periods if no data are available from 1995-2005
- Prefer complete chemical analysis (see below)

Mandatory information to be included in analysis

- Latitude and Longitude
- Date of sample collection
- pH
- DOC (mg/L) milligrams per liter
- Ca^{2+} (ueq/L) micro equivalents per liter
- Mg^{2+} (ueq/L) micro equivalents per liter
- K^+ (ueq/L) micro equivalents per liter
- Na^+ (ueq/L) micro equivalents per liter
- NH_4^+ (ueq/L) micro equivalents per liter
- SO_4^{2-} (ueq/L) micro equivalents per liter
- NO_3^- (ueq/L) micro equivalents per liter
- Cl^- (ueq/L) micro equivalents per liter

Additional chemical data helpful to the analysis

- DIC (dissolved inorganic carbon) (mg/L) milligrams per liter
- ALK (Gran titration Alkalinitiy) (mg/L) milligrams per liter
- Al (total) (umoles/L) micro moles per liter
- Al (organic) micro moles per liter
- Al (exchangeable) micro moles per liter
- F^- (ueq/L) micro equivalents per liter
- SiO_2 (mg/L) milligrams per liter
- Organic Nitrogen (mg/L) milligrams per liter
- Total N (mg/L) milligrams per liter
- Total P (mg/L) milligrams per liter

Additional information helpful to the analysis

- Surface Water Name
- State ID number for surface water sampling station
- Secchi depth (m)
- Color (platinum color units)

- Surface Water Area (ha) hectares
- Watershed Area (ha) hectares
- Q (Annual Runoff or Discharge) (m/y) meters per year
- Qs (Discharge at time of sampling) (m3/s) meters cubed per second

For a small number of samples DOC was not available, but COLOR measured in platinum color units was available. For these samples, DOC was estimated from the relationship between DOC and COLOR established in a subset of the data set.

When all required and critical supporting data were available the record was assigned a status of data completeness "A". For this analysis if critical supporting data were not available they were assumed to be zero. Samples lacking critical supporting data were assigned a status of data completeness "B".

Ancillary data accompanying surface water chemistry were obtained when available from each data source. These data included Si, Al, and P concentrations, and Secchi depth.

Surface water data represented a range of sampling times from the mid 1980s for EPA NSS and ELS data to mid 2000s for surface water data provided by several states. As the primary use of surface water data was to determine the pre-acidification (or chemical weathering generated) flux of base cations in a catchment, samples representing different time periods should not be problematic. By definition and explicit assumption in the SSWC model the pre-acidification flux of base cations ($*BC_0$)[9] is a time invariant constant[10].

Data representing multiple time periods for the sampling station were aggregated as means. When different agencies sampled the same water bodies, these were treated as different sampling stations, as the specific sampling locations were almost always different.

As time-of-sampling of stream or lake discharge data were not frequently available, no attempt was made to discharge-weight the means. Several data sets provided only single samples generally obtained by the sampling agency to be representative of either mean or spring conditions according to the goals of the specific sampling program.

---

[9] Please note that for consistency between text, graphics, and tabular data generated with statistical software, we have adopted a notation for salt corrected concentrations that is slightly different from standard usage. In standard usage the asterisk appears to the right of the chemical symbol (e.g. BC_0*, see ICP Mapping Manual 2004). For practical reasons in this document and accompanying figures, tables and data base files, salt corrected values are noted by placing the asterisk before the chemical symbol (e.g. $*BC_0$).

[10] Rapp (2001) and others have noted that the inferred values of BC_0* estimated from surface water chemistry measurements representing different time periods may be different. This results from faulty assumptions in the standard SSWC method for estimating BC_0* using the F-factor. This is an artifact of the incorrect assumptions rather than evidence that BC_0* varies over short (decadal) time periods (Rapp 2001). In terms of the explicit assumptions of a steady state modeling framework weathering and BC_0* should be taken to be constants.

Salt Correction

The assembled data exhibited extensive "salt" impacts either from marine atmospheric sources or road-deicing agents. Chloride concentrations ranged over 2 orders of magnitude from 2-9 µeq/L in remote inland locations to 1000-9800 µeq/L in coastal or road-salt impacted waters (Figure 4.1). The simple "sea-salt" correction approach based on either Na or Cl described in the ICP Mapping Manual (2004) resulted in unacceptable results (negative concentration values for corrected ion concentrations) in many samples. Therefore, a modified "salt" correction approach was developed.

4/1/10 11:01 AM
Data Table=Primary_WS-AQCL-TpH66

Distributions

Cl-(ueq/L)

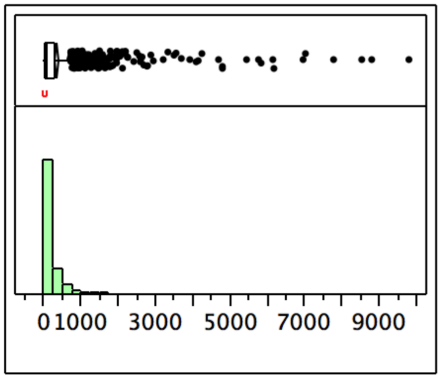

Quantiles		
100.0%	maximum	9826.7
99.5%		6192.1
97.5%		2222.8
90.0%		848.6
75.0%	quartile	318.7
50.0%	median	105.8
25.0%	quartile	48.1
10.0%		9.0
2.5%		6.2
0.5%		2.2
0.0%	minimum	0.0

Moments	
Mean	354.98956
Std Dev	812.29288
Std Err Mean	21.022422
upper 95% Mean	396.2262
lower 95% Mean	313.75292
N	1493

Figure 4.1. Frequency distribution of measured Cl- concentrations in evaluated surface waters.

The Na/Cl ratio was used to establish which ion would be the most suitable index for the salt correction for a specific location. If the sample ionic Na/Cl ratio was greater than the Na/Cl ratio in seawater, this indicated a weathering contribution of Na to the sample, thus Cl would be the more appropriate "salt" tracer at that location. A sample with an ionic Na/Cl ratio less than the ratio in seawater, indicates either a sink for Na or locally greater atmospheric Cl contribution than Cl with a marine origin. As sinks for Na could not readily be evaluated, it was assumed (implicit in the ICP method) that Na is conservative, thus Na would be a better tracer of "salt" in such a case.

Calcium, Mg, K, (Na or Cl) were corrected for the "salt" contribution of either marine or anthropogenic (road-salt) contributions by the appropriate index. For >10% of the samples this resulted in negative values for the Mg concentration and >2.5% for the K concentration, clearly implausible results. As the Na/Cl ratio guidance always selected the lesser concentration of either Na or Cl as the index for correction, choosing the alternative index ion would only make the situation worse.

The most plausible interpretations of negative salt corrected Mg or K concentrations are:

- non sea-salt source of index (Na or Cl)

- analytical error (low bias) in the Mg or K concentration
- analytical error (high bias) in the index (Na or Cl) ion concentration.

The latter explanation seems most plausible when Na was selected (Na/Cl < 0.858) as the index ion. When the Cl concentration is selected as the index it is possible that other de-icing agents (e.g. $CaCl_2$) could be the source of elevated Cl with a stoichiometry different from seawater.

To deal with this problem, background levels of $*Mg^{2+}$ and $*K^{+}$ were established with respect to $*Ca^{2+}$ from samples that were not significantly salt-impacted ($SO4^{2-}/Cl^{-}$ >1). From 565 samples with $SO4^{2-} > Cl^{-}$, the range of uncorrected Cl^{-} concentrations was 0.85 to 254 ueq/L with 90% of samples < 73 ueq/L. In these relatively dilute waters with low Cl, the "salt" correction did not produce negative corrected concentrations. With a small number of exceptions, $*Mg^{2+}$ and $*K^{+}$ were well correlated with $*Ca^{2+}$ exhibiting intercepts (minimum expected concentrations) of 8.2 and 5.6 ueq/L, respectively (Figure 4.2). Therefore, salt-corrected $*Mg^{2+}$ and $*K^{+}$ were limited to these minimum expected values when the "salt" correction produced negative values.

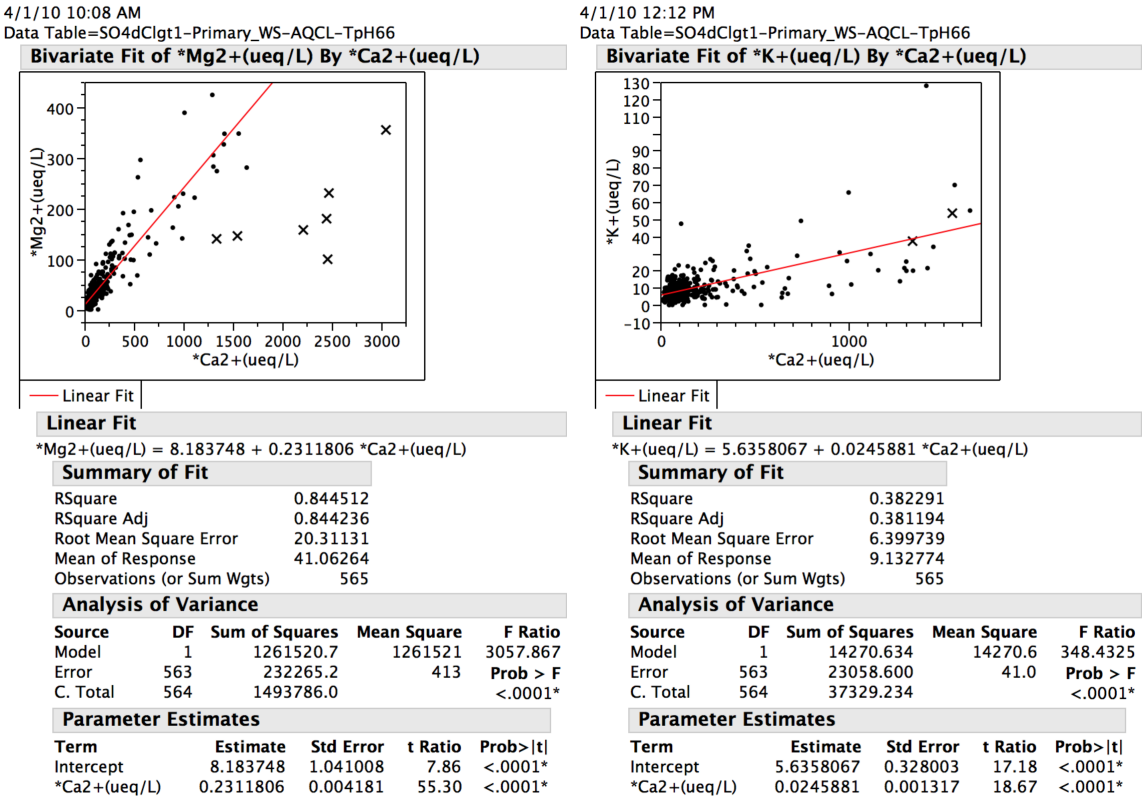

Figure 4.2. Estimation of minimum *Mg2+ and *K+ from subset of non salt-impacted waters.

Significant potential uncertainty in the corrected Ca^{2+}, Mg^{2+}, and K^{+} concentrations of "weathering dilute", "high-salt" waters is possible given expected analytical uncertainties of +/- 5-10% for Na^{+} or Cl^{-} determinations. Given a frequent order of magnitude (or higher)

difference between Na^+ or Cl^- and Ca^{2+}, Mg^{2+}, or K^+ in salt-impacted systems, errors in corrected base cation concentrations could approach 50-100%. Rather than exclude a large number of samples subject to high uncertainty based on salt-correction we maintained these samples in the data set and employed sensitivity analysis (varying the Na and Cl concentrations used for salt-correction by 5-10%) to evaluate the uncertainty in resulting critical loads and exceedances (see below).

Nitrogen in surface waters

The standard application of the SSWC (ICP Mapping Manual 2004) assumes that NO_3^- in surface water arises from nitrification within the watershed. The observed surface water NO_3^- is appropriately factored into the sum of anions expressions for computation of $*BC_0$. This convention is followed in the present analysis. However, it is also possible that measured values of NO_3^- in the surface water data used for this study may represent both atmospheric source N transmitted through the watershed (as is assumed in the model) and NO_3^- from anthropogenic point and non-point sources within the watersheds. The specific source of NO_3^- is irrelevant to estimation of $*BC_0$ as the observed surface water NO_3^- (regardless of source) is needed for the sum of anions in the computation. When computing exceedance of the critical load, the surface water NO_3^- concentration is explicitly attributed to atmospheric sources only by the SSWC. If appreciable anthropogenic point and non-point NO_3^- is contributed from sources within the watershed, the critical load will be lower than estimated in this study.

In order to harmonize with the assumptions used in the integrated terrestrial critical load modeling and exceedance calculations (Miller 2005), all atmospheric N inputs (NO_3^- and NH_4^+) are assumed to be converted to NO_3^- within the watershed for the purposes of calculating exceedance of the aquatic critical load. This conversion is implicit in the steady state assumptions (if N inputs exceed the steady state vegetative demand, C/N will decline as N accumulates until the C/N ratio associated with nitrification is reached Aber et al 1998, Galloway et al. 2003). While considerable uncertainty remains about the specific land-use history, soil, vegetation, and climatic factors that regulate short, medium, and longer-term N retention by ecosystems (Aber et al. 1998,), recent analyses catalog many systems that exhibit inorganic N leaching losses (primarily NO_3^-) equal to inorganic N inputs ($NO_3^- + NH_4^+$, see figure 5 of Galloway et al. 2003) indicating net N retention equal to zero at steady state is a reasonable assumption.

The standard application of the SSWC (ICP Mapping Manual, 2004) assumes that NH_4^+ in lake water is zero (as is typically observed in remote watersheds). This is not the case in the surface water data used for this study. Approximately 90% of samples reporting an NH_4^+ measurement exhibit measureable NH_4^+, likely arising from anthropogenic point and non-point sources in the watersheds. In these cases, the NH_4^+ contributes to base neutralizing capacity. In this study we make the assumption that NH_4^+ concentrations remain constant at the observed values at steady-state. Thus, measured NH_4^+ concentrations are added to $*BC_0$ to compute the sum of cations term for critical load evaluation. If surface water NH_4^+ concentrations increase in the future relative to the measured values the critical load will be less than estimated in this analysis. If surface water NH_4^+ concentrations decrease in the

future relative to the measured values the critical load will be greater than estimated in this analysis. As NH_4^+ contributed 4.3% or less of the sum of base cations in 97.5% samples evaluated, the influence of this assumption on the critical load of acidity are likely to be quite small, except for a few watersheds subject to large non-atmospheric non-point or point N loadings.

Atmospheric Deposition

Atmospheric deposition of sulfur, nitrogen, base cations, and chloride were estimated with Ecosystem Research Group, Ltd.'s High Resolution Deposition Model (HRDM). These data layers are described in Section 2 of this document.

Deposition estimates were generated for 2 scenarios of atmospheric concentrations of S and N representing atmospheric conditions in ~2002 (average of 1999-2003) and 2018. The concentrations in the 2002 scenario were derived from observational data, while the 2018 values were derived from a CMAQ modeling study conducted by NESCAUM (NESCAUM 2006). Section 2 of this doucment describes the process for estimating 2018 S and N atmospheric concentrations. Chloride and base cation atmospheric concentrations were assumed to remain unchanged between the two scenarios as there was no attempt to model any changes in these elements in the NESCAUM MANE-VU modeling exercise.

Runoff (Discharge)

Runoff values were generated by the HRDM climate module using 30-year (1971-2000) normal precipitation and temperature data from the National Climatic Data Center and Environment Canada. Evapotranspiration was estimated using the water-balance method of Dingman (1994) accounting for differing vegetation types and soil conditions. Briefly, this method involves iterative solution of the monthly water balance until the monthly soil moisture values converge to constant values:

$$S_m = \text{minimum } \{[(W_m - PET_m) + S_{m-1}], S_{max}\},$$

where m = month index (1,2,3,…,12), S_m = soil moisture storage at the end of the month, W_m = total monthly water inputs (rain + cloudwater), PET_m is the potential monthly evapotranspriation estimated as 0.409 times the saturation vapor pressure at the mean monthly air temperature (Malmstron 1969, Dingman 1994), and S_{max} is the maximum soil water storage capacity (a function of vegetation type and soil field capacity, permanent wilting point, and soil depth). If W_m is less than PET_m, a soil moisture deficit develops or increases

$$S_m = S_{m-1} \exp[-1 * (PET_m - W_m)/ S_{max}].$$

Runoff $= W_m - PET_m$, if $W_m > PET_m$; otherwise Runoff = 0.

These are the same runoff values used in the integrated terrestrial critical loads modeling component of this project (Miller 2006, see Section 3 of this document).

Aggregation of Atmospheric Deposition and Runoff values by Watershed

Watersheds representing the upslope contributing area with respect to each sample location were computed using the IDRISI™ (www.clarklabs.org) WATERSHED module. Due to the very large spatial domain of the study and grid-size limitations, the 30-meter resolution DEM used for atmospheric deposition and runoff modeling was resampled (bilinear interpolation) to 90-meter resolution for use in watershed delineation. Similarly the 30-m resolution deposition and runoff grids were resampled (bilinear interpolation) to 90-m resolution to facilitate the extraction of watershed-associated data.

As many samples represented multiple reaches of a single stream or multiple lakes in a chain, nesting relationships were established between watersheds representing the local drainage areas. Six levels of nesting were required to represent the data. In other words, there were several watersheds that contained within them up to six different sampling locations with 6 different nested upslope contributing areas. Complicated, multiple levels of nesting were observed. Atmospheric deposition and runoff were extracted from the raster data for each watershed. The values presented in Appendix NPSCL-TD4a.pdf are the watershed average values of all upslope drainage area contributing to a given sampling location.

Scenarios with Approach 1, SSWC

1. Target pH = 6.6, Implied ANC limit = 50 μeq/L at DOC = 0, Deposition 2002, 2018
2. Target pH = 7.15, Implied ANC limit = 100 μeq/L at DOC = 0, Deposition 2002, 2018
3. Sensitivity analysis (-10% NaCl, ANC 50 μeq/L, 2018)
4. Sensitivity analysis (+25% DOC, ANC 50 μeq/L, 2018)

Implied Steady-state ANC and pH values were computed using the SSWC and DOC correction for the 2002 and 2018 atmospheric S and N loadings. This information illustrates the potential long-term implications of critical load exceedance (implied further acidification) or non-exceedance (implied recovery). Information about the time required to reach steady-state pH values must be obtained from supplementary dynamic modeling. As some systems may take several hundred years to reach the steady-state condition (slow changes implied by a small exceedance value) the steady-state pH values are most useful to establish the direction of the pH trend (lower or higher) relative the observed (present) pH.

It is important to recognize that surface water data were assembled for this analysis opportunistically, obtaining available data collected by a variety of agencies and programs for

varying purposes. With such a sample the sample population statistics (e.g. frequency of waters with critical load exceeded or not exceeded, mean values of exceedance) are representative solely of the sample population of waters and not the regional population of waters as a whole. While the presented results are categorized by surface water type (lake/pond, stream/river, or wetland), interpretations are limited to the sample population in each category. For several of the agency data sets, only surface waters with the greatest risk to acidification were sampled, while in others a broader sample of surface waters was collected. For a second phase of analysis, (described below) extrapolating aquatic critical loads and exceedance to the full population of northeast surface waters, a broad representation of surface waters was required. The initial extrapolation method relied on the ability to model spatial variance in observed $*BC_0$ and DOC compiled in the present study using data layers developed for terrestrial critical loads modeling (e.g. Miller 2006, Section 3 of this document).

Estimated critical loads using the SSWC method ranged from negative values (indicating the ANC limit and target pH levels are unattainable in some systems) to greater than 20 keq/ha/y in extremely well buffered systems underlain by calcium carbonate rich rocks (Figures 4.3 and 4.4). Sixteen percent of the surface water sampling locations evaluated are not expected to be able to obtain or sustain the ANC=50 µeq/L at DOC=0 or pH 6.6 level of protection. Forty percent of the surface water sampling locations evaluated are not expected to be able to obtain or sustain the ANC 100 µeq/L at DOC=0 or pH 7.15 level of protection. The mean critical load for acidity was 0.25 keq/ha/y (16%) lower for the more stringent ANC=100 µeq/L at DOC=0 or pH 7.15 level of protection than the ANC=50 µeq/L at DOC=0 or pH 6.6 level of protection.

4/5/10 8:47 AM
Data Table=Primary_WS-AQCL-TpH66

Distributions

CritLoad_Target_pH=6.6, ANClimit=50 @DOC=0 (keq/ha/y)

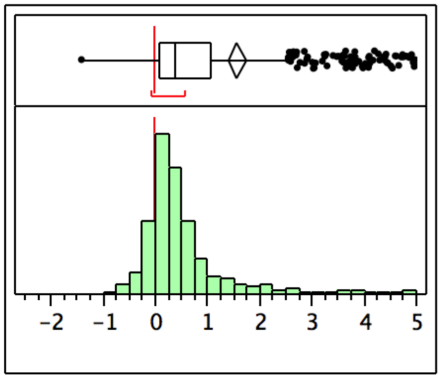

Quantiles		
100.0%	maximum	36.37
99.5%		17.52
97.5%		12.24
90.0%		5.12
75.0%	quartile	1.07
50.0%	median	0.39
25.0%	quartile	0.09314
10.0%		-0.12
2.5%		-0.48
0.5%		-0.82
0.0%	minimum	-1.40

Moments	
Mean	1.5632001
Std Dev	3.3421901
Std Err Mean	0.0868175
upper 95% Mean	1.7334983
lower 95% Mean	1.3929018
N	1482

Figure 3. Frequency Distribution of the Critical Load for Acidity estimated using the SSWC model for an ANC limit of 50 µeq/L, corresponding to a target pH of 6.6 at DOC = 0. Negative critical loads indicate that the ANC limit and target pH are not attainable due to low base cation supply from mineral weathering, high DOC or a combination of these factors.

Estimated 2002 atmospheric deposition of S+N acidity exceeded the critical load for 55% of the watersheds evaluated for the ANC=50 µeq/L at DOC=0 or pH 6.6 level of protection (Table 4.1). The percentage of watersheds with estimated 2018 atmospheric

deposition of S+N acidity exceeding the critical load dropped to 45% for this protection level (Table 4.1). There was a difference in percentage of sampled locations changing exceedance status between different surface water types. Proportionally more river and stream reaches switched from critical load exceeded to not-exceeded status than for wetlands, which improved slightly more than lakes and ponds, which in turn improved more than the small sample of reservoirs in the study.

4/5/10 8:48 AM
Data Table=Primary_WS-AQCL-TpH715

Distributions

CritLoad_Target_pH 7.15, ANClimit=100 @DOC=0 (keq/ha/y)

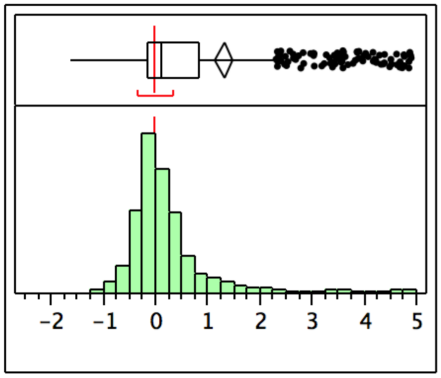

Quantiles		
100.0%	maximum	36.13
99.5%		17.32
97.5%		12.01
90.0%		4.91
75.0%	quartile	0.82
50.0%	median	0.13
25.0%	quartile	-0.17
10.0%		-0.40
2.5%		-0.80
0.5%		-1.11
0.0%	minimum	-1.63

Moments	
Mean	1.3125832
Std Dev	3.3567379
Std Err Mean	0.0871954
upper 95% Mean	1.4836227
lower 95% Mean	1.1415436
N	1482

Figure 4.4. Frequency Distribution of the Critical Load for Acidity estimated using the SSWC model for an ANC limit of 100 ueq/L, corresponding to a target pH of 7.15 at DOC = 0. Negative critical loads indicate that the ANC limit and target pH are not attainable due to low base cation supply from mineral weathering, high DOC or a combination of these factors.

Estimated 2002 atmospheric deposition of S+N acidity exceeded the critical load for 35% of the watersheds evaluated for the ANC=100 µeq/L at DOC=0 or pH 7.15 level of protection (Table 4.1). Recall that this level of protection was not attainable for 40% of watersheds, so the total surface water stations in the sample with pH < 7.15 at steady state is estimated to be 75%. The percentage of watersheds with estimated 2018 atmospheric deposition of S+N acidity exceeding the critical load dropped to 31% for this protection level (Table 4.1). As with the ANC=50 scenario, there was a difference in percentage of locations changing exceedance status between sampled different surface water types in the sample. Proportionally more river and stream reaches switched from critical load exceeded to not-exceeded status than for lakes and ponds, which improved more than wetlands. There was no change in estimated exceedance status between the 2002 and 2018 deposition scenarios for the small sample of reservoirs in the study in the ANC=100 µeq/L at DOC=0 or pH 7.15 runs.

The equations used for estimating the critical load and exceedance using the SSWC with DOC correction can be rearranged to solve for the steady-state pH value associated with a given load of acidity. Steady-state pH values associated with the 2002 and 2018 atmospheric S+N deposition scenarios were computed. These steady-state pH values can be compared with the observed (time of sampling) pH to establish the pH trend between the time of sampling condition and steady-state conditions associated with an atmospheric deposition scenario. If the steady-state pH for a deposition scenario is less than the observed

(time of sampling) pH the system is expected to acidify unless the atmospheric load is changed. If the steady-state pH for a deposition scenario is greater than the observed (time of sampling) pH the system is expected to improve (decrease acidity) unless the atmospheric load is changed. When combined with the critical load exceedance information the following classification scheme results.

- CL UNATTAINABLE, with further acidification expected
- CL UNATTAINABLE, with pH improvement (but not achievement of the target)
- CL EXCEEDED, with further acidification expected
- CL EXCEEDED, with pH improvement (but not achievement of the target)
- CL NOT EXCEEDED, with pH decline expected (but not below the target)
- CL NOT EXCEEDED, with pH increase (recovery to above the target)

Tables 4.2, 4.3, and 4.4 present the critical load exceedance status for the different deposition, protection level, and sensitivity analysis scenarios categorized by both exceedance status and pH trend (between present and steady-state implied pH). Also included in these tables are the mean exceedance values for each exceedance and pH trend category by surface water type. Generally, the 2018 deposition scenario results in anticipated pH improvement or recovery over the 2002 deposition scenario but with some exceptions.

The implications of the sensitivity analysis for uncertainty in the critical load and exceedance results is best illustrated by a comparative analysis of the cumulative frequency distributions of observed (time of sampling) pH and implied steady-state pH under the different scenarios (Figure 4.5). The difference between the results for the two atmospheric deposition scenarios is substantially greater than the difference between either the -10% NaCl or +25% DOC sensitivity analysis runs and the 2018 case (base for the sensitivitiy analysis). As also indicated in Table 4.3, the uncertainty in results arising from uncertainty in the Na and Cl analytical determinations and subsequent salt-correction calculations is typically less than a few percent. The uncertainty arising from the unknown potential future changes (likely to be increases) in DOC can be quite substantial (~30%) for high DOC waters where the target ANC and pH levels are unattainable. Therefore the degree of potential improvement (below the target level) or further degradation is highly uncertain in these systems. For systems where the target ANC and pH are attainable, the uncertainty introduced by potential changes in DOC appears to be more modest. However, individual waters and watersheds of specific concern should be evaluated for their current and potential DOC levels as changes in DOC may prevent some systems from attaining the target ANC and pH.

Table 4.1. Summary of exceedance status by surface water type under different deposition, target ANC-pH, and sensitivity analysis scenarios.

Target pH = 6.6, ANC = 50 @DOC = 0: Number of Surface Water Sampling Locations							
Year	**STATUS**	Total	*%Total*	LAKE/POND	RESERVOIR	RIVER/STREAM	WETLAND
2002	UNATTAINABLE	242	*16%*	140	1	72	29
	EXCEEDED	813	*55%*	546	23	219	25
	NOT EXCEEDED	427	*29%*	119	3	282	23
2018	UNATTAINABLE	242	*16%*	140	1	72	29
	EXCEEDED	673	*45%*	473	21	159	20
	NOT EXCEEDED	567	*38%*	192	5	342	28
Percent Change	UNATTAINABLE	0%	*0%*	0%	0%	0%	0%
	EXCEEDED	-17%	*-9%*	-13%	-9%	-27%	-20%
	NOT EXCEEDED	33%	*9%*	61%	67%	21%	22%
Target pH = 7.15, ANC = 100 @ DOC = 0: Number of Surface Water Sampling Stations							
Year	**STATUS**	Total	*%Total*	LAKE/POND	RESERVOIR	RIVER/STREAM	WETLAND
2002	UNATTAINABLE	595	*40%*	410	15	131	39
	EXCEEDED	526	*35%*	315	9	186	16
	NOT EXCEEDED	361	*24%*	80	3	256	22
2018	UNATTAINABLE	595	*40%*	410	15	131	39
	EXCEEDED	460	*31%*	278	9	158	15
	NOT EXCEEDED	427	*29%*	117	3	284	23
Percent Change	UNATTAINABLE	0%	*0%*	0%	0%	0%	0%
	EXCEEDED	-13%	*-4%*	-12%	0%	-15%	-6%
	NOT EXCEEDED	18%	*4%*	46%	0%	11%	5%
Sensitivity Analysis (2018) Target pH = 6.6, ANC = 50 @DOC = 0: % Change from Base							
Mode	**STATUS**	Total		LAKE/POND	RESERVOIR	RIVER/STREAM	WETLAND
-10% NaCl	UNATTAINABLE	1.2%		0.7%	0.0%	1.4%	3.4%
	EXCEEDED	0.6%		0.6%	0.0%	0.0%	5.0%
	NOT EXCEEDED	-1.2%		-2.1%	0.0%	-0.3%	-7.1%
+25% DOC	UNATTAINABLE	29%		22%	400%	35%	31%
	EXCEEDED	-7%		-5%	-19%	-6%	-25%
	NOT EXCEEDED	-4%		-3%	0%	-4%	-14%

Table 4.2. Summary of exceedance status and pH trend by surface water type under 2002 and 2018 estimated atmospheric deposition with a target pH of 6.6 corresponding to and ANC limit = 50 µeq/L at DOC = 0. The pH trend refers to direction of pH change indicated by the model between the present observed pH and the steady state modeled scenario pH. Undetermined refers to the situation where no present (observed) pH information was available.

Target pH = 6.6, ANC = 50 @DOC = 0							**Mean(EX(keq/ha/y))**			
STATUS(2002)	**pHTrend(2002)**	Total	LAKE/POND	RESERVOIR	RIVER/STREAM	WETLAND	LAKE/POND	RESERVOIR	RIVER/STREAM	WETLAND
UNATTAINABLE	ACIDIFYING	239	137	1	72	29	1.206	1.511	1.124	1.163
UNATTAINABLE	IMPROVING	3	3	0	0	0	1.366			
EXCEEDED	UNDETERMINED	1	0	0	1	0			0.598	
EXCEEDED	ACIDIFYING	738	495	21	197	25	0.620	0.841	0.473	0.434
EXCEEDED	IMPROVING	74	51	2	21	0	0.461	0.187	0.217	
NOT EXCEEDED	UNDETERMINED	8	0	0	8	0			-2.983	
NOT EXCEEDED	ACIDIFYING	89	25	0	48	16	-0.366		-4.752	-4.636
NOT EXCEEDED	RECOVERING	330	94	3	226	7	-1.437	-0.491	-5.388	-2.182
UNATTAINABLE		242	140	1	72	29				
EXCEEDED		813	546	23	219	25				
NOT EXCEEDED		427	119	3	282	23				
STATUS(2018)	**pHTrend(2018)**	Total	LAKE/POND	RESERVOIR	RIVER/STREAM	WETLAND	LAKE/POND	RESERVOIR	RIVER/STREAM	WETLAND
UNATTAINABLE	ACIDIFYING	209	108	1	71	29	0.896	1.217	0.868	0.948
UNATTAINABLE	IMPROVING	33	32	0	1	0	0.937		1.677	
EXCEEDED	UNDETERMINED	1	0	0	1	0			0.190	
EXCEEDED	ACIDIFYING	476	309	19	128	20	0.423	0.507	0.305	0.274
EXCEEDED	IMPROVING	196	164	2	30	0	0.323	0.584	0.285	
NOT EXCEEDED	UNDETERMINED	8	0	0	8	0			-3.318	
NOT EXCEEDED	ACIDIFYING	103	24	0	58	21	-0.260		-4.046	-3.694
NOT EXCEEDED	RECOVERING	456	168	5	276	7	-1.048	-0.507	-4.690	-2.383
UNATTAINABLE		242	140	1	72	29				
EXCEEDED		673	473	21	159	20				
NOT EXCEEDED		567	192	5	342	28				
Percent Change (2018 - 2002) Target pH = 6.6, ANC = 50 @DOC = 0										
STATUS	**pH Trend**	Total	LAKE/POND	RESERVOIR	RIVER/STREAM	WETLAND	LAKE/POND	RESERVOIR	RIVER/STREAM	WETLAND
UNATTAINABLE	ACIDIFYING	-13%	-21%	0%	-1%	0%	-26%	-19%	-23%	-19%
UNATTAINABLE	IMPROVING	1000%	967%				-31%			
EXCEEDED	UNDETERMINED	0%			0%				-68%	
EXCEEDED	ACIDIFYING	-36%	-38%	-10%	-35%	-20%	-32%	-40%	-36%	-37%
EXCEEDED	IMPROVING	165%	222%	0%	43%		-30%	212%	31%	
NOT EXCEEDED	UNDETERMINED	0%			0%				11%	
NOT EXCEEDED	ACIDIFYING	16%	-4%		21%	31%	-29%		-15%	-20%
NOT EXCEEDED	RECOVERING	38%	79%	67%	22%	0%	-27%	3%	-13%	9%
UNATTAINABLE		0%	0%	0%	0%	0%				
EXCEEDED		-17%	-13%	-9%	-27%	-20%				
NOT EXCEEDED		33%	61%	67%	21%	22%				

Table 4.3. Percent change from standard run in exceedance status and pH trend by surface water type under 2018 estimated atmospheric deposition with a target pH of 6.6 corresponding to and ANC limit = 50 μeq/L at DOC = 0 under different sensitivity analysis assumptions. The pH trend refers to direction of pH change indicated by the model between the present observed pH and the steady state modeled scenario pH. Undetermined refers to the situation where no present (observed) pH information was available.

Sensitivity Analysis (2018) Target pH = 6.6, ANC = 50 @DOC = 0										
Percent Change with -10% NaCl										
STATUS	**pHTrend**	Total	LAKE/POND	RESERVOIR	RIVER/STREAM	WETLAND	LAKE/POND	RESERVOIR	RIVER/STREAM	WETLAND
UNATTAINABLE	ACIDIFYING	1.0%	0.0%	0.0%	1.4%	3.4%	0.3%	1.4%	0.3%	-1.3%
UNATTAINABLE	IMPROVING	3.0%	3.1%		0.0%		1.1%		-0.1%	
EXCEEDED	UNDETERMINED	0.0%			0.0%				-3.3%	
EXCEEDED	ACIDIFYING	0.8%	0.3%	0.0%	1.6%	5.0%	0.1%	0.7%	-0.2%	-9.3%
EXCEEDED	IMPROVING	0.0%	1.2%	0.0%	-6.7%		-2.4%	2.0%	7.2%	
NOT EXCEEDED	UNDETERMINED	0.0%			0.0%				-0.1%	
NOT EXCEEDED	ACIDIFYING	-4.9%	-20.8%		3.4%	-9.5%	12.8%		-3.5%	11.4%
NOT EXCEEDED	RECOVERING	-0.4%	0.6%	0.0%	-1.1%	0.0%	-2.2%	-2.0%	1.5%	2.1%
UNATTAINABLE		1.2%	0.7%	0.0%	1.4%	3.4%				
EXCEEDED		0.6%	0.6%	0.0%	0.0%	5.0%				
NOT EXCEEDED		-1.2%	-2.1%	0.0%	-0.3%	-7.1%				
Percent Change with +25% DOC										
STATUS	**pHTrend**	Total	LAKE/POND	RESERVOIR	RIVER/STREAM	WETLAND	LAKE/POND	RESERVOIR	RIVER/STREAM	WETLAND
UNATTAINABLE	ACIDIFYING	35%	32%	400%	35%	31%	5%	-27%	9%	9%
UNATTAINABLE	IMPROVING	-12%	-13%		0%		5%		4%	
EXCEEDED	UNDETERMINED	0%			0%				25%	
EXCEEDED	ACIDIFYING	-6%	-6%	-16%	-3%	-25%	0%	0%	2%	-14%
EXCEEDED	IMPROVING	-8%	-5%	-50%	-20%		-4%	-8%	2%	
NOT EXCEEDED	UNDETERMINED	0%			0%				0%	
NOT EXCEEDED	ACIDIFYING	7%	-17%		22%	-10%	15%		31%	18%
NOT EXCEEDED	RECOVERING	-7%	-1%	0%	-10%	-29%	0%	0%	-2%	-28%
UNATTAINABLE		29%	22%	400%	35%	31%				
EXCEEDED		-7%	-5%	-19%	-6%	-25%				
NOT EXCEEDED		-4%	-3%	0%	-4%	-14%				

Table 4.4. Summary of exceedance status and pH trend by surface water type under 2002 and 2018 estimated atmospheric deposition with a target pH of 7.15 corresponding to an ANC limit = 100 μeq/L at DOC = 0. The pH trend refers to direction of pH change indicated by the model between the present observed pH and the steady state modeled scenario pH. Undetermined refers to the situation where no present (observed) pH information was available.

Target pH = 7.15, ANC = 100 @ DOC = 0							**Mean(EX(keq/ha/y))**			
STATUS(2002)	**pHTrend(2002)**	Total	LAKE/POND	RESERVOIR	RIVER/STREAM	WETLAND	LAKE/POND	RESERVOIR	RIVER/STREAM	WETLAND
UNATTAINABLE	ACIDIFYING	568	385	15	129	39	1.221	1.200	1.208	1.265
UNATTAINABLE	IMPROVING	27	25	0	2	0	1.232		1.449	
EXCEEDED	UNDETERMINED	1	0	0	1	0			0.876	
EXCEEDED	ACIDIFYING	440	262	7	155	16	0.636	0.969	0.593	0.521
EXCEEDED	IMPROVING	85	53	2	30	0	0.290	0.404	0.274	
NOT EXCEEDED	UNDETERMINED	8	0	0	8	0			-2.765	
NOT EXCEEDED	ACIDIFYING	58	10	0	33	15	-0.583		-6.642	-4.718
NOT EXCEEDED	RECOVERING	295	70	3	215	7	-1.654	-0.264	-5.434	-1.956
UNATTAINABLE		595	410	15	131	39				
EXCEEDED		526	315	9	186	16				
NOT EXCEEDED		361	80	3	256	22				
STATUS(2018)	**pHTrend(2018)**	Total	LAKE/POND	RESERVOIR	RIVER/STREAM	WETLAND	LAKE/POND	RESERVOIR	RIVER/STREAM	WETLAND
UNATTAINABLE	ACIDIFYING	468	299	14	116	39	0.913	0.876	0.978	1.048
UNATTAINABLE	IMPROVING	127	111	1	15	0	0.961	0.921	0.910	
EXCEEDED	UNDETERMINED	1	0	0	1	0			0.468	
EXCEEDED	ACIDIFYING	264	133	6	110	15	0.475	0.588	0.403	0.319
EXCEEDED	IMPROVING	195	145	3	47	0	0.263	0.388	0.203	
NOT EXCEEDED	UNDETERMINED	8	0	0	8	0			-3.099	
NOT EXCEEDED	ACIDIFYING	56	9	0	31	16	-0.363		-7.259	-4.609
NOT EXCEEDED	RECOVERING	363	108	3	245	7	-1.329	-0.558	-5.043	-2.157
UNATTAINABLE		595	410	15	131	39				
EXCEEDED		460	278	9	158	15				
NOT EXCEEDED		427	117	3	284	23				
Percent Change (2018 - 2002) Target pH = 6.6, ANC = 50 @DOC = 0										
STATUS	**pH Trend**	Total	LAKE/POND	RESERVOIR	RIVER/STREAM	WETLAND	LAKE/POND	RESERVOIR	RIVER/STREAM	WETLAND
UNATTAINABLE	ACIDIFYING	-18%	-22%	-7%	-10%	0%	-25%	-27%	-19%	-17%
UNATTAINABLE	IMPROVING	370%	344%		650%		-22%		-37%	
EXCEEDED	UNDETERMINED	0%			0%				-47%	
EXCEEDED	ACIDIFYING	-40%	-49%	-14%	-29%	-6%	-25%	-39%	-32%	-39%
EXCEEDED	IMPROVING	129%	174%	50%	57%		-9%	-4%	-26%	
NOT EXCEEDED	UNDETERMINED	0%			0%				12%	
NOT EXCEEDED	ACIDIFYING	-3%	-10%		-6%	7%	-38%		9%	-2%
NOT EXCEEDED	RECOVERING	23%	54%	0%	14%	0%	-20%	111%	-7%	10%
UNATTAINABLE		0%	0%	0%	0%	0%				
EXCEEDED		-13%	-12%	0%	-15%	-6%				
NOT EXCEEDED		18%	46%	0%	11%	5%				

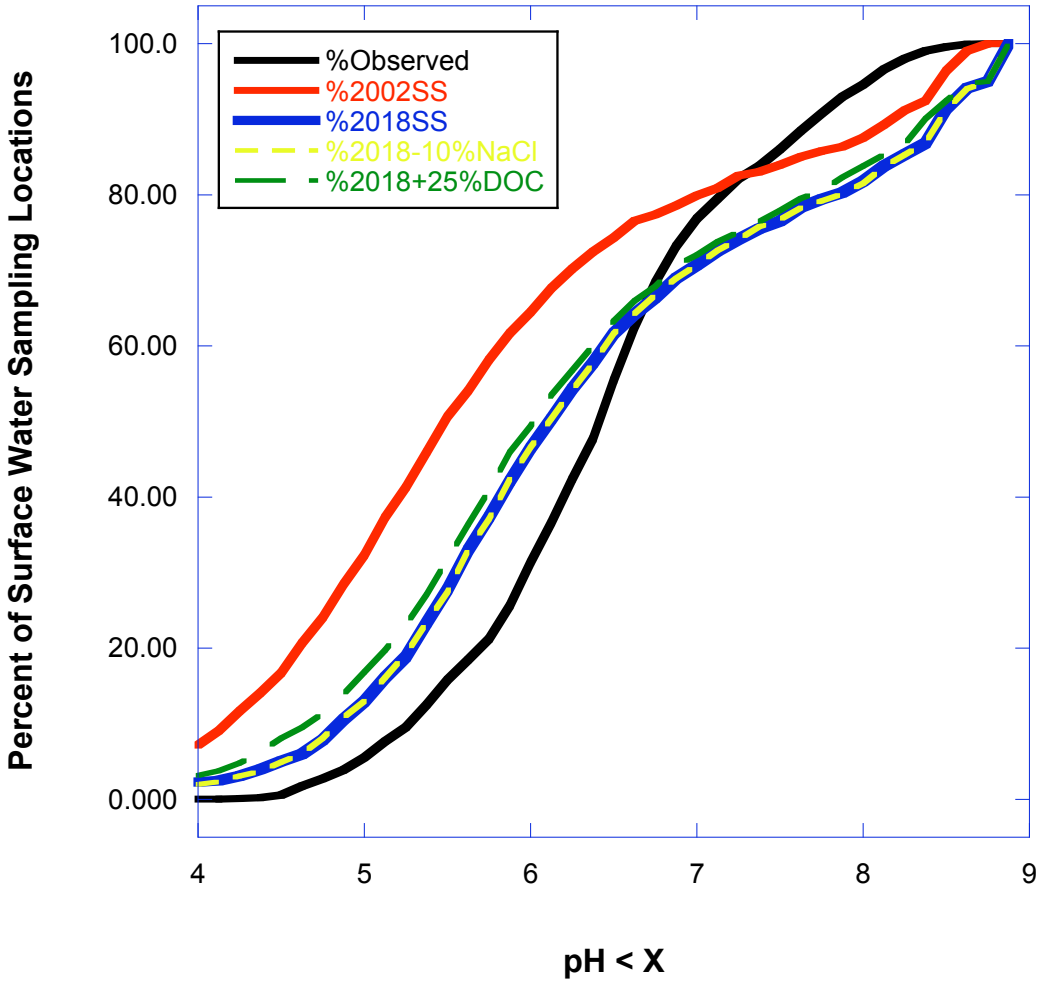

Figure 4.5. Cummulative frequency distributions of evaluated surface water stations for observed (present) pH (black line), 2002 deposition scenario implied steady-state pH (red line), 2018 deposition secenario implied steady-state pH (blue line), 2018 deposition secenario with -10% NaCl implied steady-state pH (dashed yellow line), and 2018 deposition secenario with +25% DOC implied steady-state pH (dashed green line).

Attempted spatial extrapolation of SSWC watershed results

One approach explored for obtaining a regional assesmment of critical loads for all surface waters in the northeast was to attempt to generalize the results of the 1482 specific water-body analyses described above. The project plan called for exploring and developing an empirical statistical extrapolation of the specific water body results by relating either the critical load or components of the critical load calculation to landscape information from the terrestrial ecosystem assessment and other available sources. Watershed average (or total as appropriate) values of all available data layers were computed. These values were systematically explored via general linear modeling for predictive ability with respect to the SSWC critical load and components of the critical load calculation.

No model to directly predict the critical load could be produced that explained more than 40% of variance across all types of water bodies. However, there was large amount of variance associated with critical loads greater than 3 keq/ha/y, a very high rate of S+N deposition not frequently expected for the region. Therefore, the variance in critical load was compressed by capping critical load values at 3 keq/ha/y. This capping of the critical load improved the amount of variance explained to only 58% (Figure 4.6). Allthough this model could explain 58% of the capped critical load variance, the residuals were frequently quite large for well-studied water bodies.

4/19/10 8:34 PM
Data Table=extrap-set2-TpH66

Response Midpoint Cap3-CL(keq/ha/y)

Summary of Fit

RSquare	0.579964
RSquare Adj	0.569118
Root Mean Square Error	0.74133
Mean of Response	0.855373
Observations (or Sum Wgts)	1312

Analysis of Variance

Source	DF	Sum of Squares	Mean Square	F Ratio
Model	33	969.7684	29.3869	53.4725
Error	1278	702.3512	0.5496	Prob > F
C. Total	1311	1672.1196		<.0001*

Effect Tests

Source	Nparm	DF	Sum of Squares	F Ratio	Prob > F
LATITUDE	1	1	41.847204	76.1453	<.0001*
LONGITUDE	1	1	19.855379	36.1289	<.0001*
Outlet-Elevation(m)	1	1	27.900815	50.7684	<.0001*
WS-BCflux	1	1	3.550206	6.4600	0.0112*
FlowAvg-Qflux(cm)	1	1	6.632170	12.0679	0.0005*
WS-BCflux*FlowAvg-Qflux(cm)	1	1	21.457521	39.0442	<.0001*
LONGITUDE*Outlet-Elevation(m)	1	1	60.817478	110.6636	<.0001*
WS-BCflux*Outlet-Elevation(m)	1	1	7.704036	14.0183	0.0002*
CaDep(keq/ha/y)	1	1	25.017815	45.5225	<.0001*
ClDep(keq/ha/y)	1	1	3.511702	6.3899	0.0116*
PRISM-ppt(cm/y)	1	1	7.847218	14.2788	0.0002*
SW_TYPE	3	3	99.574591	60.3954	<.0001*
FlowAvg-Boreal	1	1	14.035748	25.5395	<.0001*
FlowAvg-Wetland	1	1	7.431461	13.5223	0.0002*
FlowAvg-Boreal*FlowAvg-Wetland	1	1	3.718661	6.7665	0.0094*
NLCD-WetlandCell	1	1	4.094119	7.4497	0.0064*
QsurfCode	6	6	25.436064	7.7139	<.0001*
Cell-Toposhape	9	9	9.823742	1.9861	0.0376*

Figure 4.6. Best-fit SSWC regional extrapolation model with critical load capped at 3 keq/ha/y.

Landscape Mass-Balance (LMB) Approach

The "Landscape Mass Balance Approach" developed here[11] is conceptually similar to the first-order acidity balance and SSWC approaches in that that they are all derived from the steady-state mass balance framework (Hindar et al. 2000, ICP Mapping Manual 2004).

[11] In the initial submission of this report the method was simply categorized as a form of the FAB approach. As one reviewer strongly objected to this designation, we have changed the name of the approach to the "Landscape Mass-Balance Approach" (LMB) to emphasize the integration of sources and sinks of acidity over the entire landscape upstream of a given stream reach, lake or pond. We are not trying to make a claim of developing a "new" method by using this nomenclature, rather we are trying to accommodate different reviewer sensibilities. Two out of 3 reviewers were satisfied with the designation of this approach under the FAB umbrella. We consider the approach (like the FAB) to be a variant of the simple steady-state-mass balance method (ICP Mapping Manual 2004). An additional difference between LMB and FAB is that FAB makes the implicit assumption that observations of inlet and outlet chemistry can provide a good estimate of steady-state in-lake processing of N and BC. As discussed elsewhere in this document, few systems are currently in steady-state so this is a poor assumption. We have avoided this weakness in the LMB.

CL (S+N Acidity) $= BC_0 - ANC_{limit}$
$= Q * ([BC]_0 - [ANC]_{limit})$

However, in the LMB, BC_0 is estimated directly[12] from the watershed sinks for acidity and the acidity source related to base cation uptake as:

$BC_0 = TBC_{wx} + BC_{dep} - TBC_{uptake}$ *(flow-weighted average),*

where all of the terms on the right hand side are flow-weighted averages (described below) rather than from observations of water chemistry. In the implmentation in this project total base cation weathering (TBC_{wx}) is taken from the terrestrial ecosystem soil estimate (Soil Layer BC_{wx}) modified by a factor related to the character of the bedrock (calcareous / other) and surfical materials (Soller 1990) mapped in a grid cell.

TBC_{wx} = Soil Layer BC_{wx} (from terrestrial assessment) * QSURF

where QSURF was the the mean ratio between a given surfical material class and the thin till type class of BC_0 calcuated for the training sites from surface water data. It was assumed (based on the design of the terrestrial analysis) that Soil Layer BC_{wx} was representative of weathering rates in thin till type soils. The Soil Layer BC_{wx} rates were modified accordingly by geologic material class (calcareous bedrock, thin till, deep till, coarse-grained stratified sediment, fine-grained stratified sediment, and organic sediment).

Geologic Material	**Ratio to Thin Till Class BC_0 Estimate**
Calcareous bedrock	2.90
Fine-grained stratified sediment	2.22
Coarse-grained stratified sediment	1.62
Deep Till	1.44
Thin Till	1.0
Organic sediment	1.0

The net sources of acidity are similarly calculated from the watershed data as:

Total Acidity = $Cl_{dep} + S_{dep} + N_{dep} - TN_{uptake}$ *(flow-weighted average)*

where again, the terms on the right hand side are the flow-weighted averages (described below).

[12] as opposed to by inference from observed surface water chemistry with all of the difficulties associated by the assumptions used in the standard inference methods (see text above).

Flow-weighted average data in the LMB approach

Surface waters for the LMB approach were defined as any grid cell classified as water in the USGS NLCD. LMB calculations (described above) were carried out for every landscape grid cell in the model domain as if each cell were a water chemistry sampling location. The contribution of acidity sources and sinks from upstream grid cells (land and water) were determined using IDRISI™ software with the required data layers from the terrestrial ecosystem analysis (see Section 3 of this document). The proceedure was as follows:

1. The flow network was calculated from the 90-meter DEM after pit-removal (Figure 4.7) using the IDRISI FLOW and PITREMOVAL tools.
2. Parameter values at each grid cell contributing flow were accumulated along the flow network using the IDRISI™ RUNOFF tool.
3. At each grid cell along the flow network, the contributing watershed area was calculated as well as the number of contributing grid cells calculated using the IDRISI™ RUNOFF tool.
4. The flow-accumulated parameter value totals were divided by the number of contributing grid cells or contributing area (whichever was appropriate) to yield the average value of a parameter associated with water flowing into each grid cell.

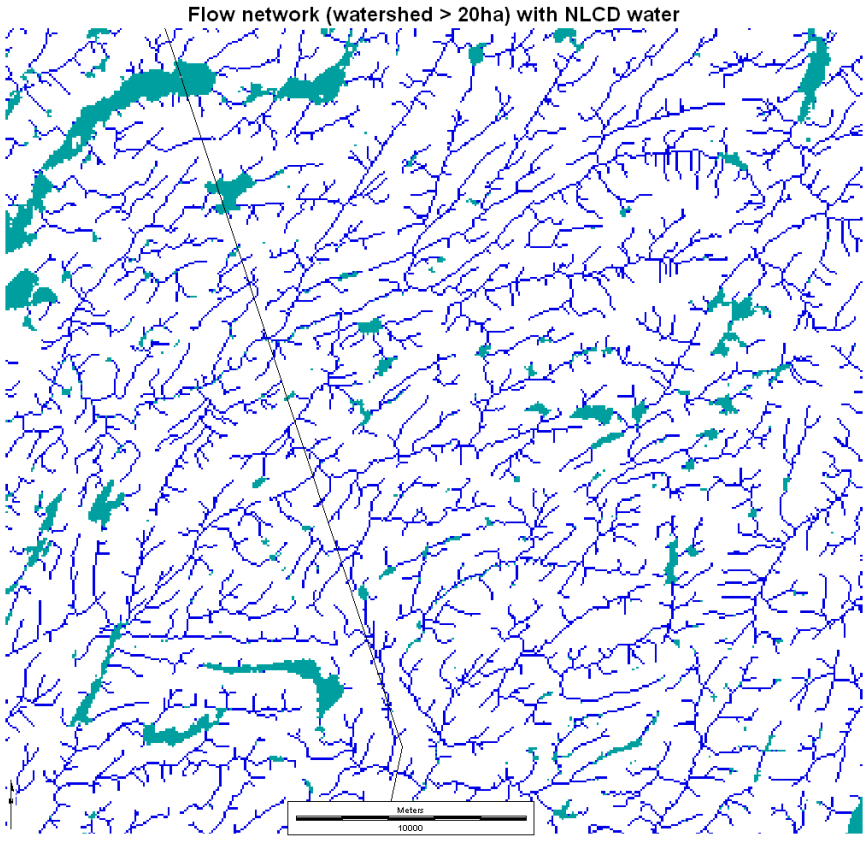

Figure 4.7. Flow network calculated from the 90-meter DEM. Blue areas are flow network segmenst with watershed contributing areas greater than 20 ha. Green areas are classified as water in the NLCD.

LMB calculations on these flow-accumulated source/sink grids yeilded a continuous representation of the aquatic ecosystem critical load across the landscape (Figure 4.8). Thus, values reprsenting the accumlated watershed contribution to the aquatic critical load at any grid cell on the flow network are stored in each grid cell representing land while the effective critical load for a surface water reach or element is represented in the grid cells classified as water.

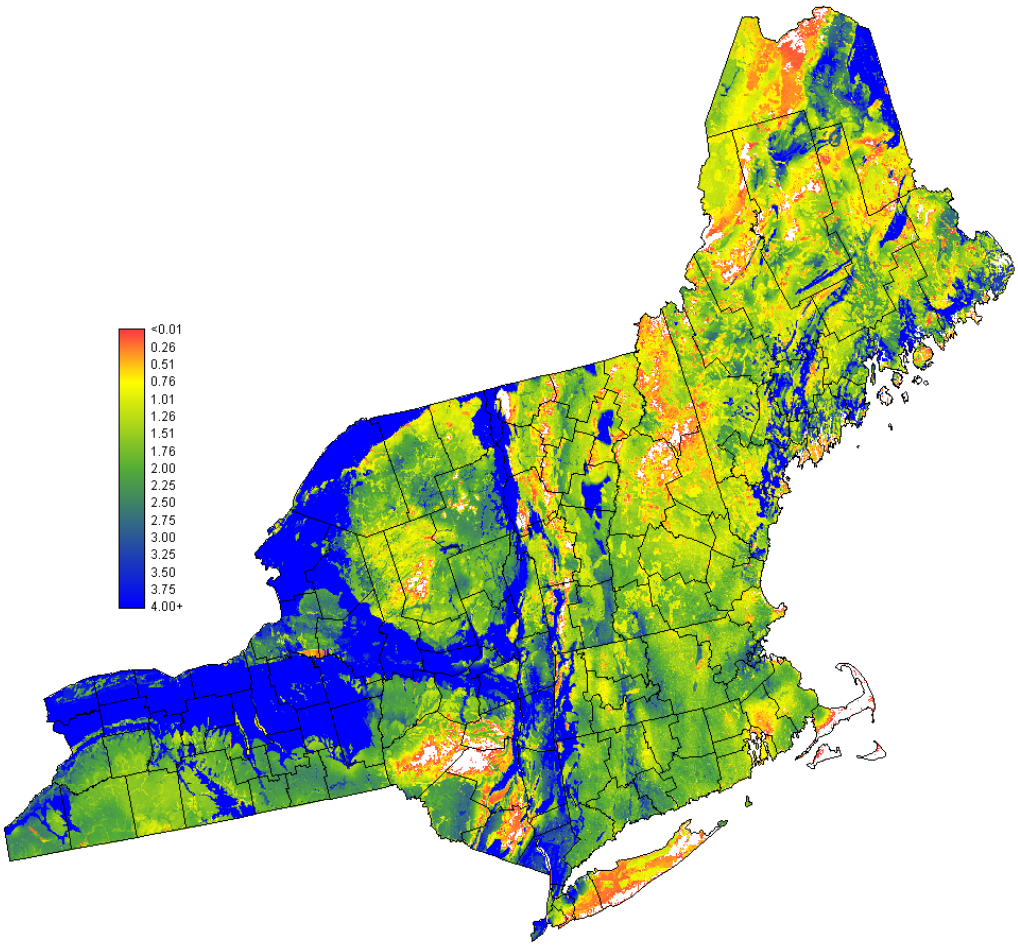

Figure 4.8. Continuous representation of LMB aquatic critical load (keq/ha/y S+N deposition) associated with a target pH of 6.6. The critical load is calculated for each grid cell in the flow network including land areas of a watershed. White areas internal to the figure are regions where the critical load is less than zero. This means that geologic, DOC, and other condtions are such that the target pH can not be reached.

Scenarios with Approach 2, LMB

Landscape mass-balance modeling (LMB) was conducted for two critical threshold scenarios, each with two atmospheric deposition scenarios.

1. Target pH = 6.6, Implied ANC limit = 50 μeq/L at DOC = 0, Deposition 2002, 2018

2. Target pH = 7.15, Implied ANC limit = 100μeq/L at DOC = 0, Deposition 2002, 2018

The results are continuous grids of representing the flow-averaged contribution of all upstream watershed area to the aquatic ecosystem critical load at a given grid cell (Figure 4.8). The end user is free to tabluate these results in different ways depending on the goals of each end user's analysis. A value representing the critical load representative of a specific water body (lake, pond) may be obtained by extracting the data for the grid cell associated with the lake outlet. Care should be taken to check for georeferencing errors and to be sure the sample point coordinates extract the appropriate value from the grid. Similarly, the critical load for any given stream reach can be retrieved by extracting the value for either the highest or the lowest elevation point on the reach stream reach. Selecting the value corresponding to the highest elevation point on a reach would generally provide the lowest critical load (as critical loads tend to increase downstream) for the reach. Selecting the value associated with the lowest elevation point on the reach would typicaly provide the maximum critical load for the reach.

Because there are a large number of valid ways to tablulate and/or map the aquatic critical loads and exceedances developed for the regional assessment only two examples of the possibilites are provided here (Figures 4.8 and 4.9).

Significant sources of uncertainty in the aquatic critical loads assessment

Less than 50% of variance in training site DOC concentration was explained by the regional model for surface water DOC. As the regionalized DOC estimate was used to adjust the ANC_{limit} to produce the desired target pH, the uncertainty in DOC estimates translates directly to uncertainty in the ANC_{limit}. The terrestrial root zone soil mineral weathering rate scaled by surficial geology class was used to estimate weathering inputs of base cations to the aquatic systems. There is evidence of considerable weathering at the soil/bedrock interface in shallow soils (Miller et al. 1993, Munroe et al. 2007) and in deep till and stratified sediments of large aquifers. The simple empirical scheme for increaseing the soil-layer weathering rate to account for deeper layer weathering could be considerably improved. Still, any method based on available data for the entire region would not be able to account for subsurface (or unmapped) geologic variations from the surface map that influence conditions in a deep flow path. There were no data available suitable for evaluating the effects of internal SO_4 retention/release on the SSWC BC_0 estimates used to calibrated deep weathering rates for the LMB the model. However, there were strong indications of SO_4 retention or release for many of the training sites and the phenomena have been established as frequently important in the region (Mitchell et al. 2010).

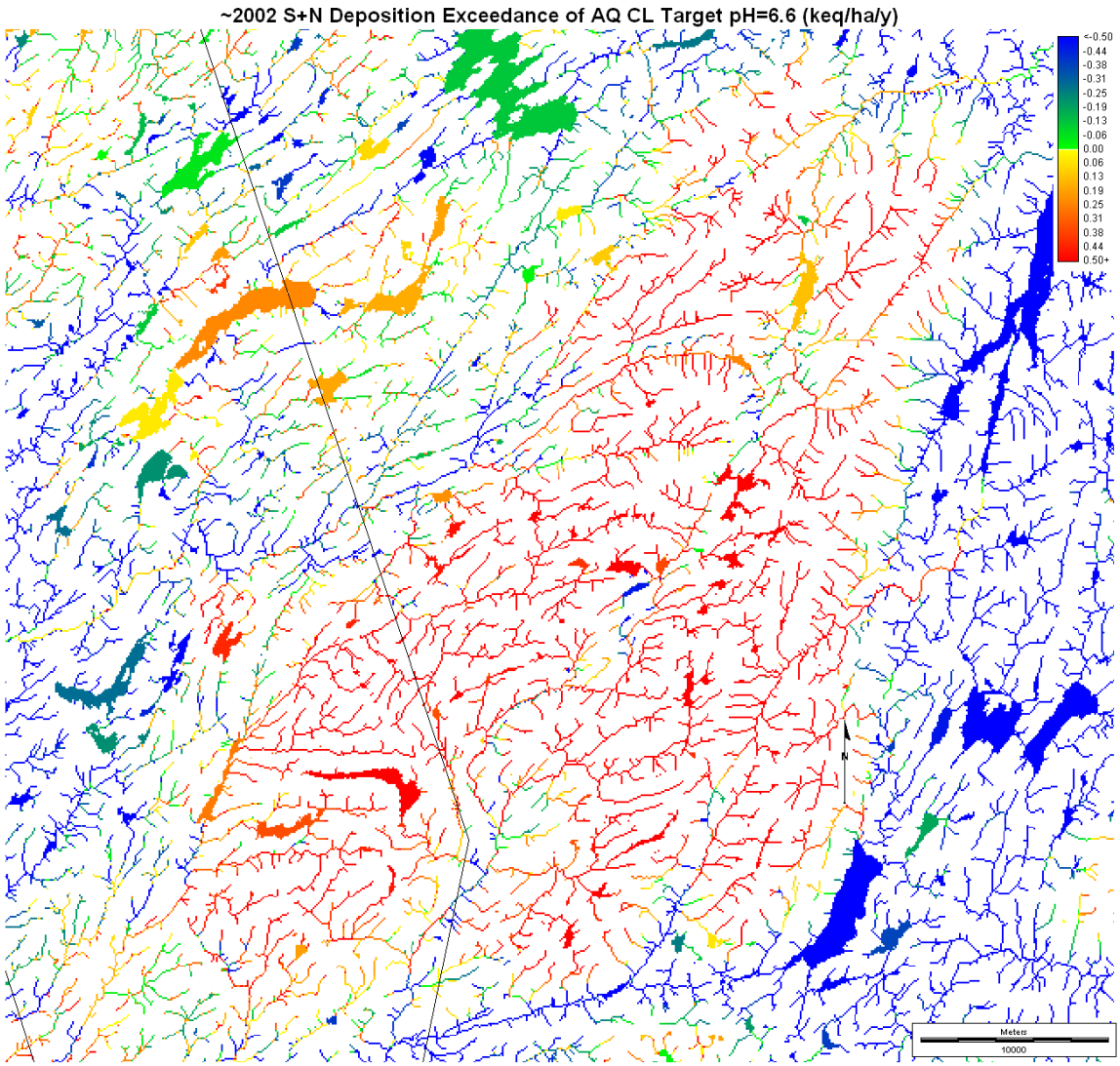

Figure 4.9. Example of flow network (locations with upstream watershed area greater than 20 ha) representation of 2002 critical load exceedance for a target pH of 6.6 in the southwestern Adirondack Mountains, NY.

Comparison of LMB steady-state critical load and exceedance results to indpendent metrics of surface water acid sensitivity

As stated above, few (if any) ecosystems in the Northeastern US are currently at steady state with respect to atmospheric deposition, climatic, and land-use conditions. Therefore, the end-user of this assessment should not harbor the expectation that a map of steady-state critical load exceedance should have a 1:1 correspondence with current or historic observations of ecosystem condtions (e.g. pH, ANC). The maps produced using the LMB analysis convey information about a ***potential future condition*** of the ecosystem ***if it were to reach steady-state*** with respect to the inputs and conditions of the modeled scenario. Given this constraint associated with steady-state modeling how can we compare the model with observations in a meaningful way? Such comparisons are difficult if not impossible (Rapp 2001). However, we can reasonably argue that systems for which the observed surface water pH has remained above the critical threshold of pH 6.6 for the entire period of record are less acid sensitive than systems that have exhibited a pH of 6.6 or lower during the period as a result of historical and recent atmospheric deposition levels. We compared the LMB estimates of critical load and exceedance to this simple "pH status" metric to determine if the LMB approach was indicating the relative acid sensitivity of surface waters similarly to the "pH status" metric over the full Northeastern domain and in the well-studied Adirondack Park Region of NY state.

The LMB modeled critical loads for S+N acidity seem to reasonably reflect the observed differences in acid sensitivity as reflected by surface water pH in the Adirondack Park Region sampled during 1992-2008 (ALSC[13], Driscoll et al. 2003). There was a statistically significant difference (one-sided t-test, unequal variances, $p = 0.0051$) in the lake-watershed spatial averages of the modeled aquatic steady-state pH 6.6 critical load between lakes that have exhibited a pH < 6.6 (mean CL =1.19 keq/ha/y) and lakes for which pH remained >= 6.6 (mean 1.90 keq/ha/y). This correspondence between a model result and the observations suggests that the critical load modeling process and underlying data layers are discriminating observed differences in acid sensitivity in the Adirondack Region.

There was also a statistically significant difference (one-sided t-test, unequal variances, $p < 0.0001$) in the percentage of lake-watershed area where 2002 estimated atmospheric deposition exceeded the modeled aquatic steady-state pH 6.6 critical load for lakes that have exhibited a pH < 6.6 (mean = 32.6%) and lakes for which pH remained >= 6.6 (mean = 3.7%) for the ALSC data. Thus, the critical load exceedance estimates based on 2002 atmospheric deposition are also consistent with observed differences in acid sensitivity in the Adirondack Region.

The findings of consistency between the steady-state critical loads and exceedance estimates of acid sensitive areas and surface water based measures of acid sensitivity (observed pH above or below the critical threshold) that were apparent in the Adirondack region are also apparent when compared to surface water observations from throughout the Northeast. The average LMB estimate of aquatic steady-state critical load (relative to a critical threshold of pH 6.6) estimated for the watersheds associated with sample points

[13] http://www.adirondacklakessurvey.org/ltmpage.html

described above for the SSWC analysis (including lakes, ponds, and stream reaches) was significantly less (one-sided t-test, unequal variances, $p < 0.0001$, n=1200) for watersheds exhibiting surface water pH < 6.6 (mean = 1.28 keq/ha/y) than for watersheds exhibiting pH >= 6.6 (mean 1.93 keq/ha/y). Similarly, the average LMB estimate of aquatic steady-state critical load exceedance estimated for the watersheds associated with sample points (including lakes, ponds, and stream reaches) was significantly greater (one-sided t-test, unequal variances, $p < 0.0001$, n=1200) for watersheds exhibiting surface water pH < 6.6 (mean = -0.31 keq/ha/y) than for watersheds with surface waters exhibiting pH >= 6.6 (mean -1.00 keq/ha/y).

The LMB regional steady-state analysis results are also consistent with the spatial patterns evident in published accounts of aquatic systems that are observed to be **on a path to** recovery (increasing pH or ANC trends) and those that are not recovering or continuing to acidify. The results of our analysis generally agree with spatial patterns described in earlier studies (e.g., Stoddard et al. 2003; Burns et al. 2006), which indicated initial signs of recovering surface water ANC and pH in the Adirondack Mountains region (relatively Ca-rich anorthosite bedrock) but a more limited recovery in the Catskill Mountains (sandstone, base-poor geology) and no recovery in much of New England (in areas of less base-rich metamorphic rocks and sandstone). Differences in rates of base cation removal due to timber harvesting between the regions (see sections 3 and 5) also likely play a significant role in the observed spatial patterns of projected recovery (or lack of recovery).

The indication given by the LMB regional steady-state assessment that 2002 estimated atmospheric deposition of S and N did not exceed the steady state critical load for large areas of the Adirondacks is consistent with the result of Driscoll et al. (2003). Driscoll et al. 2003 state:

"For the entire group, 29 of the 48 ALTM lakes had significant trends of increasing ANC ($p < 0.1$) for the period 1992-2000. Twenty-one of the 26 thin till drainage lakes exhibited increases in ANC. This pattern of increasing ANC has never been previously reported for large numbers of Adirondack Lakes. The mean rate of ANC increase for lakes showing a significant trend over the 1992-2000 interval was 1.60 μequiv L^{-1} yr^{-1}. This recent increase in ANC can be attributed to the fact that both SO_4^{2-} and NO_3^- concentrations have been decreasing, resulting in a marked rate of decline in the sum of strong acid anions."

References – Section 4

Burns, D.A., M.R. McHale, C.T. Driscoll, and K.M. Roy. 2006. Response of surface water chemistry to reduced levels of acid precipitation: comparison of trends in two regions of New York, USA. Hydrological Processes, 20: 1611-1627.

Dingman, S.L. (1994). *Physical Hydrology*. Macmillan College Publishing Company, New York 575p.

Driscoll, C.T., K.M. Driscoll, K.M. Roy and M.J. Mitchell. 2003. Chemical response of lakes in the Adirondack region to declines in acidic deposition. *Environ. Sci. Technol.* 37:2036-2042.

Dupont, J., T.A. Clair, C. Gagnon, D.S. Jeffries, J.S. Kahl, S J. Nelson, and J.M. Peckenham. 2005. Estimation of critical loads of acidity for lakes in northeastern United States and eastern Canada. *Environmental Monitoring and Assessment* 109:275-291.

Henriksen A., and M. Posch. 2001. Steady-state models for calculating critical loads of acidity for surface waters. *Water, Air and Soil Pollution Focus* 1:375-398.

Hindar A., M. Posch, A. Henriksen, J. Gunn, and E. Snucins. 2000. Development and application of the FAB model to calculate critical loads of S and N for lakes in the Killarney Provincial Park (Ontario, Canada). Report SNO 4202-2000, Norwegian Institute for Water Research, Oslo, Norway, 40 pp.

ICP Mapping Manual (2004) International Cooperative Programme on Modelling and Mapping of Critical Loads and Levels and Air Pollution Effects, Risks and Trends, UNECE Convention on Long-range Transboundary Air Pollution. *Manual on Methodologies and criteria for Modelling and Mapping of Critical Loads and Levels and Air Pollution Effects, Risks and Trends.* (http://icpmapping.org/cms/zeigeBereich/5/manual-und-downloads.html)

Miller, E.K., J.D. Blum and A.J. Friedland (1993) Determination of Soil Exchangeable-Cation Loss and Weathering Rates Using Sr Isotopes, *Nature*, 362:438-441.

Miller, E.K. 2006. Assessment of Forest Sensitivity to Nitrogen and Sulfur Deposition in Maine. Technical report prepared on behalf of the Conference of New England Governors' and Eastern Canadian Premiers' Forest Mapping Group, 15 December 2006, for the Maine Department of Environmental Protection, Bureau of Air Quality, Statehouse Station #17, Augusta, ME 04333.

Mitchell, M.J., G. Lovett, S. Bailey, F. Beall, D. Burns, D. Buso. T. A. Clair, F. Courchesne, L. Duchesne, C. Eimers, D.Jeffries, S. Kahl,, G. Likens, M.D. Moran, C. Rogers, D. Schwede, J. Shanley, K. Weathers and R. Vet. 2010. Comparisons of Watershed Sulfur Budgets in

Southeast Canada and Northeast US: New Approaches and Implications. *Biogeochemistry* (In Press).

Monteith, D.T., J.L. Stoddard, C.D. Evans, H.A. de Wit, M. Forsius, T. Hogasen, A. Vilander, B.L. Skjelkvale, D.S. Jeffries, J. Vuorenmaa, B. Keller, J. Kopacek, and J. Vesely (2007) Dissolved organic carbon trends resulting from changes in atmospheric deposition chemistry. *Nature* 450: 537-540.

Morel, F.M-M. and J.G. Hering. 1993. *Principles and Applications of Aquatic Chemistry*. Wiley, New York. 588p.

Munroe, J.S., G. Farrugia, and P.C. Ryan. 2007. Parent material and chemical weathering in alpine soils on Mt. Mansfield, Vermont, USA. Catena 70: 39-48.

NESCAUM, 2006. Contributions to Regional Haze in the Northeast and Mid-Atlantic United States, Technical Report for the MANE-VU Regional Planning Organization, NESCAUM, Boston, MA, August, 2006 (See http://www.nescaum.org/documents/ contributions-to-regional-haze-in-the-northeast-and-mid-atlantic--united-states/)

NHDES 2004. Total Maximum Daily Load (TMDL) for 65 Acid Impaired New Hampshire Ponds (FINAL). R-WD-04-17, NHDES, Concord, NH.

Rapp, L. 2001. Critical Loads of Acid Deposition for Surface Water - Exploring existing models and a potential alternative for Sweden. Doctor's dissertation. ISSN 1401-6230, ISBN 91-576-6091-3

Rapp, L. and K. Bishop. 2009. Surface water acidification and critical loads: exploring the F-factor. *Hydrology and Earth System Sciences* 13: 2191-2201.

Soller, D.R. 1990. Text and References to Accompany "Map Showing the Thickness and Character of Quaternary Sediments in the Glaciated States East of the Rocky Mountains". USGS Bulletin 1921. 80pp.

Stoddard JL, Kahl JS, Deviney F, Dewalle D, Driscoll C, Herlihy A, Kellogg J, Murdoch P, Webb J, Webster K. 2003. Response of surface waters to the Clean Air Act Amendments of 1990. EPA/620/R-03/001, US Environmental Protection Agency, Washington, DC.

VTDEC 2003. Total Maximum Daily Loads for 30 Acid Impaired Lakes. VTDEC, Waterbury, VT.

Section 5 – Integrated Terrestrial and Aquatic Critical Loads and Exceedance

This section describes the terrestrial and aquatic critical loads and exceedance estimates for NY and New England. A primary objective of this project was to produce compatible aquatic and terrestrial critical loads assessments that could be integrated to identify the lowest critical load or highest exceedance (terrestrial or aquatic) for a given landscape segment. Compatibility goals were to use – to the greatest extent possible – similar data sources, spatial scales, and model constructs. In addition, aquatic critical loads needed to be estimated region wide for all watersheds and surface waters rather than for a subset of the region's waters as has been the practice in previous studies.

Tight integration between the aquatic and terrestrial critical loads assessments was achieved by adopting the landscape mass-balance (LMB) form of the general steady-state critical loads model (section 4 of this document). This form of aquatic assessment allowed full use of the data layers developed for the terrestrial analysis, directly integrating data sources. The LMB approach follows the simple mass-balance approach used in the terrestrial assessment (see Section 3 of this document). The LMB approach was also practical for generating continuous grids of the aquatic critical load with respect to all upslope drainage area contributions (see details in Section 4 of this document). The continuous grids (rather than watershed polygons established for arbitrary sized stream reaches, and with nesting complications) simplify the comparison of terrestrial and aquatic critical loads and exceedance at any point on a stream reach or at any point within a watershed. Direct comparisons for any externally defined watershed require only a simple data extraction. The end user of the assessment data is free to aggregate the continuous grid data into stream-reach, lake or pond watersheds as fits their specific analysis needs.

Critical Loads

The estimated forest ecosystem steady-state critical load of sulfur plus nitrogen for New York and the New England states is shown in Figure 5.1. Estimated aquatic ecosystem steady-state critical loads for the pH 6.6 critical threshold are shown in Figure 5.2. Critical loads are highest in areas of sediments and metasediments containing limestone, dolomite, or calcite vein fillings. Critical loads are moderate in the Adirondack Mountains region due to the anorthosite bedrock present there. Areas of low critical loads occur in the higher elevations of the Adirondack, Catskill, Green, and White Mountains where cooler temperatures and thin soils reduce weathering rates. The metamorphic and igneous rocks of the Green and White Mountains and the southwestern Adirondacks have minerals more resistant to weathering than Adirondack anorthosite or the limestones, dolomites, and calcareous sediments found in southern New England and western New York. Significant base-cation removals due to timber harvesting also contributed to low critical loads in northern Maine, New Hampshire, and Vermont. Very low critical loads occur in the Catskill Mountains of New York, northern areas of New York, and Maine, and south coastal areas were sandstone bedrock prevails, especially where significant timber removals are indicated. The aquatic critical load analysis indicates some areas that naturally would not be expected to exhibit a surface water pH equal to or greater than 6.6 (Figure 5.2). High estimated DOC concentrations and very low estimated weathering rates (typically in sandstone or base-poor metamorphic rocks) result in these expectations of low pH values. The aquatic critical load may be locally underestimated in coastal regions and the Lake Champlain Basin where buried marine sediment layers exist that were not captured in the geologic mapping resources used for the study. In these regions, surface water pH varies from values less than 6.6 (consistent with bedrock mapping) to greater than 7.1 (influenced by marine sediments) depending on aquifer interaction with these sediments (e.g., O'Malley 2008).

Table 5.1 compares statewide averages of the critical load and its key components. New York has lower statewide estimated base cation removals due to harvesting than the New England states. In contrast, New York has a high statewide average weathering rate and a high statewide average critical load relative to the New England states due to the abundance of calcareous rocks and anorthosite in the state. New York, with its large land area, has a wide range of geologic materials and a wide range of climatic conditions leading to a large variance in the weathering rate.

Due to the nature of the data sets there are multiple ways to combine the terrestrial and aquatic critical loads estimates for joint analysis. The method of combination should be dependent on the goals of the end-user's analysis. For example, the simplest combination is to map the minimum value of either the terrestrial or aquatic critical load at any grid cell. Another logical combination would be to extract the aquatic critical load values for all grid cells classified as surface water and overlay these values on the terrestrial critical load grid. However, with the latter type of combination, information is lost on which terrestrial components of a watershed are contributing to a low aquatic critical load in adjacent surface waters. The end user should carefully consider the implications of any method selected for combining the terrestrial and aquatic critical loads.

Table 5.1. Statewide average values of key components of the forest and aquatic ecosystem critical load.

State	Base Cation Harvest keq ha^{-1} y^{-1}	Soil Base Cation Weathering keq ha^{-1} y^{-1}	WX SD[1]	Forest Ecosystem Critical Load keq ha^{-1} y^{-1}
Maine	0.41	2.44	1.87	1.28
New Hampshire	0.26	1.80	0.43	1.35
Vermont	0.23	2.50	2.09	1.60
Rhode Island	0.33	2.20	0.33	1.13
Massachusetts	0.21	2.27	1.24	1.77
Connecticut	0.17	2.68	1.15	2.29
New York	0.13	6.50	11.6	5.30

[1] One standard deviation of the weathering rate estimated for different locations in the state expressed as keq ha^{-1} y^{-1} of base cations released.

Table 5.2. Estimated statewide average total atmospheric acidity (sulfur plus nitrogen) loading in the 2002 reference period and the 2018 scenario.

State	Est. 2002 S+N Deposition keq ha^{-1} y^{-1}	Est. 2018 S+N Deposition keq ha^{-1} y^{-1}
Maine	0.66	0.48
New Hampshire	0.88	0.61
Vermont	0.99	0.71
Rhode Island	1.21	0.89
Massachusetts	1.24	0.87
Connecticut	1.29	0.91
New York	1.36	0.99

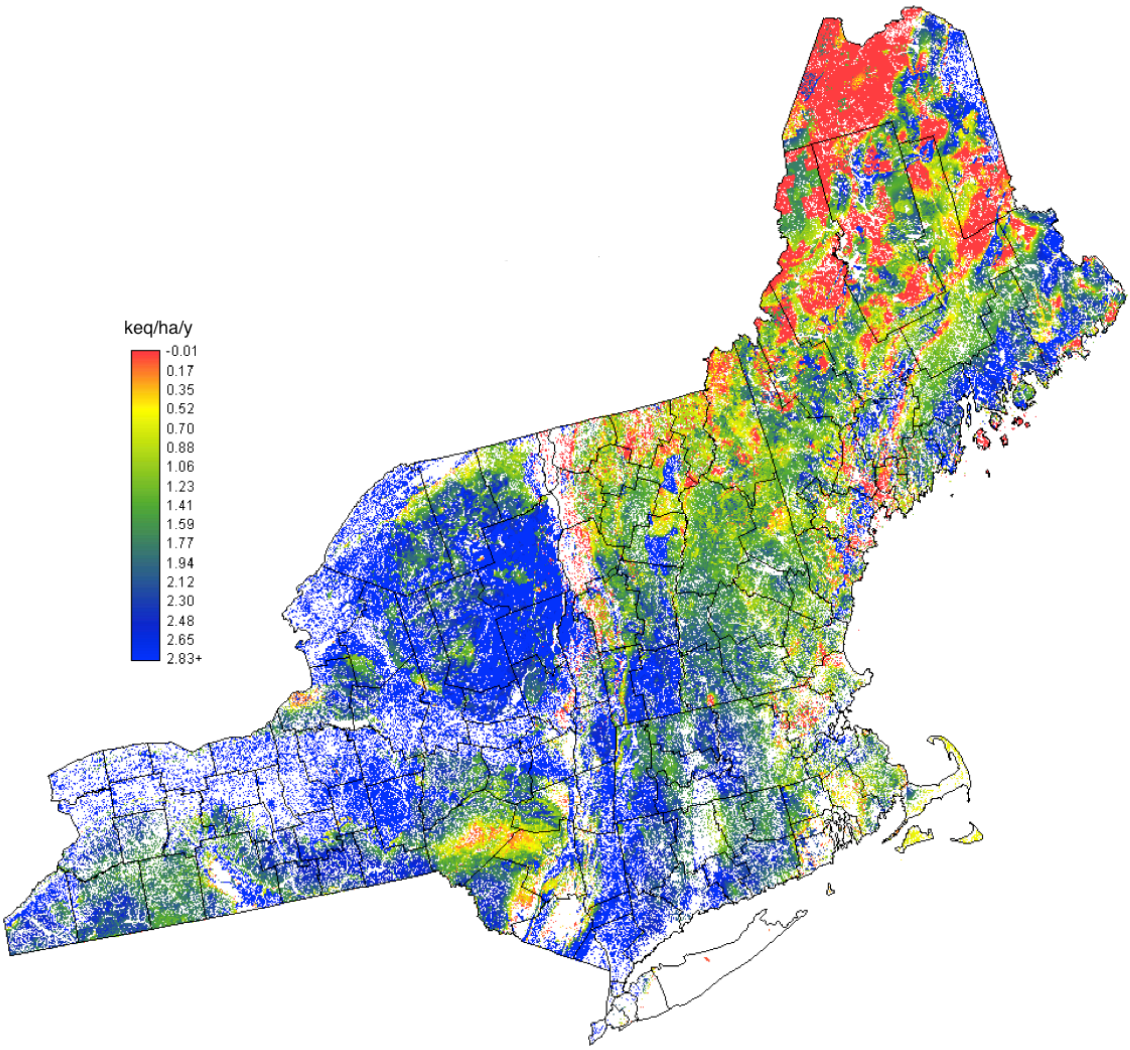

Figure 5.1. Steady-state critical load of sulfur plus nitrogen deposition for forested ecosystems of the northeastern US. White areas represent non-forest cover types identified in the USGS 30-meter resolution National Land Cover Data for 1999 (NLCD).

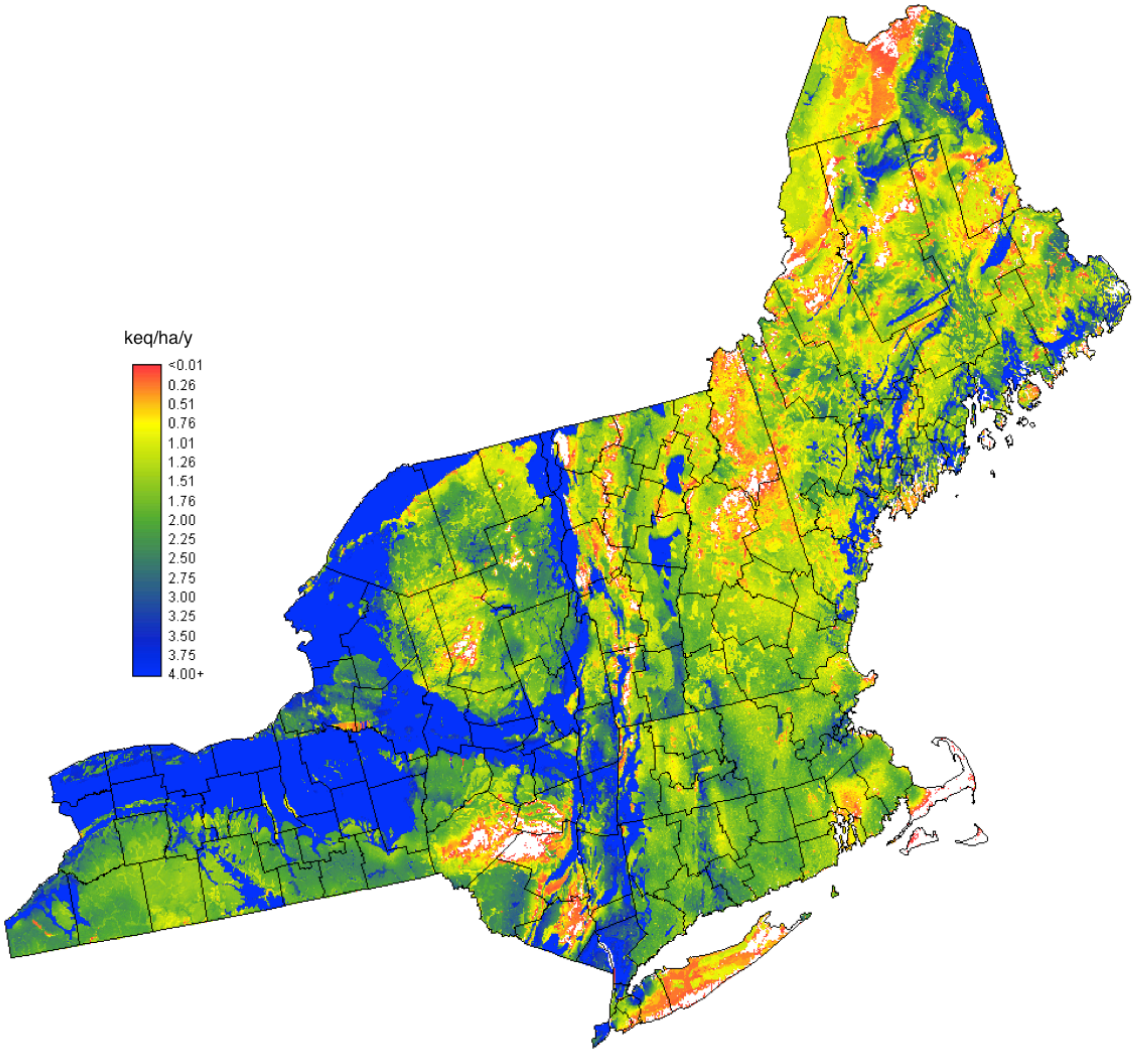

Figure 5.2. Fresh-water aquatic ecosystem steady-state critical load for sulfur plus nitrogen deposition in the northeastern US. The aquatic ecosystem critical load is mapped to all contributing land areas in a watershed for visualization. Mapped to only surface water grid cells, the results would not be interpretable at a regional scale. White areas represent locations where the critical load is less than zero, indicating that the critical pH of 6.6 is not attainable even with zero sulfur and nitrogen deposition. Such a situation may arise when weathering rates are very low, DOC values are high, or timber harvesting is significant (or a combination of these factors).

Exceedance of Critical Loads

The difference between the critical load and atmospheric deposition, termed "exceedance" (ICP 2004), indicates the severity of the nutrient imbalance or the capacity of an ecosystem to tolerate additional deposition. At sites where the deposition exceeds the critical load, the time required for the manifestation of declines in forest health and growth rate is governed, in part, by the size of the soil-exchangeable pool of nutrient cations. Exchangeable cations are those that are loosely retained in the soil, and can be thought of as the short-term supply of nutrients, while soil mineral weathering provides the long-term supply. If the exchangeable pool is large, the forest may be able to buffer a small nutrient input-output imbalance for tens to hundreds of years, delaying the onset of health and growth limitations. This buffering period allows time for the implementation of air pollution emissions reductions. If, as is likely the case for much of the northeastern US, exchangeable base cation pools have been substantially diminished by past decades of elevated sulfur and nitrogen deposition (Johnson et al. 1994; Lawrence and Huntington 1999), a small net positive cation balance (small negative exceedance) will move the system only slowly toward the critical levels of base saturation or surface water pH. Thus, when the steady-state exceedance is estimated to be slightly negative (deposition slightly less than the critical load), ecosystems may remain in a degraded (low soil base saturation, low aquatic pH) state for long periods of time as recovery proceeds slowly (see Lawrence and Huntington 1999, Driscoll et al. 2001, Stoddard et al. 2003).

Because the critical load exceedance is being evaluated at steady state, all nitrogen deposited to an ecosystem in excess of vegetative demand is assumed to be converted to nitrate.[14] At steady-state, there is no net retention or release of sulfate. Therefore, for the purpose of calculating steady-state critical load exceedance, sulfur and nitrogen deposition can be expressed as a sum of the oxidized forms in units of anionic charge (keq/ha/y, Table 5.2).

Figure 5.3 shows the areas where sulfur plus nitrogen atmospheric deposition is estimated to exceed the steady-state critical load for forested ecosystems for New York and New England under c.a. 2000 and 2018 atmospheric deposition rates. All states show a reduction in estimated forest area where deposition exceeds the steady-state critical load between 2002 and 2018. Figure 5.4 shows the areas where sulfur plus nitrogen atmospheric deposition is estimated to exceed the steady-state aquatic critical loads for pH 6.6 and 7.1 under atmospheric deposition estimated for 2002. Figure 5.5 illustrates the change in watershed area where the steady-state critical load for a critical pH of 6.6 is exceeded as deposition changes from 2002 to project 2018 levels. Circa 2018 deposition is projected to reduce the area of the forest and aquatic resources where the steady-state critical load is exceeded in all states (Table 5.3). This suggests a potential for a 30% reduction in forest and aquatic resources subject to continued degradation from acidification as a result of current air pollution control programs. Where ecosystems have transitioned from exceedance to non-

[14] At steady state, nitrogen deposition deposited in excess of the annual growth requirement will have accumulated in the system driving the C/N ratio to the nitrification range (see Aber et al. 1998, Galloway et al. 2003, Ouimet et al. 2006).

exceedance of the critical load, they are likely to be in the initial stages of recovery (modest soil base saturation increases, slow increases in surface water ANC and pH). *When deposition falls below the steady-state critical load, a system is expected to begin to evolve toward the critical threshold values.* However, this process of recovery may take a long time, especially when prior depletion has been extensive and the steady-state base cation mass balance is only slightly positive.

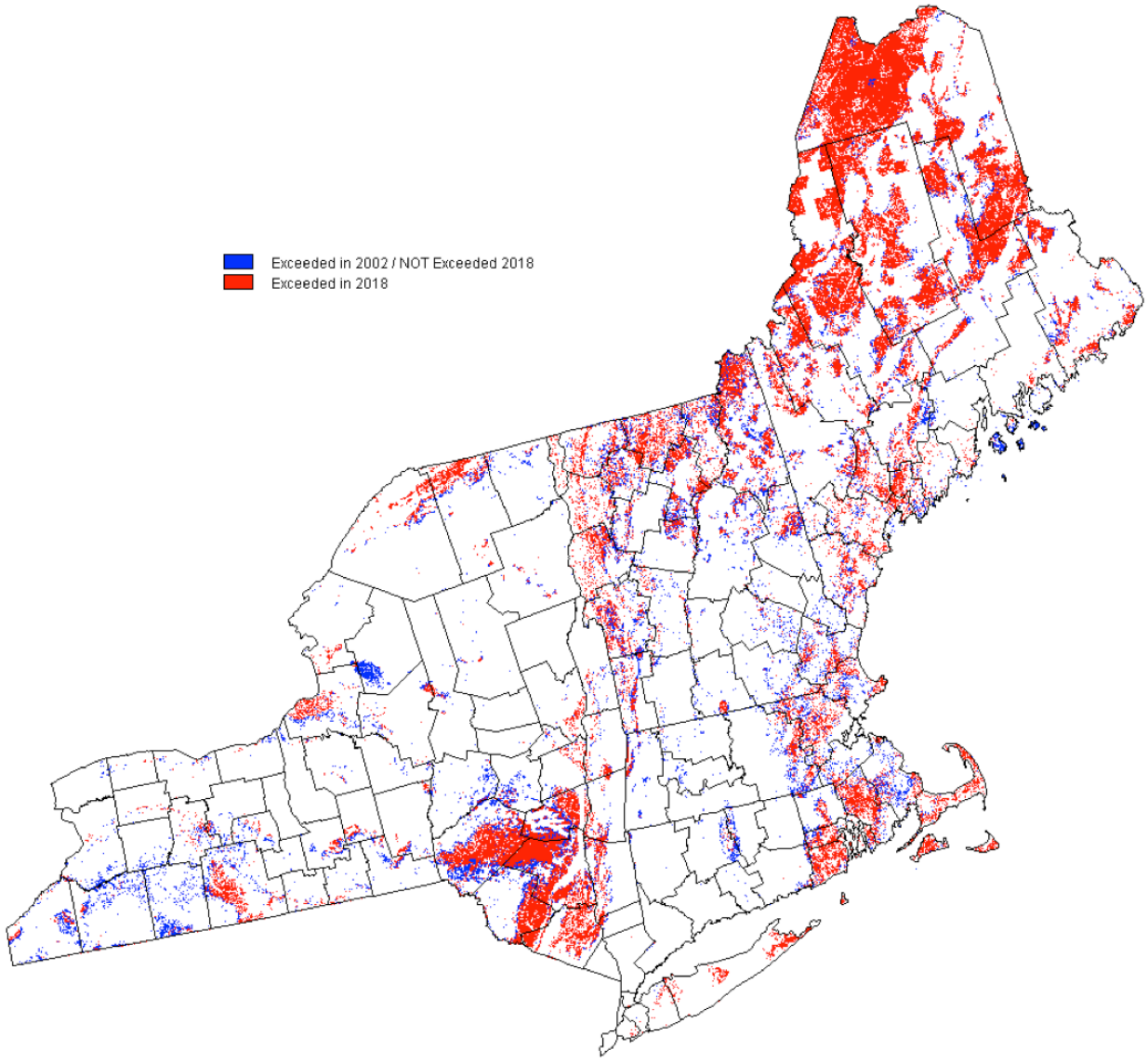

Figure 5.3. Estimated changes between 2002 and 2018 in the amount of forested area where the steady-state forest ecosystem critical load of sulfur plus nitrogen is exceeded. Blue shading indicates areas where the critical load was estimated to be exceeded in 2002 but is not projected to be exceeded in 2018. Red shading indicates areas where the critical load is estimated to be exceeded in both 2002 and 2018. There are substantial estimated reductions in the area where the critical load is exceeded over the period. Still, for four out of seven Northeastern states, atmospheric deposition of sulfur plus nitrogen will likely exceed 20% of forested area in 2018.

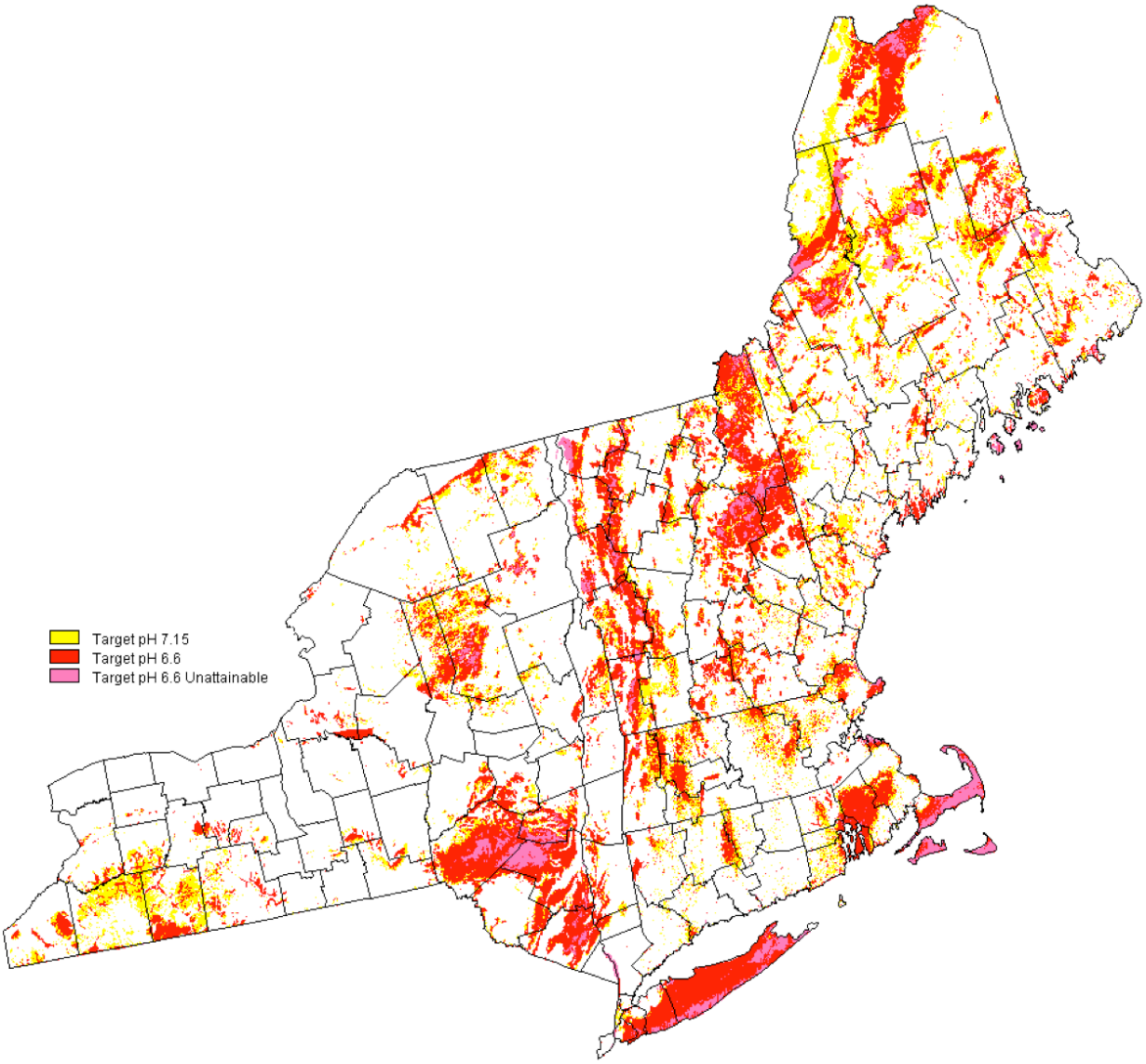

Figure 5.4. Watershed contributing areas where 2002 sulfur plus nitrogen deposition is estimated to exceed the steady-state aquatic ecosystem critical load for a critical surface water pH of 7.15 (yellow) or 6.6 (red). In some areas (pink), the critical pH of 6.6 is not attainable due to low weathering rates, high DOC concentrations, or intensive timber harvesting (or a combination of these factors).

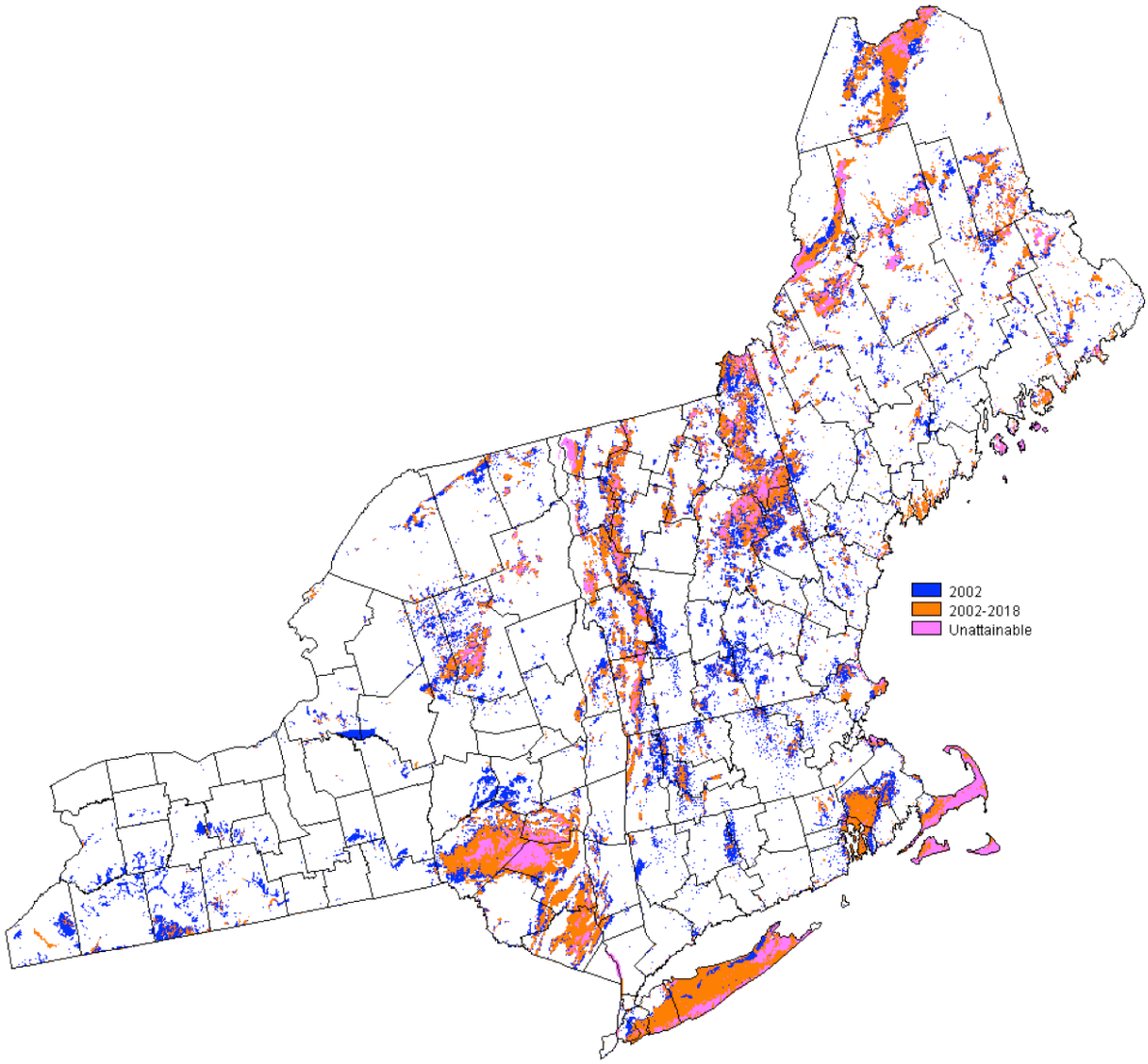

Figure 5.5. Estimated changes between 2002 and 2018 in the amount of contributing watershed area where the steady-state aquatic ecosystem critical load of sulfur plus nitrogen for a critical pH of 6.6 is exceeded. In some areas (pink), the critical pH of 6.6 is not attainable due to low weathering rates, high DOC concentrations, or intensive timber harvesting (or a combination of these factors).

Table 5.3. Percent of watershed area with atmospheric deposition of sulfur plus nitrogen in excess of either the forest or aquatic ecosystem steady-state critical load for the 2002 reference period and 2018 atmospheric deposition scenario.

State	2002	2018
Connecticut	7.1%	1.6%
Maine	34.7%	28.8%
Massachusetts	31.1%	18.0%
New Hampshire	35.7%	18.1%
New York	18.7%	11.8%
Rhode Island	47.9%	36.1%
Vermont	35.6%	23.9%
Northeast Region	26.7%	18.4%

The results of this analysis generally agree with spatial patterns described in earlier studies (e.g., Stoddard et al. 2003, Burns et al. 2006), which indicated initial signs of recovering surface water ANC and pH in the Adirondack Mountains region (relatively Ca-rich anorthosite bedrock) but a more limited recovery in the Catskill Mountains (sandstone, base-poor geology) and no recovery in much of New England (in areas of less base-rich metamorphic rocks and sandstone). Differences in rates of base cation removal due to timber harvesting between the regions (Table 5.1) also likely play a significant role in the observed spatial patterns of projected recovery (or lack of recovery).

Areas identified in this study as possibly transitioning from a state of critical load exceedance to non-exceedance would be good locations to focus future data collection and time-series modeling efforts in order to better evaluate the likely trajectory of recovery. Such studies could determine the extent of additional reductions in deposition rates required to restore soil base saturation or surface water pH to critical levels in a reasonable time frame. Similarly, areas where 2018 deposition is likely to continue to exceed the critical load also should be the focus of data collection and time-series modeling to ascertain the degree of further degradation likely without implementation of additional air pollution controls. The areas where the absolute value of steady-state critical load exceedance is small (see supplemental material) should be the focus of more detailed study to quantify risk of ecosystem harm due to sulfur and nitrogen deposition.

Integrated critical load exceedance estimates may be derived by calculating separately the aquatic and terrestrial exceedance and then combining or by calculating the exceedance with respect to an integrated critical load (see above). Table 5.3 represents a simple form of integration – the case where either the terrestrial or aquatic critical load (relative to the pH 6.6 target) is exceeded. As with critical loads, there are multiple ways to combine the critical load exceedance estimates. The best choice of combination method is dependent on the questions to be addressed by the end-user's analysis.

Conclusions

Air pollution control programs currently envisioned and in-place are likely to produce a reduction in the area of forest and aquatic ecosystems continuing to be degraded by sulfur and nitrogen deposition. Areas transitioning from exceedance to nonexceedance of the critical load will likely only slowly improve given the small difference between deposition and the steady-state critical load. The project produced maps (Figures 5.3 through 5.5) identifying areas where observation programs should be focused to support time-series modeling to evaluate future trajectories of critical ecosystem properties. Better geologic mapping and more sample collection to define mineralogy, improved estimates of soil parameters such as depth and texture, and improved spatial modeling of surface water DOC could improve future regional assessments.

References – Section 5

Aber, J., W. McDowell, K. Nadelhoffer, A. Magill, G. Berntson, M. Kamakea, S. McNulty, W. Currie, L. Rustad., and I. Fernandez. 1998. *Bioscience*. 48:921-934.

Burns, D.A., M.R. McHale, C.T. Driscoll, and K.M. Roy. 2006. Response of surface water chemistry to reduced levels of acid precipitation: comparison of trends in two regions of New York, USA. Hydrological Processes, 20: 1611-1627.

Driscoll, C.T., G.B. Lawrence, A.J. Bulger, T.J. Butler, C.S. Cronan, C. Eagar, K.F. Lambert, G.E. Likens, J.L. Stoddard, and K.C. Weathers. 2001. Acidic Deposition in the Northeastern United States: Sources and Inputs, Ecosystem Effects, and Management Strategies. *BioScience*. 51: 180-198.

Dupont, J., T.A. Clair, C. Gagnon, D.S. Jeffries, J.S. Kahl, S J. Nelson, and J.M. Peckenham. 2005. Estimation of critical loads of acidity for lakes in northeastern United States and eastern Canada. *Environmental Monitoring and Assessment*. 109:275-291.

Driscoll, C.T., G.B. Lawrence, A.J. Bulger, T.J. Butler, C.S. Cronan, C. Eagar, K.F. Lambert, G.E. Likens, J.L. Stoddard, and K.C. Weathers. 2001. Acidic Deposition in the Northeastern United States: Sources and Inputs, Ecosystem Effects, and Management Strategies. *BioScience*. 51: 180-198.

Galloway, J.N., J.D. Aber, J.W. Erisman, S.P. Seitzinger, R.W. Howarth, E.B. Cowling, and B.J. Cosby. 2003. The Nitrogen Cascade. *Bioscience*. 53:341-356.

ICP Mapping Manual (2004) International Cooperative Programme on Modelling and Mapping of Critical Loads and Levels and Air Pollution Effects, Risks and Trends, UNECE Convention on Long-range Transboundary Air Pollution. *Manual on Methodologies and criteria for Modelling and Mapping of Critical Loads and Levels and Air Pollution Effects, Risks and Trends.* (http://icpmapping.org/cms/zeigeBereich/5/manual-und-downloads.html)

Johnson. A.H., Friedland, A.J., Miller, E.K., and Siccama, T.G. 1994. Acid rain and soils of the Adirondacks. III. Rates of soil acidification in a montane spruce-fir forest at Whiteface Mountain, New York. *Canadian Journal of Forest Research*, v. 24, pp. 663-669.

Lawrence, G.B. and T.G. Huntington. 1999. Soil-calcium depletion linked to acid rain and forest growth in the eastern United States. USGS WRIR98-4267 (http://bqs.usgs.gov/acidrain).

O'Malley, T.M. 2008. *Analysis of surface water quality and ground water flow in the Carmans River Watershed, Long Island, New York*. M.S. Thesis. State University of New York, College of Environmental Science and Forestry, Syracuse, New York. 123 pp.

Ouimet, R., P. Arp, S. Watmough, J. Aherne, and I. DeMercant. 2006. Determination and mapping critical loads of acidity and exceedances for upland forest soils in Eastern Canada. *Water, Air, and Soil Pollution* 172: 57-66.

Stoddard JL, Kahl JS, Deviney F, Dewalle D, Driscoll C, Herlihy A, Kellogg J, Murdoch P, Webb J, Webster K. 2003. Response of surface waters to the Clean Air Act Amendments of 1990. EPA/620/R-03/001, US Environmental Protection Agency, Washington, DC.

Section 6 – Uncertainty in Critical Loads and Exceedance Estimates

All critical loads and exceedance estimates are recognized to be subject to considerable uncertainty due to both data limitations and the limitations of models used to represent ecosystem processes (see Hodsen and Langen 1999, Alveteg et al. 2000, Skeffington 2006, CASAC 2011). By their nature, regional estimates of critical loads and exceedance such as the present study exhibit higher uncertainties due to the need for extensive parameter estimation (see Li and McNulty 2007, Koseva et al. 2010); whereas, site-specific studies often have access to direct measurements of key model parameters (Koseva et al. 2010). Specific sources of uncertainty in the present regional assessment have been discussed in detail in Sections 1-4 of this document. These discussions are collected and summarized here in order to provide the end user of the data with a comprehensive picture of sources of uncertainty in the regional estimates of critical loads and exceedance.

Exhaustive uncertainty analysis (e.g. Hall et al. 2001, Li and McNulty 2007) was beyond the scope and budget of the present project. The following discussion is intended to familiarize the end user of the project data and results with the potential sources of uncertainty in the regional assessment, to discuss trade offs made between different sources of uncertainty, and to review general uncertainty issues common to all steady-state critical loads assessments. The end user is encouraged to review the uncertainty analyses referenced in this section and consider the methods and data sources used and their associated uncertainties when interpreting any critical loads and exceedance estimates.

The primary goal of the present study was to provide regional air quality managers with a comprehensive (entire landscape evaluated) regional estimate of the percentage and location of areas where sulfur and nitrogen deposition exceed either the terrestrial or aquatic ecosystem critical load. To achieve this goal it was necessary to trade off the additional uncertainty related to parameter estimation for the ability to evaluate the entire landscape rather than a small number of locations where model parameter measurements were available. The current study adopted strategies for estimating the most important parameters that minimized uncertainty in the critical load calculations. For example, it is well understood that critical loads are most sensitive to the base cation weathering rate (Hodsen and Langen 1999, Hall et al. 2001, Li and McNulty 2007). Therefore, considerable effort was made in the present study to develop estimates of the base cation weathering rate in the most robust manner possible for a regional assessment. The methods used account for the specific mineralogical composition of soils and use the PROFILE model (Sverdrup and Warfinge, 1993) that has been established as the most reliable method of regional weathering rate estimation by studies in Europe and North America (see Koseva et al. 2010).

The end user of critical load and exceedance estimates should review the excellent and extensive reviews of uncertainty in steady-state mass balance type critical loads assessments provided by (Hodsen and Langen 1999, Alveteg et al. 2000, Hall et al. 2001, Skeffington 2006, Li and McNulty 2007, and Koseva et al. 2010). These studies point out that the application of different estimation methods for parameters used in simple mass balance models may lead to

widely differing estimates of critical loads and exceedance. These studies also make clear that much additional research is needed to refine and improve methods of estimating model parameters in order to reduce uncertainties. As was the intention of the present study, consideration of parameter and aggregate uncertainties indicates that regional assessments are best used to identify areas where additional fieldwork would be most cost-effective in providing the necessary observations and measurements needed to reduce uncertainties in critical loads estimates. With proper understanding of the existing uncertainties, regional estimates such as the present study are also useful in establishing the likely direction, magnitude, and areal percentage changes in exceedance in response to anticipated deposition changes.

The steady-steady state critical loads analysis in this study was designed to provide an objective approach for identifying ecosystems where recovery is possible and where recovery is unlikely under present and future atmospheric deposition scenarios. This study identified areas where additional data should be collected in order to conduct additional modeling to estimate the likelihood of and the expected recovery trajectory toward a specific target soil base saturation or a surface water pH. The study was not designed to be a final assessment of risk to terrestrial and aquatic ecosystems, but rather as an initial step toward objectively identifying areas that may be in early stages of recovery or that likely will continue to degrade under the anticipated 2018 deposition. Resource managers can use the results of this study to identify areas where the detailed field studies required before calibrated dynamic modeling would be most cost-effective for estimating the temporal response of ecosystems to future changes in atmospheric deposition.

Uncertainty in atmospheric deposition estimates

Estimates of sulfur, nitrogen, chloride, and base cation deposition are described in Section 2 of this document. The approach combined interpolation of network observations, inferential modeling using the HRDM (Miller et al. 2005), and emissions-transport modeling using CMAQ (NESCAUM 2006). The c.a. 2002 deposition scenario is subject to uncertainty from interpolation of sparse network observations (see Miller et al. 2005), although the interpolation method did insure fidelity of concentrations at the observation points. The HRDM (Miller et al. 2005) was developed to provide atmospheric deposition estimates that include the influence landscape variance and receptor characteristics on < 1 km spatial scales. Using inferential deposition estimates at 30-meter ground resolution reduced a known bias associated with coarse-scale (1km or greater) deposition estimates that "average away" known high deposition environments in high-elevation regions with complex topography. Data comprising 1971-2000 normal climate fields generated from the NOAA network of observing stations (Miller et al. 2005) were used to drive the HRDM. Using climate normals rather than individual year climate is more appropriate for developing input layers for steady-state critical loads modeling. The steady state loads need to represent long-term average climatic conditions rather than conditions in a specific year. Using 30-year climate normals substantially reduced uncertainty in steady-state critical loads and exceedance estimates that would have been introduced by using a specific year or a shorter-term average for climate (temperature, precipitation, evapotranspiration, runoff) as there is a large year-to-year spatial

variance in climate parameters of a magnitude that would significantly alter exceedance estimates.

To estimate c.a. 2018 deposition rates results from 2002 and 2018 CMAQ model simulations (NESCAUM 2006) were combined with c.a. 2002 HRDM estimates (see Section 2). Evaluation of CMAQ results (Figure 6.1, see also NESCAUM 2006, Section 2 and Appendix NPSCL-TD2a-ComparativeAnalysis.pdf) revealed under prediction of S and N in the Northeastern US relative to NADP and CASTNET data (Figure 6.1) and prior HRDM runs based on NADP and CASTNET observations with 30-year normal climate (see Appendix NPSCL-TD2a-ComparativeAnalysis.pdf). CMAQ performance and EPA's correction routines have been optimized for both the national model domain and a much larger eastern domain that includes the Mid-Atlantic States. While CMAQ performance is reasonable when summarized over the full model domain or the eastern domain, there are areas of better and poorer model performance. The northeastern US is an area where the level of disagreement between model output and observations is large enough to be significant when calculating critical load exceedances. The apparent model bias in the northeastern US, ***while not large in the context of deposition variance across the nation***, is of the same order of magnitude as the anticipated changes in Northeastern US deposition resulting from the combined effects of CAIR, Federal Fuel and Motor Vehicle Programs, and SIPs. Therefore, the present project used the ratio of NESCAUM (2006) CMAQ results for 2018 relative to 2002 multiplied by the 2002 estimates generated by the HRDM. This approach produced deposition estimates with a higher fidelity to the observed magnitudes and spatial patterns, but with inference on the spatial distribution of the direction and magnitude of change by 2018 provided by the CMAQ modeling.

Comparison of CMAQ results with NADP observations

Ratio of CMAQ run estimated deposition (kg/ha/y) to NADP observed deposition (kg/ha/y)

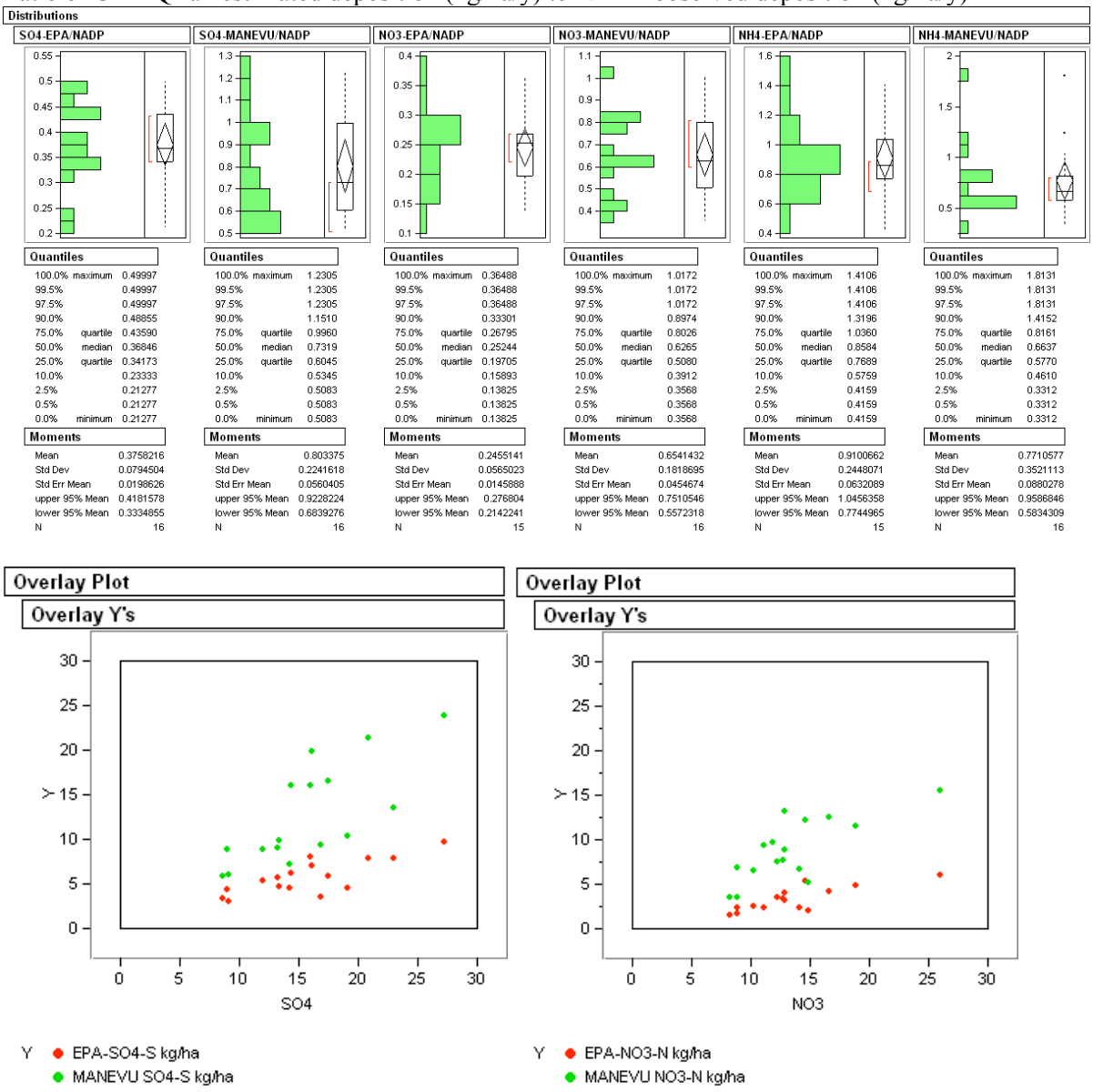

Figure 6.1. Comaparison of NESCAUM (2006) MANE-VU CMAQ estimated 2002 deposition, EPA CMAQ estimated 2002 deposition (Robbing Dennis, USEPA Personal Communication) and NADP observed deposition for the northeastern US. See Appendix NPSCL-TD2a-ComparativeAnalysis.pdf for further discussion and figures.

Uncertainty in ecosystem critical threshold values

The critical load of sulfur + nitrogen is the level of deposition below which, to the best of available knowledge, no harmful ecological effects occur in an ecosystem. Critical load estimates depend on a value termed the critical threshold. After extensive deliberation and international peer review, the NEG/ECP Forest Sensitivity Mapping Initiative adopted a forest ecosystem steady-state critical threshold corresponding to a condition of all nutrient base cation mass balances equal to zero (NEG/ECP 2001) and this threshold value was adopted for the present study. If the steady-state Ca, Mg, or K mass-balance is negative, this indicates the ecosystem is on a path to reduced critical nutrient availability (a state of nutrient depletion). While this threshold selection is based on considerable theoretical and observational evidence (see Section 3, Schaberg et al. 2001, Moore and Ouimet 2006, and Schaberg et al. 2007) from northeastern North America and has been adopted for use elsewhere (e.g. Nasr et al. 2010), it is possible the threshold could underestimate risk for some ecosystem components.

For aquatic ecosystems subject to acidification by sulfur and nitrogen, the parameter most often related to the condition of key organism and aquatic ecosystem health is pH (ICP Mapping Manual, 2004, Dupont et al. 2005). For historical reasons – due primarily to the complications associated with modeling DOC (discussed below) a target pH critical threshold has been translated to a corresponding value of the acid neutralizing capacity termed the ANC limit (see discussion in Dupont et al. 2005). This is done because the charge-balance form of the acid neutralizing capacity (see Morel and Hering 1993) is simpler to model than pH in a steady-state context with limited data (ICP Mapping Manual 2004). We developed an empirical function from training site data representative of the region to relate pH to charge-balance ANC and DOC that explains 80% of variance in pH observations (Figure 6.2, see also section 4, Appendix NPSCL-TD4a-DOC-correction-of-ANC-limit.pdf). Use of DOC in conjunction with ANC reduces uncertainty in predicted pH (Figure 6.2). However, DOC then becomes a model parameter that needs to be estimated for regional assessment.

Approximately 46% of variance in training site DOC concentration was explained by the best obtainable regional model for surface water DOC (Appendix NPSCL-TD4a-DOC-correction-of-ANC-limit.pdf). This is only 2% less variance than the 48% of variance in surface water DOC explained by Canham etl al. (2004) in the Adirondack region using a higher spatial resolution (10 m x 10 m grid) model. Canham et al. (2004) acheieved a slightly higher proportion of variance explained (55%) for a sample of 355 headwaters lakes only. However the appropriate comparison to the present study is Canham et al.'s (2004) evaluation of model performance over 428 lakes representing headwaters and more typical compound (multiple lakes chained along flowage systems) lakes, which remains biased (83% headwaters lakes in sample) to headwaters (simpler) systems. The present study compares predictions against primarily compound lakes and samples from stream reaches. Therefore, the level of explanation of variance in DOC explained by the current study represents the current "state of the science" for the Northeast for compound lakes and stream reaches. This is clearly an area where additional research effort should be focused to reduce the uncertainty in critical load and exceedance estimates.

As the regionalized DOC estimate was used to adjust the ANC_{limit} to produce the desired target pH, uncertainty in DOC estimates translates directly to uncertainty in the ANC_{limit}.

Furthermore, DOC concentrations are known to be varying with time at present in the Northeast (Monteith et al. 2007), probably are not representative of steady-state DOC concentrations. Thus, uncertainty in the steady-state critical load predictions is introduced by the possibility that the available 1984-2005 DOC observations used to generate the spatial model of DOC may not reflect the long-term average DOC values, therefore use represents (similar the harvesting rate selection) a somewhat arbitrary choice for steady state conditions. However, sensitivity analysis indicated only a minor effect of a 25% decrease in DOC on the cumulative frequency distribution of the results (see Tables 4.1 and 4.2). The large temporal range of DOC observations likely contributes to unexplained variance in the spatial model of DOC derived from the available observations.

In the present study critical pH thresholds were selected based on guidance provided by EPA (based on recent work by CASAC) and consultation with the multi-agency funding group in collaboration with state air and water resource agencies. Two pH thresholds were evaluated. A pH of 6.6 was selected as a threshold providing protection to important fish species of interest (see Driscoll et al. 2001, Dupont et al. 2005) while pH 7.15 was selected as a threshold providing protection to Atlantic salmon (Perry 1990, Haines et al. 1990, Dill et al. 2002) and many sensitive plankton species of the region (Dixit et al. 1999). Some unquantified uncertainty exists in the adequacy of these thresholds as they were empirically derived from subpopulations of surface waters from the region. The reader is encouraged to review the extensive discussions in materials developed by the EPA CASAC (2011) for more information on critical thresholds related to biological conditions in aquatic ecosystems.

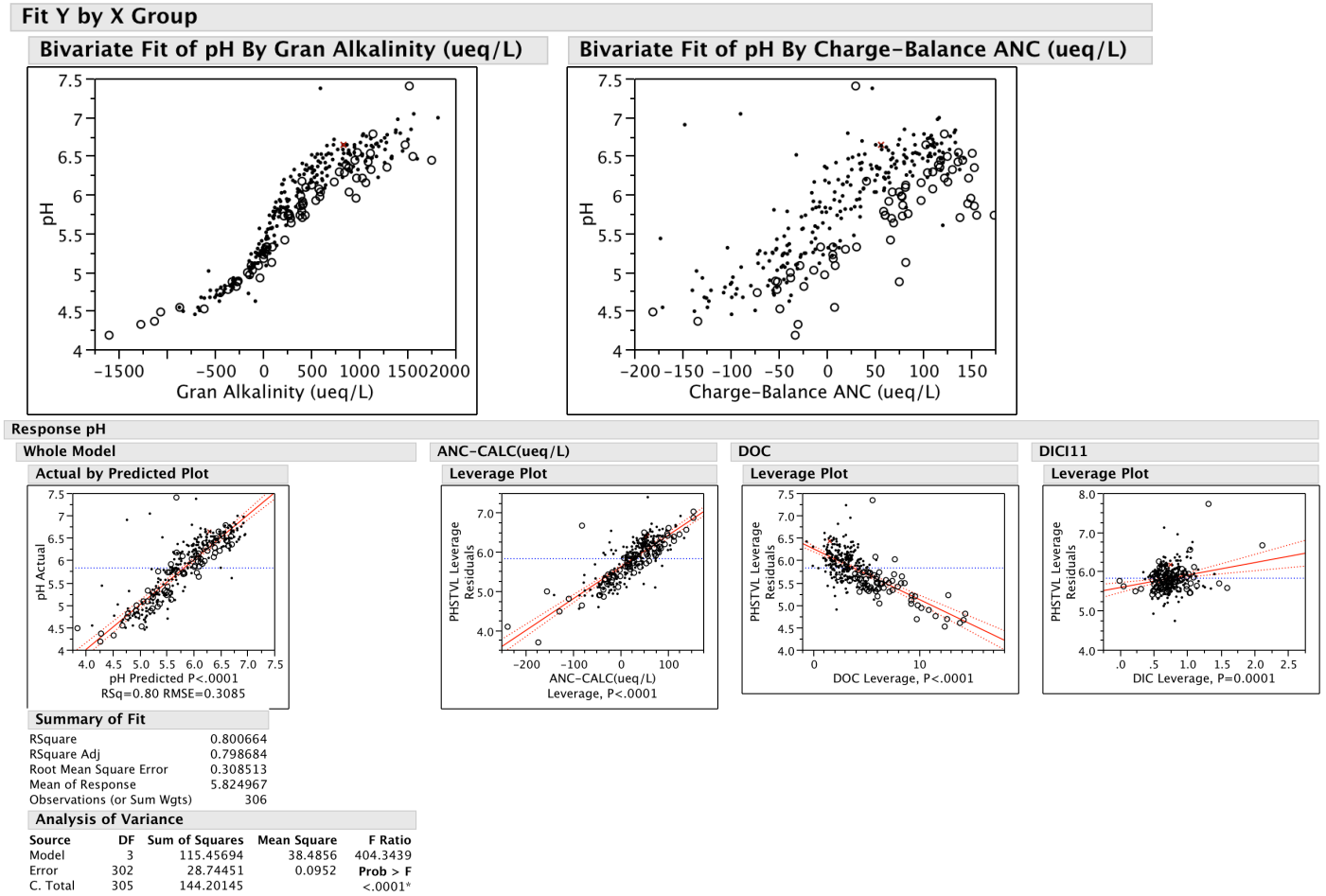

Figure 6.2. The relationships between pH and Alkalinity and charge-balance ANC (top). Regression model for pH as a function of CBANC, DOC and DIC (bottom).

Response DOC(mg/L)

Actual by Predicted Plot

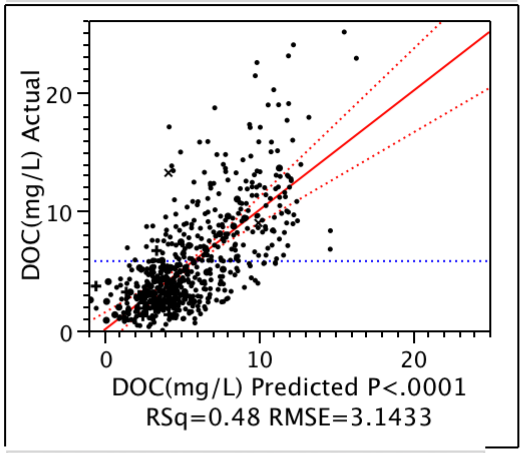

Summary of Fit

RSquare	0.475484
RSquare Adj	0.457783
Root Mean Square Error	3.143252
Mean of Response	5.804496
Observations (or Sum Wgts)	583

Analysis of Variance

Source	DF	Sum of Squares	Mean Square	F Ratio
Model	19	5042.483	265.394	26.8616
Error	563	5562.457	9.880	**Prob > F**
C. Total	582	10604.940		<.0001*

Figure 6.3. Predictive ability of the regional surface water DOC estimate. Observed values are from the training site data set described in NPSCL-TD4-Aquatic-CL.pdf.

Uncertainties common to terrestrial and aquatic critical loads estimates

As both terrestrial and aquatic critical loads estimates rely on the root-zone soil layer mass balance (see Sections 3 and 4) uncertainties in components of the mass balance affect both critical loads in the same way.

As described in detail in the Appendix NPSCL-TD3b-Biomass-Extraction.pdf there is considerable uncertainty associated with estimates of base cation exports due to harvesting. The uncertainty primarily results from statutory limitations on access to USDA FIA timber removal data. As timber removal data were only available to the project at county level by rough forest type and land use categories, the method for distributing the countywide average rates imparts uncertainty. Furthermore, the USFS FIA characterization of timber removals from inventory without distinction to a periodic removal for recurring harvest or a permanent removal due to land development leads to a likely positive bias in county-wide estimates of "harvest" removals. This bias is likely greatest in rapidly urbanizing areas. Given that parcel-specific management information is not available on a regional scale, the average removal rate for a given category of land use (private, public) by forest type was assigned to each landscape element. Some parcels will have more aggressive cutting than other parcels due to differences in management strategies and will differ from the countywide averages, thus imparting considerable uncertainty at the local parcel scale. The end user of this assessment information that is interested in management of a specific parcel is encouraged to compare what is known about parcel-specific management history and plans to the countywide averages used in this study. Adjustments can easily be made to the estimates provided here to account for local harvesting information.

The uncertainty associated with forest-type assignments has been well quantified for the New England States (see Appendix NPSCL-TD3a-Forest-Type-Model.pdf). The uncertainty associated with forest type assignments in New York is unknown as there was no funding available for ground truth assessment of this component in New York. The uncertainty associated with plant nutrient content has been well characterized (see Pardo et al. 2005).

The chemical breakdown of rock-forming minerals and their conversion to soil minerals, termed *soil mineral weathering*, is the primary means of replenishing the nutrients Ca, Mg and K that are lost from soils via acidic deposition-induced leaching and/or biomass removal. The landscape and geologic factors that control the rate of weathering are: 1) mineral assemblage, 2) climate, and 3) physical properties of the soil. Common minerals that may co-occur in the same rock or soil may have widely varying Ca, Mg, and K contents and inherent rates of chemical breakdown that could vary by up to 8 orders of magnitude (Table 3.1 and see Lasaga et al. 1994). Thus, the proportion of easily weathered minerals (which are often the highest in Ca and Mg) exerts the dominant control on the overall soil weathering rate (Koseva et al. 2010). The mineral assemblage is governed by the geologic history of a site including the bedrock mineralogy, transport of minerals to the site by water, wind or glaciers, and the length of time the assemblage has been subject to weathering. Weathering rates increase with increasing temperature and water flux through a soil. The more mineral surface area that is exposed to water, the higher the weathering rate and this factor is governed by soil mineralogy, texture, and climate. The depth to which roots can penetrate the soil (a function of both plant and soil characteristics) and the presence or absence of a fluctuating

water table at this depth influence the volume of soil over which weathering is relevant to plant nutrition. Not surprisingly, the weathering rate is a highly localized parameter and very difficult to evaluate on a regional basis given the complexity of factors involved and data required. The estimation approach employed in this project provides values of the average weathering rate for upland soils (NEG/ECP-FMG, 2001). Local weathering rates may depart substantially from the averages derived, but the estimates provide a rational basis for differentiating the ability of different areas within the region to replenish lost nutrients.

In areas with upwelling groundwater, weathering rates would include deep till and bedrock contributions below the root zone and along 3-dimensional ground water transport pathways. To attempt to include such upwelling water contributions in the weathering rate estimates would require complex and data intensive groundwater modeling that was beyond the scope and budget of this project. Thus, the end user of the information in this report must be aware that the weathering rates used represent the minimum likely weathering rates in areas of upwelling waters.

Koseva et al. (2010) affirmed the utility of the PROFILE modeling approach used in this study to estimate weathering rates. Koseva et al. (2010) and many other studies make clear the importance of providing PROFILE with representative mineral compositions in order to obtain the best estimates of weathering rates. The method employed in the current study takes into account glacial redistribution of bedrock mineralogy, thus reducing uncertainty over methods dependent on bedrock mineralogy alone or in combination with soil textural data. Koseva et al. (2010) point out the significant errors and bias that accompanies the often-used soil textural analysis approach (STA) in comparison to a PROFILE-based approach. As described in detail in Section 3, the metamorphic geology of New England generates many base-poor, but clay-rich soils, confounding the standard STA calibrations. Nevertheless, some uncertainty must be attributed to errors in geologic mapping, sub map scale bedrock variations and lack of samples to populate the bedrock mineralogy database (see detailed discussion in Section 3). Lack of funding also limited bedrock sample collection in New York relative the effort conducted in New England resulting in lower confidence in bedrock mineralogy estimates for New York. Lack of funding limited field calibration of the glacial redistribution model beyond Vermont. Therefore, all of New England and New York was modeled using the Vermont based glacial dispersion calibration.

Considerable uncertainty in soil depth and texture estimates resulted from use of the STATSGO soil database (see Section 3 and Li and McNulty 2007).

Uncertainties specific to aquatic critical loads

Uncertainties in salt corrections contribute to uncertainties in the “deep weathering” correction ratios derived from the training site data. Although with respect to the variance in weathering rates across the region due to geology and climate, this uncertainty is small (see Figure 4.5)

The terrestrial root zone soil mineral weathering rate scaled by surficial geology class was used to estimate weathering inputs of base cations to the aquatic systems. There is evidence of considerable weathering at the soil/bedrock interface in shallow soils (Miller et al.

1993, Munroe et al. 2007) and in deep till and stratified sediments of large aquifers. The simple empirical scheme for increaseing the soil-layer weathering rate to account for deeper layer weathering could be considerably improved. Still, any method based on available data for the entire region would not be able to account for subsurface (or unmapped) geologic variations from the surface map that influence conditions in a deep flow path. There were no data available suitable for evaluating the effects of internal SO_4 retention/release on BC_0 estimates for the SSWC model. However, SO_4 retention or release was observed to be significant at many of the training sites and the phenomena have been established as frequently important in the region (Mitchell et al. 2010).

References – Section 6

Alvateg, M., A. Barkman, and H. Sverdrup. 2000. Integrated Environmental Modelling – Uncertainty in Critical Load Assessments. Final Report of the Swedish Subproject, EU/LIFE Project. http://www2.chemeng.lth.se/Publications.

CASAC 2011. ***http://www.epa.gov/ttn/naaqs/standards/no2so2sec/)***

Canham, C.D., M.L. Pace, M.J. Papaik, A.G.B. Primack, K.M. Roy, R.J. Maranger, R.P. Curran, and D.M. Spada. 2004. A spatially explicity watershed-scale analysis of dissolved organic carbon in Adirondack Lakes. *Ecological Applications*, 14(3), 839-854.

Dill. R., C. Fay, M. Gallagher, D. Kirheis, S. Mierzykowski, M. Whiting, and T. Haines (2002). Water quality issues as potential limiting factors affecting juvenile Atlantic salmon life stages in Maine Rivers. Report to Maine Atlantic Salmon Technical Advisory Committee by the Ad Hoc Committee on Water Quality. Atlantic Salmon Commision. Bangor, ME. 28pp.

Dixit, S.S., J.P. Smol, D.F. Charles, R.M. Hughes, S.G. Paulsen, and G.B. Collins. 1999. Assessing water quality changes in the lakes of the northeastern United States using sediment diatoms. *Can. J. Fish. Aquat. Sci*. 56: 131-152.

Driscoll, C.T., G.B. Lawrence, A.J. Bulger, T.J. Butler, C.S. Cronan, C. Eagar, K.F. Lambert, G.E. Likens, J.L. Stoddard, and K.C. Weathers. 2001. Acidic Deposition in the Northeastern Unites States: Sources and Inputs, Ecosystem Effects and Management Strategies. *BioScience* 51:180-198.

Dupont, J., T.A. Clair, C. Gagnon, D.S. Jeffries, J.S. Kahl, S J. Nelson, and J.M. Peckenham. 2005. Estimation of critical loads of acidity for lakes in northeastern United States and eastern Canada. *Environmental Monitoring and Assessment* 109:275-291.

Haines, T. S. Norton, J. Kahl, C. Fay, S. Pauwels, and C. Jagoe. 1990. Intensive studies of stream fish populations in Maine. U.S. Environmental Protection Agency, Office of Acid Deposition, Environmental Monitoring and Quality Assurance. EPA/600/3-90-043.

Hall, J., B. Reynolds, S. Langon, M. Hornung, F. Kennedy, and J. Aherne. 2001. Investigating the Uncertainties in the Simple Mass Balance Equation for Acidity Critical Loads for Terrestrial Ecosystems in the United Kingdom. *Wat. Air and Soil Pollution: Focus* 1: 43-56.

Hodson, M.E., and S.J. Langen. 1999. Considerations of uncertainty in setting critical loads of acidity of soils: the role of the weathering rate determination. *Environ. Pollution* 106:73-81.

ICP Mapping Manual (2004) International Cooperative Programme on Modelling and Mapping of Critical Loads and Levels and Air Pollution Effects, Risks and Trends, UNECE Convention on Long-range Transboundary Air Pollution. *Manual on Methodologies and criteria for Modelling and Mapping of Critical Loads and Levels and Air Pollution Effects, Risks and Trends.* (http://icpmapping.org/cms/zeigeBereich/5/manual-und-downloads.html)

Koseva, I.S., S.A. Watmough, and J. Aherne. 2010. Estimating base cation weathering rates in Canadian forest soils using a simple texture-based model. *Biogeochemistry* 101:183-196.

Lasaga, A.C., J.M. Soler, J.G. Ganor, T.E. Burch, and K.L. Nagy. 1994. Chemical weathering rate laws and global geochemical cycles. *Geochim. et Cosmochim. Acta* 58:2361-2386.

Li, H. and S.G. McNulty. 2007. Uncertainty analysis on simple mass balance model to calculated critical loads for soil acidity. *Environ. Pollution* 149: 315-326.

Miller, E.K., J.D. Blum and A.J. Friedland (1993) Determination of Soil Exchangeable-Cation Loss and Weathering Rates Using Sr Isotopes, *Nature*, 362:438-441.

Miller, E.K., A. VanArsdale, G.J. Keeler, A. Chalmers, L. Poissant, N. Kamman, and R. Brulotte. 2005. Estimation and Mapping of Wet and Dry Mercury Deposition Across Northeastern North America. *Ecotoxicology* 14: 53-70.

Mitchell, M.J., G. Lovett, S. Bailey, F. Beall, D. Burns, D. Buso. T. A. Clair, F. Courchesne, L. Duchesne, C. Eimers, D.Jeffries, S. Kahl,, G. Likens, M.D. Moran, C. Rogers, D. Schwede, J. Shanley, K. Weathers and R. Vet. 2010. Comparisons of Watershed Sulfur Budgets in Southeast Canada and Northeast US: New Approaches and Implications. *Biogeochemistry* (In Press).

Monteith, D.T., J.L. Stoddard, C.D. Evans, H.A. de Wit, M. Forsius, T. Hogasen, A. Vilander, B.L. Skjelkvale, D.S. Jeffries, J. Vuorenmaa, B. Keller, J. Kopacek, and J. Vesely (2007) Dissolved organic carbon trends resulting from changes in atmospheric deposition chemistry. *Nature* 450: 537-540.

Moore, J-D. and R. Ouimet. 2006. Ten-year effect of dolomitic lime on the nutrition, crown vigor, and growth of sugar maple. *Canadian Journal of Forest Research* 36:1834-1841.

Morel, F.M-M. and J.G. Hering. 1993. *Principles and Applications of Aquatic Chemistry*. Wiley, New York. 588p.

Munroe J.S., Ryan P.C., Carlson H.A., and Miller E.K., 2008, Testing Latest Wisconsinan Ice Flow Directions in Vermont through Quantitative X-ray Diffraction Analysis of Soil Mineralogy. *Northeastern Geology and Environmental Sciences*, 29(4): 263-275.

Nasr, M., M. Castonguay, J. Ogilvie, B.A. Raymond, and P.A. Arp. 2010. Modelling and mapping critical loads and exceedances for the Georgia Basin, British Columbia, using a zero base-cation depletion criterion. *J. Limnol.* 69 (Suppl. 1): 181-292.

NEG/ECP Forest Mapping Group. 2001. Protocol for assessment and mapping of forest sensitivity to atmospheric S and N deposition. The Conference of the New England Governors and Eastern Canadian Premiers. 76 Summer St. Boston, MA 02110. 79 pp.

NESCAUM, 2006. Contributions to Regional Haze in the Northeast and Mid-Atlantic United States, Technical Report for the MANE-VU Regional Planning Organization, NESCAUM, Boston, MA, August, 2006 (See http://www.nescaum.org/documents/ contributions-to-regional-haze-in-the-northeast-and-mid-atlantic--united-states/).

Pardo, L.H., M. Robin-Abbott, N. Duarte, and E.K. Miller. 2005. Tree Chemistry Database (Version 1.0). USFS General Technical Report NE-324. USDA Forest Service, 11 Campus Blvd. Suite 2000, Newtown Square, PA.

Perry, C.M. (1990) Chronic effects of low pH on length and weight of Atlantic salomon, Salmo salar. *Environmental Biology of Fishes* 27: 153-155.

Schaberg, P.G., D.H. DeHayes, and G.J. Hawley. 2001. Anthropogenic Calcium Depletion: A Unique Threat to Forest Ecosystem Health? *Ecosystem Health* 7: 214-228.

Schaberg, P.G., Miller, E.K., Eagar, C. Assessing the Threat that Anthropogenic Calcium Depletion Poses to Forest Health and Productivity. 2007. USDA Forest Service General Technical Report PNW-GTR-806 (a peer-reviewed, combined publication of the Southern and Pacific Northwest Research Stations) and a chapter on the web-based forestry encyclopedia: www.threats.forestencyclopedia.net

Skeffington, R.A. 2006. Quantifying Uncertainty in Critical Loads: (a) Literature Review. *Wat. Air. Soil Pollution.* 169-3-24.

Sverdrup, H. and P. Warfvinge. 1993. Calculating field weathering rates using a mechanistic geochemical model PROFILE. *Applied Geochemistry* 8: 273-283.